Construction Materials Research Center

Mississippi State University
CMRC
Construction Materials Research Center
"An Industry, Agency & University Partnership"

Prototype and Full Scale Instrumented Testing of Wood Construction Platforms

Final Report
CMRC-08-01

Written and Performed By:
Isaac L. Howard, PhD-Mississippi State University
Martin F. Stroble III-Mississippi State University

June 30, 2008

JAMES WORTH BAGLEY
COLLEGE OF ENGINEERING
MISSISSIPPI STATE UNIVERSITY
CIVIL & ENVIRONMENTAL ENGINEERING

Technical Report Documentation Page

1. Report No. CMRC-08-1	2. Government Accession No.	3. Recipient's Catalog No.
4. Title and Subtitle Prototype and Full Scale Instrumented Testing of Wood Construction Platforms		5. Report Date June 30, 2008
		6. Performing Organization Code
7. Author(s) Isaac L. Howard, PhD, Assistant Professor, Mississippi State University Martin F. Stroble III, Graduate Assistant, Mississippi State University		8. Performing Organization Report No. CMRC-08-1
9. Performing Organization Name and Address Mississippi State University Civil and Environmental Engineering Department 501 Hardy Road: P O Box 9546 Mississippi State, MS 39762		10. Work Unit No. (TRAIS)
		11. Contract or Grant No.
12. Sponsoring Agency Name and Address MODUMAT 705 Main Street Leakesville, MS 39451		13. Type of Report and Period Covered Final Report
		14. Sponsoring Agency Code
Supplementary Notes: Work performed under Mississippi State University research project titled: Instrumentation and Analysis of Wood Matting Systems		

16. Abstract

This report contains testing and preliminary analysis of 63 instrumented wood construction platforms. Of these, 54 were of prototype scale (generally 1/6th scale), and 9 were full scale. Four wood types were evaluated: 1) white ash, 2) hickory-pecan, 3) southern pine, and 4) sweetgum. The mats were constructed into 17 different geometries with differing amounts of repetition for each. A total of 150 foil strain gages were used during testing. Results are presented in terms of ultimate strength, deflection, strain, and relaxation (load and strain) under brief sustained load pauses. In general, a small number of the geometric configurations were promising. Recommendations for future work are presented that would improve the current data set.

17. Key Words Construction Platforms, Wood, Instrumentation	18. Distribution Statement Unclassified		
19. Security Classif. (of this report) Unclassified	20. Security Classif. (of this page) Unclassified	21. No. of Pages 114	22. Price

Form DOT F 1700.7 (8-72) **Reproduction of completed page authorized**

TABLE OF CONTENTS

LIST OF FIGURES

LIST OF TABLES

CHAPTER 1-INTRODUCTION

1.1 General and Background Information

Wood matting systems have application in a variety of temporary to short term applications, with construction over soft soils being one of the most prevalent. They are capable of protecting the environment, ensuring health and safety of workers, and are highly portable. *Green*, safe construction is feasible using laminated wood mats where no residual material (e.g. stone from haul roads) is left behind but during service the mats are adequate; possibly highly over designed. Permanent access to many areas is neither needed nor wanted, and removal of many solutions can cause pollution and/or erosion problems (Mason and Greenfield 1995).

Pipeline construction has utilized timber mats dating as far back as the early 1960's (Anon 1961). These mats often support large objects such as cranes, which heightens the need for exhaustive testing programs prior to use. Beavers et al. (2006) reported crane related fatalities represent more than 8% of all construction fatalities investigated by OSHA, and that mobile cranes (candidates to operate over wood mats) account for 84% of crane related fatalities. Instrumented testing is capable of providing invaluable data in optimizing wood mats that would, in turn, have a reduced mass resulting in reduced energy costs and material usage while not sacrificing functionality or worker safety.

A total of 63 wood mats were tested (54 prototype and 9 full scale), that were instrumented with a total of 150 foil strain gages. The materials tested varied from hardwoods to softwoods, and a total of thirteen prototype geometric configurations and five full scale geometric configurations were investigated. The remainder of the report discusses the testing and analysis of the mats and provides recommendations for future investigation.

1.2 Objectives and Scope

The objective of this report is to provide a large volume of instrumented test data of prototype (i.e. scaled) and full scale wood construction platforms. The data is analyzed to a level of detail that provides insight into the overall quality of a particular wood type and geometric configuration. Basic mechanics principles are also applied to the mats to determine their suitability in further analysis. No design procedures or direct recommendations related to a specific end use of a particular wood type and geometric configuration are provided. This level of information is beyond the scope of the report.

1.3 Brief Literature Review

The field of wood construction platforms is primarily industry driven, especially in terms of the current knowledge base. A literature review was conducted that demonstrates research incorporating instrumentation and numerical analysis is scarce in both the engineering and forest products disciplines. The literature review was conducted to investigate testing programs used for wood mats and instrumentation used in wood mat testing. Most testing and analysis of wood construction mats has followed a protocol consisting of testing to failure and observing the results. This model appears to be somewhat consistent in the military and civil works of the US Army Corps of Engineers (Kestler et al.

1999; Santoni et al. 2001), the USDA (Hislop 1996), and other works (Mason and Greenfield 1995).

Mason and Greenfield (1995) tested five products including wood pallets and wood mats (100 mm and 150 mm (4 and 6 in)) mostly in Florida for the Forest Service. All testing was qualitative in nature (e.g. surface deformation measurements) and further evaluation was recommended for all methods. Schweitzer and Marinello (1996) incorporated wood mats in Texas and Louisiana for utility construction through environmentally sensitive marsh and wetlands. The wood mat construction cost was 10-15% of building conventional temporary roads when mitigation was considered.

Hislop (1996) evaluated techniques including wood pallets and wood mats to prevent low volume road rut development in short and unstable sections. The field evaluation in Florida showed wood surfaces were successful at reducing rutting and simultaneously reducing environmental impacts. Hislop (1996a) reported the wood pallets and mats reduced rut depths, on average, by 127 mm (5 in) for the low volume roads considered that were maintained by the Forest Service.

Kestler et al. (1999) tested four methods including two types of wood mats (on site construction using lightweight materials and oak Unimats) over very weak and unstable soils in Wisconsin. All evaluation was either empirical or subjective: e.g. rutting, lateral expansion, and driver ratings. Wood mats were shown to be effective, durable, able to withstand tank motions, and a decision aid was developed for the products and conditions. Santoni et al. (2001) tested many products including hardwood mats over very soft soils (California Bearing Ratio-$CBR \leq 1$). The full scale experimental program included no instrumentation and consisted primarily of rut depth measurements and visual observations. It was found that two layers of SOLOCO wood mats were capable of sustaining 2,000 passes of military trucks.

Instrumentation does not appear to be commonplace in wood mats. Laboratory programs and on ground testing of mats do not appear to be making use of the technology. Review of literature found two instances where instrumentation was used for timber bridges (Franklin et al. 1999; Wipf et al. 1996). Franklin et al. (1999) used DCDT displacement transducers to measure deflections for two portable timber bridges to quantify effects of dynamic loading. Similarly, Wipf et al. (1996) tested the dynamic response of timber bridges using potentiometer transducers (DCPT) and accelerometers.

CHAPTER 2-EXPERIMENTAL PROGRAM

2.1 Experimental Program Overview

The experimental program consisted of testing multiple prototype and full scale mats manufactured from 4 different wood types and into 18 different geometries (13 prototype and 5 full scale). A total of 63 mats were tested: 1) 34 pine, 12 gum, 4 ash, and 4 hickory prototype mats; and 2) 9 pine full scale mats. Photos of all 18 geometries can be seen in Appendix A. The prototype mats were tested in 3-point bending while measuring load, deflection, and strain, while the full scale mats were tested in 4-point bending while measuring the same properties. Advancement of loading was paused for one minute at various intervals to capture relaxation behaviors of the respective configurations. Additional details of prototype and full scale testing can be found in the following sub-sections.

2.1.1 Prototype Mats Experimental Program

A summary of the prototype testing program can be seen in Table 2.1. The mats were labeled 1 to 54 based on the order they were tested. The mats were also identified according to geometry. Drawings of each of the 13 geometries can be found in Appendix B, where both instrumentation and geometric configurations can be seen.

Table 2.1 - Summary of Prototype Testing Program

Geometry	No. Tested	Mat Type (Mat Numbers)*
1	1	P(1)
2	1	P(23)
3	1	P(10)
4	2	P(15,16)
5	1	P(5)
6	2	P(21,22)
7	3	P(27,28,29)
8	5	P(4,11,12,13,14)
9	5	P(3,17,18,19,20)
10	8	P(8,24,25,26) G(9,52,53,54)
11	8	P(6,46,47,48) G(7,49,50,51)
12	16	P(38,39,40,41) G(30,31,32,33) A(34,35,36,37) H(42,43,44,45)
13	1	P(2)

** P = Pine, G = Gum, A = Ash, and H = Hickory.*

Prototype geometry 1 was used to assess the viability of the testing procedure. This mat was 81 cm (32 in) long (twice as long as the remaining mats). Both the mat performance and the test procedure were deemed acceptable, and the remaining mats tested were built to 1/6th of full scale (20 cm wide by 41 cm long (8 in by 16 in)). All mats were purely bonded by adhesive and were tested very quickly after manufacture.

Photos of the 3-point bending prototype testing can be found in Appendix A. Therein, the load frame, deflection gages, and other noteworthy items can be seen. Noteworthy items included: 1) the elastic pad placed between the mat and load block, 2) the metal load block that distributed the load evenly across the sample, and 3) the instrumentation used to collect all data.

Deformation was taken at the top and bottom of the mats. The top reading was used to account for slack and fixturing, as well as to determine when to begin the test. A seating load of 44 kg (20 lb) was sufficient to eliminate the slack. This event was indicated by a reversal of deflection of the top gage (the magnitude of the reversal was around 0.025 mm (0.001 in)). During load pauses, deflection readings remained constant indicating the load frame was capable of holding a constant position on the mats.

2.1.2 Full Scale Mats Experimental Program

A summary of the full scale testing program can be seen in Table 2.2. The mats were labeled 55 to 63 based on the order they were tested. The mats were also identified according to geometry. Photos of the five geometries can be seen in Appendix A. All instrumentation was located near the center of the mats (as discussed in Section 2.3), so detailed location drawings were not necessary.

Table 2.2 - Summary of Full Scale Testing Program

Geometry	No. Tested	Mat Type (Mat Numbers)*
14	1	P(55)
15	2	P(56, 57)
16	4	P(58, 59, 60, 61)
17	1	P(62)
18	1	P(63)

** P = Pine.*

The clear span during full scale testing was 226.1 cm (89 in). The two load patches were 171.5 mm (6.75 in) wide. The distance from the supports to the edge of the load patches was 66.4 cm (26 in), and the interior spacing between load patches was 59.6 cm (23.5 in).

The mats were manufactured using only 2 by 6, 2 by 8, and 2 by 10 lumber. All small sections were made by ripping larger lumber sections. One of the mats was made by ripping a 2 by 10 into three pieces. Key properties of each mat can be seen in Table 2.3.

Table 2.3 – Summary of Full Scale Mat Geometric Properties

			Ply Thickness-mm (in)[4]				
G[1]	Thickness[2] mm (in)	Screws[3]	No 1	No 2	No 3	No 4	No 5
14	184.2 (7.25)	Y	73.0 (2.9)	37.5 (1.5)	73.0 (2.9)	---	---
15	139.7 (5.5)	N	139.7 (5.5)	---	---	---	---
16	112.5 (4.5)	Y	37.5 (1.5)	37.5 (1.5)	37.5 (1.5)	---	---
17	112.5 (4.5)	Y	112.5 (4.5)	112.5 (4.5)	112.5 (4.5)	---	---
18	190.5 (7.5)	Y	37.5 (1.5)	37.5 (1.5)	37.5 (1.5)	37.5 (1.5)	37.5 (1.5)

1: G = Geometry
2: Total thickness
3: Y = three rows of 100 mm (4 in) screws running across the full width spaced longitudinally at 3rd points, N = no screws
4: Ply numbering begins at the top of the mat as it was tested

2.2 Material Properties of Mats Tested

The materials tested were: 1) white ash (ash); 2) sweetgum (gum); 3) hickory-pecan (hickory); and 4) southern pine (pine). Southern yellow pine contains loblolly, longleaf, shortleaf, and slash species; the species isn't routinely tracked and was unknown for the pine materials tested. These materials were selected to provide a wide range of materials that could be used during large scale manufacturing. Pine was the highest utilized material in that it is common and available in the area served by the *Mississippi* forest industry. Key properties of the materials needed for further analysis can be found in Table 2.4. They were obtained from the Wood Handbook (1999). As is commonly known, wood is an orthotropic material; i.e. unique properties in all directions. The longitudinal axis is parallel to the grain, and the radial/tangential directions are in the plane corresponding to the end of standard lumber. All prototype and full scale mats were loaded perpendicular to the fiber (grain) direction.

Table 2.4 – Properties of Wood Materials Tested

Material	MOR MPa (10^3 psi)	MOE[2] GPa (10^6 psi)	μ[3]
White Ash	103.0 (15.0)	12.0 (1.74)	0.41
Sweetgum	86.0 (12.5)	11.3 (1.64)	0.36
Hickory-Pecan	94.0 (13.7)	11.9 (1.73)	---[4]
Southern Pine[1]	97.5 (14.2)	13.0 (1.90)	0.36
Loblolly	88.0 (12.8)	12.3 (1.79)	0.31
Longleaf	100.0 (14.5)	13.7 (1.98)	0.35
Shortleaf	90.0 (13.1)	12.1 (1.75)	----
Slash	112.0 (16.3)	13.7 (1.98)	0.42

1: Average properties of four pine species listed below
2: Value in longitudinal direction that accounts for shear deflection. Bending only modulus should be increased by 10%
3: Average value of Poisson's Ratio for deformation along radial/tangential axis for stress along longitudinal axis
4: Not a commonly used wood species so property was not readily available

According to the Wood Handbook (1999) the properties displayed in Table 2.4 represent pieces of wood that are "clear" and "straight grained" and do not contain properties such as knots, cross grain checks, or splits. The wood industry refers to these specimens as homogeneous. The properties shown represent the average properties of the species. Note that all full scale mats were manufactured of *No 3 Southern Pine*.

Moisture contents of the wood during testing would resemble *air dry* conditions. All the material (prototype and full scale) was kiln dried and dimensioned. Kiln drying requires a moisture content below 19%, while Wood Handbook (1999) uses a 12% moisture content to represent *air dry* conditions. Manufacture experience estimated 12 to 15% moisture at the time of testing. As a point of reference *green* woods typically have on the order of 100% moisture. Forest products experts often approximate the wet strength (i.e. green) to be on the order of 90% of the air dry strength.

The full scale mats are typically manufactured to 2.4 by 4.9 m (8 by 16 ft). The full scale mats tested were 1.2 by 2.4 m (4 ft by 8 ft). The components tested would have twice the dimension in each direction and are symmetrical. An in service mat would be four of the mats tested. The size was reduced to fit into the test frame, for material savings, and since the testing performed provides the same quantity of full scale data. A portion of the mats contained 100 mm (4 in) screws. They were applied during pressing of the glue and wood together. Approximately 36 kPa (750 lb/ft^2) of pressure was used. In general, *Construction Adhesive* (an elastomeric material) was used and the manufacturer selected a low pressure to avoid squeezing of excessive glue.

2.3 Instrumentation and Data Acquisition

Continuous data acquisition was performed at a rate of 5 Hz using *National Instruments NI CompaqDaq 9172* chassis and *NI 9237* I/O modules. Foil strain gages manufactured by *Vishay Micro Measurements* were used for all testing. Survivability of the strain gages on prototype mats was 95%; 115 recorded strain plots were obtained from 121 desired strain locations. Similarly, 97% of the 36 full scale strain gages survived. Photos of the instrumentation can be found in Appendix A. The gages proved to be an economical instrumentation choice that yielded satisfactory results. Standard dial gages were used to measure deflection.

The drawings in Appendix B show the instrument locations of the prototype mats. The full scale mats were instrumented with four gages installed in a 25 mm (1 in) square in the center of the mat. Strain on all full scale mats was in the longitudinal direction.

CHAPTER 3-RESULTS AND DISCUSSION

3.1 Overview of Results

Information was obtained pertaining to the mats strength, mass, deflection, strain, and relaxation. These behaviors are discussed in the following sections. Note that all mats evaluated in the program are new and have not been aged due to sunlight exposure, moisture, chemical attack, and similar. The data should be taken as the day 1 service properties of the mats. In general, prototype geometries 7 to 12 (See Appendix B) were the only mats tested with sufficient repetition to allow meaningful discussion at that scale. Values from the other mats are mentioned, but the reader should note that any number of parameters can affect the results from any one test. Discussion of all full scale mats was performed in absence of substantial repetition

3.2 Strength Results

3.2.1 Prototype Strength Results

Table 3.1 summarizes the prototype strength results obtained from testing. Table 3.2 provides the density of each mat at the time of testing. A key component of the analysis is the strength to density ratio (*S/D*), which has been provided for each geometry and wood configuration in Table 3.3. Note the density was calculated as a freight density (i.e. the total mass of the mat divided by the total volume occupied within its length, width, and depth). The mean values shown in Tables 3.1 and 3.2 were used in the S/D ratio calculations.

Table 3.1 – Prototype Strength Results

G*	Wood	Mats	Ultimate Strength-kN (*Mean Value*)	Ultimate Strength-lb (*Mean Value)*
1	Pine	1	9.74 (***9.74***)	2190 (***2190***)
2	Pine	23	35.96 (***35.96***)	8085 (***8085***)
3	Pine	10	8.14 (***8.14***)	1830 (***1830***)
4	Pine	15, 16	13.01, 12.28 (***12.65***)	2925, 2760 (***2843***)
5	Pine	5	16.55 (***16.55***)	3720 (***3720***)
6	Pine	21, 22	8.41, 5.67 (***7.04***)	1890, 1275 (***1583***)
7	Pine	27, 28, 29	11.81, 10.54, 9.34 (***10.56***)	2655, 2370, 2100 (***2375***)
8	Pine	4, 11, 12, 13, 14	9.54, 10.12, 15.15, 13.81, 15.21 (***12.77***)	2145, 2275, 3405, 3105, 3420 (***2870)***
9	Pine	3, 17, 18, 19, 20	9.34, 10.34, 10.81, 10.88, 10.14 (***10.32***)	2100, 2325, 2430, 2445, 2280 (***2316***)
10	Pine	8, 24, 25, 26	12.14, 12.48, 17.48, 12.14 (***13.56***)	2730, 2805, 3930, 2730 (***3049***)
10	Gum	9, 52, 53, 54	12.68, 14.15, 14.59, 14.61 (***14.01***)	2850, 3180, 3280, 3285 (***3149***)
11	Pine	6, 46, 47, 48	19.68, 14.01, 17.28, 18.13 (***17.28***)	4425, 3150, 3885, 4075 (***3884***)
11	Gum	7, 49, 50, 51	20.19, 21.15, 21.82, 21.42 (***21.40***)	4540, 4755, 4905, 4815 (***4754***)
12	Pine	38, 39, 40, 41	15.68, 13.88, 14.88, 25.42 (***17.47***)	3525, 3120, 3345, 5715 (***3926***)
12	Gum	30, 31, 32, 33	20.95, 21.95, 23.42, 21.35 (***21.92***)	4710, 4935, 5265, 4800 (***4928***)
12	Ash	34, 35, 36, 37	9.81, 17.08, 18.42, 17.68 (***15.75***)	2205, 3840, 4140, 3975 (***3540***)
12	Hickory	42, 43, 44, 45	26.16, 26.02, 27.27, 26.42 (***26.47***)	5880, 5850, 6135, 5940 (***5951***)
13	Pine	2	12.28 (***1228***)	2760 (***2760***)

** G = Geometry*

Table 3.2 – Prototype Mat Densities at Time of Testing

G*	Wood	Mats	Density-kN/m^3 (*Mean Value*)	Density-lb/ft^3 (*Mean Value)*
1	Pine	1	5.04 (***5.04***)	32.0 (***32.0***)
2	Pine	23	5.86 (***5.86***)	37.3 (***37.3***)
3	Pine	10	5.99 (***5.99***)	38.0 (***38.0***)
4	Pine	15, 16	5.61, 5.11 (***5.36***)	35.7, 32.5 (***34.1***)
5	Pine	5	4.95 (***4.95***)	31.4 (***31.4***)
6	Pine	21, 22	5.07, 4.53 (***4.80***)	32.2, 28.8 (***30.5***)
7	Pine	27, 28, 29	5.24, 4.61, 4.70 (***4.85***)	33.3, 29.3, 29.9 (***30.8***)
8	Pine	4, 11, 12, 13, 14	5.03, 6.07, 5.11, 5.24, 5.28 (***5.35***)	32.0, 38.6, 32.5, 33.3, 33.6 (***34.0***)
9	Pine	3, 17, 18, 19, 20	4.78, 4.86, 4.95, 4.86, 5.07 (***4.91***)	30.4, 30.9, 31.4, 30.9, 32.2 (***31.2***)
10	Pine	8, 24, 25, 26	5.49, 5.03, 5.53, 4.91 (***5.24***)	34.9, 32.0, 35.1, 31.2 (***33.3***)
10	Gum	9, 52, 53, 54	5.61, 5.15, 5.32, 5.20 (***5.32***)	35.7, 32.8, 33.8, 33.0 (***33.8***)
11	Pine	6, 46, 47, 48	6.53, 5.74, 5.99, 6.36 (***6.15***)	41.5, 36.5, 38.0, 40.4 (***39.1***)
11	Gum	7, 49, 50, 51	7.15, 6.36, 6.40, 6.11 (***6.51***)	45.4, 40.4, 40.7, 38.8 (***41.4***)
12	Pine	38, 39, 40, 41	5.40, 5.40, 5.77, 7.06 (***5.91***)	34.3, 34.3, 36.7, 44.8 (***37.5***)
12	Gum	30, 31, 32, 33	6.20, 6.79, 6.68, 6.63 (***6.57***)	39.4, 43.1, 42.5, 42.1 (***41.8***)
12	Ash	34, 35, 36, 37	5.40, 6.84, 6.95, 6.63 (***6.45***)	34.3, 43.5, 44.2, 42.1(***41.0***)
12	Hickory	42, 43, 44, 45	8.02, 8.23, 8.07, 7.54 (***7.96***)	51.0, 52.3, 51.3, 47.9 (***50.6***)
13	Pine	2	4.95 (***4.99***)	31.7 (***31.7***)

** G = Geometry*

As seen in Table 3.1, the highest ultimate strength was achieved with Geometry 2 at 35.96 kN (8,085 lb). This would be expected since the mat was the thickest mat tested and was solid throughout. Since only one of these style mats was tested, further analysis is not pertinent. Within Geometries 7 to 12, hickory mats of geometry 12 were found to have the highest strength. The maximum strength achieved with any of the pine mats was found to be 17.47 kN (3,926 lb). Within Geometry 12, Ash was the weakest of all woods when tested in a common geometry.

Table 3.3 – Prototype Strength to Density (S/D) Ratios

G*	Wood	Mats	***S/D* – per m^3**	***S/D* – per ft^3**
1	Pine	1	1.93	68.4
2	Pine	23	6.14	217.0
3	Pine	10	1.36	48.1
4	Pine	15, 16	2.36	83.4
5	Pine	5	3.34	118.3
6	Pine	21, 22	1.47	51.9
7	Pine	27, 28, 29	2.18	77.0
8	Pine	4, 11,12, 13, 14	2.39	84.5
9	Pine	3, 17, 18, 19, 20	2.10	74.3
10	Pine	8, 24, 25, 26	2.59	91.6
10	Gum	9, 52, 53, 54	2.63	93.1
11	Pine	6, 46, 47, 48	2.81	99.3
11	Gum	7, 49, 50, 51	3.25	115.0
12	Pine	38, 39, 40, 41	2.96	104.6
12	Gum	30, 31, 32, 33	3.33	117.9
12	Ash	34, 35, 36, 37	2.44	86.3
12	Hickory	42, 43, 44, 45	3.32	117.6
13	Pine	2	2.46	87.0

** G = Geometry*

3.2.2 Full Scale Strength Results

Table 3.4 summarizes the full scale strength results obtained from testing. Table 3.5 provides an estimate of the volume of each mat at the time of testing. A key component of the analysis is the strength to volume ratio (*S/V*), which has been provided for each geometry and wood configuration in Table 3.6. Since none of the mats have areas where material was removed (as in the prototype mats), the thicknesses were variable, and the material used was the same, S/V was used in lieu of S/D as in the prototype mats. The mean values shown in Tables 3.4 and 3.5 were used in the S/V ratio calculations.

Table 3.4 – Full Scale Strength Results

G*	Wood	Mats	Ultimate Strength-kN (*Mean Value*)	Ultimate Strength-10^3*lb (*Mean Value)*
14	Pine	55	355 ***(355)***	79.7 (***79.7)***
15	Pine	56, 57	605, 630 ***(618)***	135.9, 141.6 ***(138.9)***
16	Pine	58, 59, 60, 61	127, 136, 111, 124 ***(125)***	28.5, 30.7, 25.0, 27.9 ***(28.0)***
17	Pine	62	72 ***(72)***	16.2 ***(16.2)***
18	Pine	63	194 ***(194)***	43.6 ***(43.6)***

** G = Geometry*

Table 3.5 – Full Scale Mat Volumes at Time of Testing

G*	Wood	Mats	Volume-m^3 (*Mean Value*)	Volume-ft^3 (*Mean Value)*
14	Pine	55	0.55	19.3
15	Pine	56, 57	0.42	14.7
16	Pine	58, 59, 60, 61	0.33	12.0
17	Pine	62	0.33	12.0
18	Pine	63	0.57	20.0

** G = Geometry*

Table 3.6 – Full Scale Strength to Volume (S/V) Ratios

G*	Wood	Mats	*S/V* – kN/m^3	*S/V* – 10^3*lb/ft^3
14	Pine	55	646	4.13
15	Pine	56, 57	1114	9.45
16	Pine	58, 59, 60, 61	379	2.33
17	Pine	62	218	1.35
18	Pine	63	340	2.18

** G = Geometry*

Note a density of 5.5 kN/m^3 (35 lb/ft^3) was assumed for the calculations

The highest strength was easily obtained by geometry 15. This geometry also was easily the highest in terms of *S/V* ratio. The geometries using the most material (14 and 18) did not prove to be the most efficient systems. It would appear based solely on the limited data that the orientation of the material within the mat is more significant than the amount of material when strength in a single direction of primary concern. This behavior is intuitive.

3.3 Deflection Results

3.3.1 Prototype Deflection Results

Complete deflection plots can be found in Appendix C. Table 3.7 provides the peak deflections recorded during testing. Deflection was recorded until failure for the prototype mats.

Table 3.7 - Summary of Deflection Results

G*	Wood	Mats	Ultimate Deflection-mm (*Mean Value*)	Ultimate Deflection-in(10^{-3}) (*Mean Value*)
1	Pine	1	N/A	N/A
2	Pine	23	13.4 (***13.4***)	526 (**526**)
3	Pine	10	19.8 (***19.8***)	778 (***778***)
4	Pine	15, 16	12.9, 9.4 (***11.2***)	506, 372 (***439***)
5	Pine	5	14.6 (***14.6***)	574 (***574***)
6	Pine	21, 22	12.1, 10.6 (***11.3***)	476, 417 (***447***)
7	Pine	27, 28, 29	11.8, 13.6, 9.0 (***11.5***)	466, 535, 356 (***452***)
8	Pine	4, 11, 12, 13, 14	13.4, 11.3, 13.7, 13.5, 13.1 (***13.0***)	527, 444, 541, 533, 515 (***512***)
9	Pine	3, 17, 18, 19, 20	18.4, 11.8, 15.7, 13.5, 11.1 (***14.1***)	724, 463, 617, 530, 438 (***555***)
10	Pine	8, 24, 25, 26	16.4, 11.2, 13.7, 11.9 (***13.3***)	645, 441, 541, 467 (***524***)
10	Gum	9, 52, 53, 54	15.8, 15.9, 14.0, 14.6 (***15.1***)	622, 626, 550, 573 (***593***)
11	Pine	6, 46, 47, 48	15.6, 14.7, 12.2, 12.8 (***13.8***)	616, 577, 481, 505 (***545***)
11	Gum	7, 49, 50, 51	17.9, 12.6, 14.2, 14.6 (***14.8***)	705, 496, 559, 574 (***584***)
12	Pine	38, 39, 40, 41	13.4, 11.8, 12.2, 15.3 (***13.2***)	527, 465, 481, 601 (***519***)
12	Gum	30, 31, 32, 33	13.9, 12.5, 14.4, 13.0 (***13.5***)	549, 491, 566, 513 (***530***)
12	Ash	34, 35, 36, 37	10.0, 12.5, 13.0, 13.3 (***12.2***)	392, 493, 512, 523 (***480***)
12	Hickory	42, 43, 44, 45	18.1, 15.2, 17.4, 19.3 (***17.5***)	711, 597, 684, 761 (***688***)
13	Pine	2	N/A	N/A

** G = Geometry*

3.3.2 Full Scale Deflection Results

Complete deflection plots can be found in Appendix C. As seen in these plots, only the early stage deflections were measured. With standard dial gages, measuring deflection to failure was not safe with the full scale mats. It was not deemed appropriate to go to the additional effort to use electronic displacement transducers. Table 3.8 provides the modulus of elasticity (*MOE*) values of the full scale mats based on standard bending theory.

Table 3.8 – Full Scale Modulus of Elasticity (*MOE*) Results

G*	Wood	Mats	*MOE*-GPa (*Mean Value*)	*MOE*-10^6*psi (*Mean Value*)
14	Pine	55	4.34 ***(4.34)***	0.63 ***(0.63)***
15	Pine	56, 57	13.44, 13.58 ***(13.51)***	1.95, 1.97 ***(1.96)***
16	Pine	58, 59, 60, 61	10.20, 9.60, 7.03, 9.65 ***(9.12)***	1.48, 1.39, 1.02, 1.40 ***(1.32)***
17	Pine	62	6.69 ***(6.69)***	0.97 ***(0.97)***
18	Pine	63	4.62 ***(4.62)***	0.67 ***(0.67)***

** G = Geometry*

3.4 Strain Results

3.4.1 Prototype Strain Results

Complete strain plots can be found in Appendix D. Table 3.9 provides the peak strains recorded during testing. Note that recording a true peak strain is often difficult since malfunction (particularly delamanation) is very likely as failure approaches. There is a large discrepancy in failure strains, and as a result the maximum (rather than mean) value of any mat of a particular wood type and geometry is the most significant value. The time to failure of strains varies widely from measurement to measurement. Also note that locations between geometries should not be compared since a given location must be coupled with its geometry. See Appendix B for drawings and locations of each strain gage for that geometry. Note that *L1, L2, L3,* and/or *L4* are commonly used herein to denote the locations of the strain gages.

Table 3.9 - Summary of Prototype Scale Maximum Strain Results

G*	Wood	Mats	Location 1	Location 2	Location 3	Location 4
1	Pine	1	5156	294	-1075	-258
2	Pine	23	13379	-----	-----	-----
3	Pine	10	6602	9525	1649	3306
4	Pine	15, 16	-----	7781	2525	-----
5	Pine	5	6848	-----	6532	144
6	Pine	21, 22	1090	3415	3244	-----
7	Pine	27, 28, 29	2996	7436	4813	-----
8	Pine	4, 11,12, 13, 14	13294	1217	3580	-----
9	Pine	3, 17, 18, 19, 20	664	10388	9594	-----
10	Pine	8, 24, 25, 26	6376	5723	6970	-----
10	Gum	9, 52, 53, 54	12733	7720	5511	-----
11	Pine	6, 46, 47, 48	12515	2914	980	-----
11	Gum	7, 49, 50, 51	12406	4039	4900	-----
12	Pine	38, 39, 40, 41	10843	-----	-----	-----
12	Gum	30, 31, 32, 33	13925	-----	-----	-----
12	Ash	34, 35, 36, 37	16586	-----	-----	-----
12	Hickory	42, 43, 44, 45	17876	-----	-----	-----
13	Pine	2	5983	2485	3066	221

** G = Geometry*

The strain relaxation of the mats when held at a fixed position for 1 min was found using Eq. (3.1) and (3.2). Refer to Section 2.1 for details on the experimental program. Figure 3.1(a) serves as an example of how to determine the first data point in Figure 3.1(b). As seen Figure 3.1(b), Eq. (3.1) computes the *y*-axis value, while Eq. (3.2) computes the *x*-axis value.

$$\varepsilon_{ult}\,(\%) = \frac{(1)}{(3)} \tag{3.1}$$

$$\mathrm{Re}\,laxation\ (\%) = \frac{(1)-(2)}{(3)} \tag{3.2}$$

Where,
(1) = strain at beginning of pause

(2) = strain at the conclusion of the pause
(3) = strain value of Table 3.9

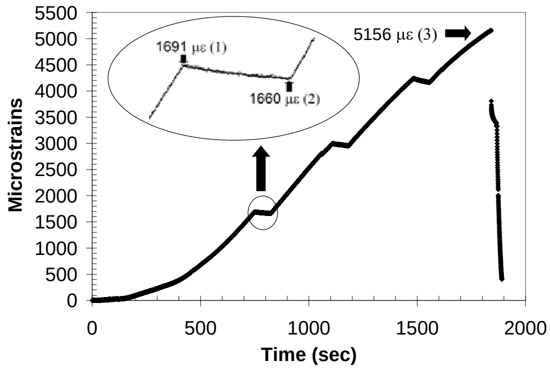

(a) Figure D1(a) Reproduced as Example

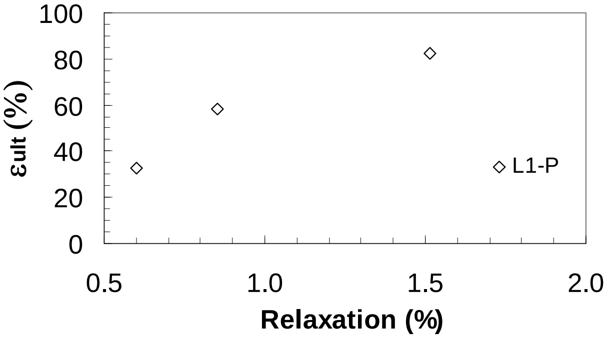

(b) Relaxation of Mat 1 from Figure D1(a)

Figure 3.1 - Determination of the Mats Strain Relaxation Behavior: Geometry 1

Figure 3.2 plots the relaxation behavior for the pine mats tested without duplication. All strain measurements were plotted that were applicable to relaxation during pauses. This was also the case for all remaining mat geometries discussed in the remainder of this section. Figure 3.3 plots the strain relaxation behavior for mats tested in duplicate, and Figures 3.4 through 3.11 plot strain relaxation behavior for the remaining geometries that have multiple mats for each wood type.

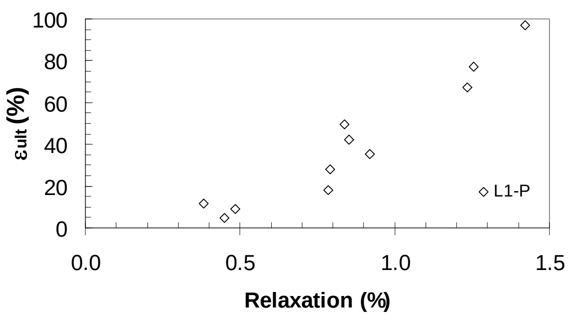

(a) Geometry 2

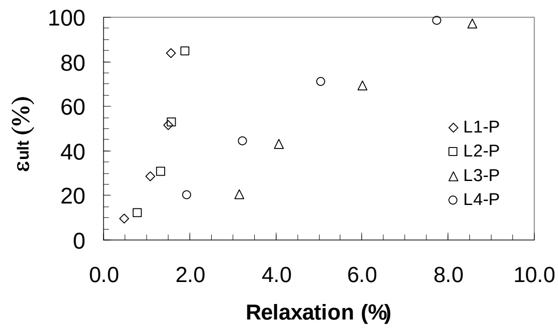

(b) Geometry 3

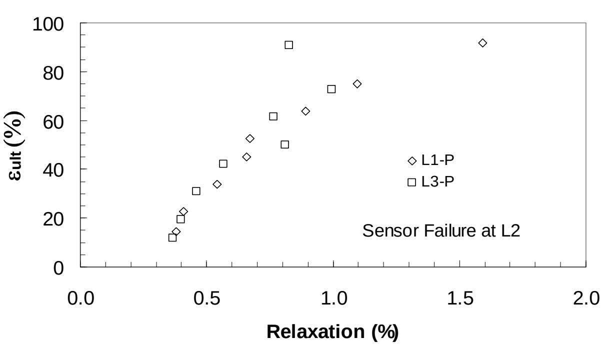

(c) Geometry 5

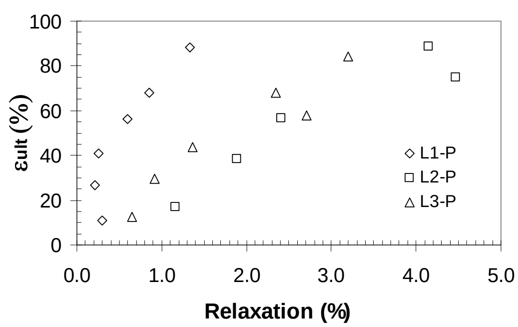

(d) Geometry 13

Figure 3.2 - Strain Relaxation Behavior for Pine Mats Tested Without Replication

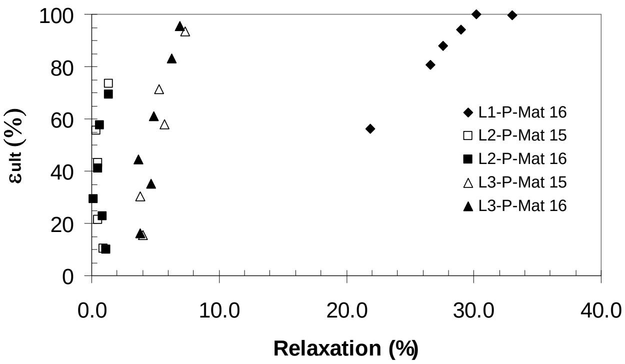

(a) Geometry 4

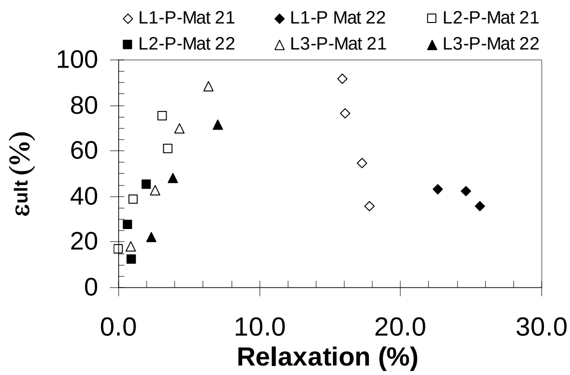

(b) Geometry 6

Figure 3.3 - Strain Relaxation Behavior for Pine Mats Tested in Duplicate

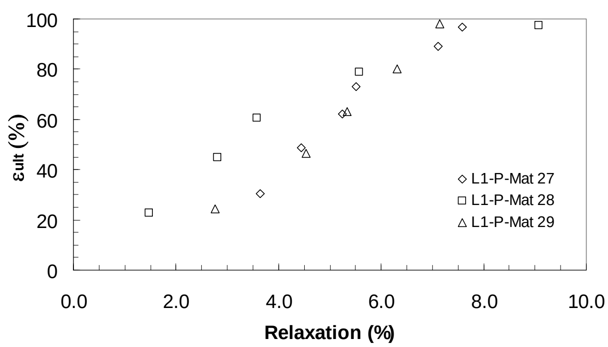

(a) Location 1 of Figure B7

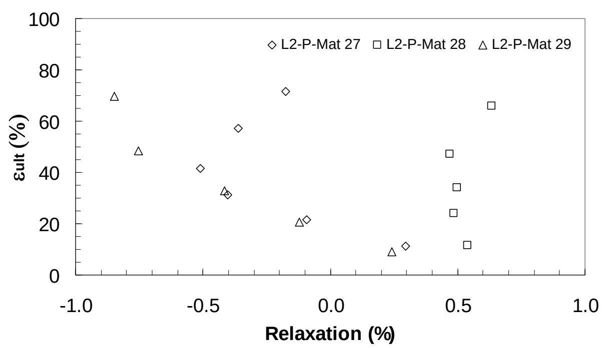

(b) Location 2 of Figure B7

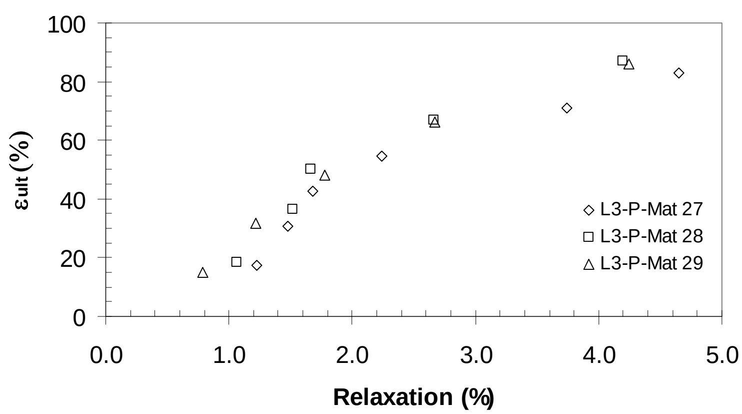

(c) Location 3 of Figure B7

Figure 3.4 - Strain Relaxation Behavior for Geometry 7 (Pine)

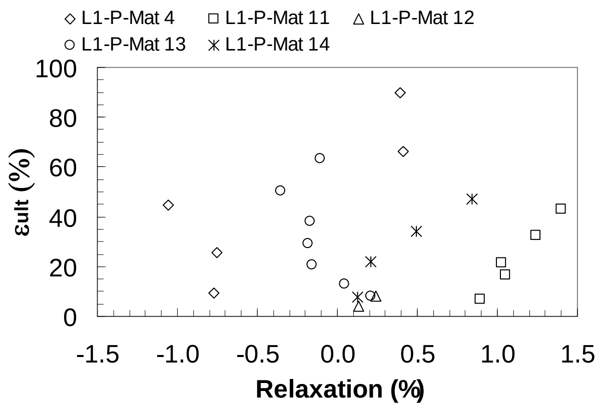

(a) Location 1 of Figure B8

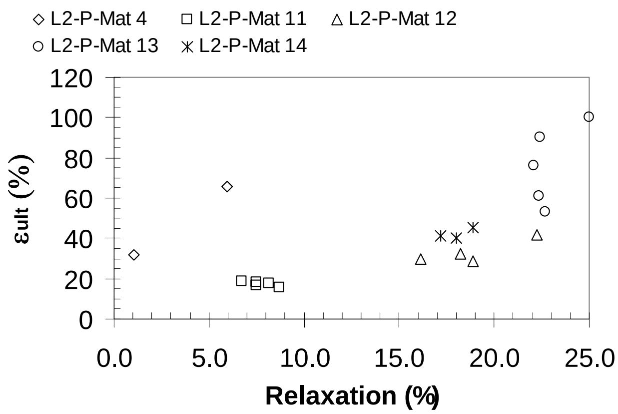

(b) Location 2 of Figure B8

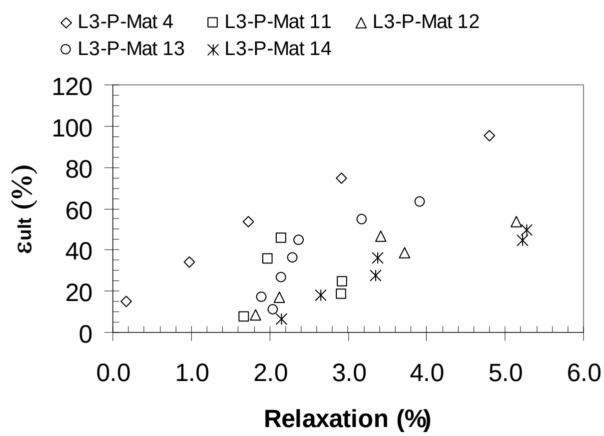

(c) Location 3 of Figure B8

Figure 3.5 - Strain Relaxation Behavior for Geometry 8 (Pine)

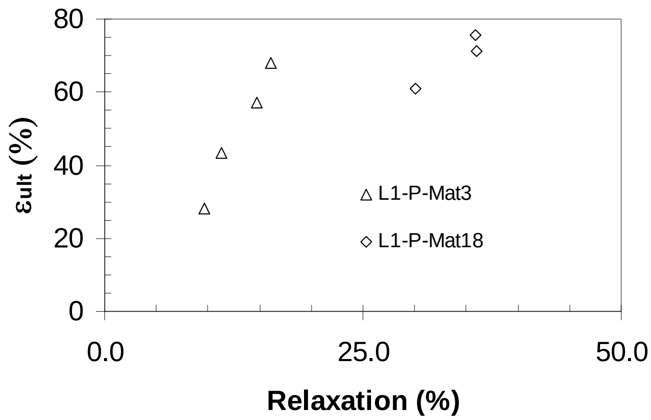

(a) Location 1 of Figure B9

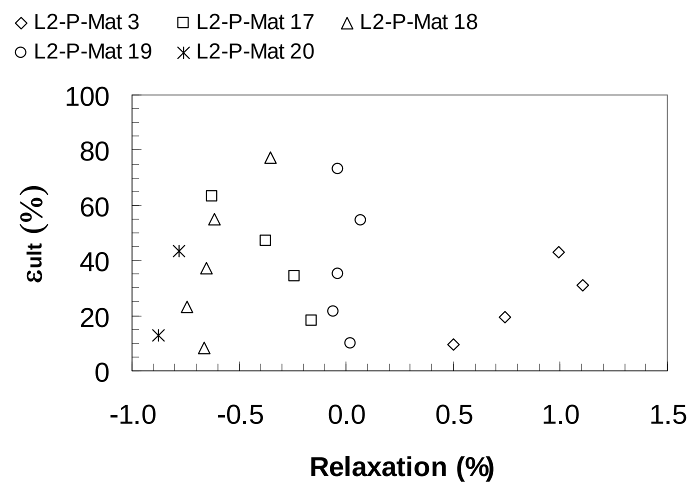

(b) Location 2 of Figure B9

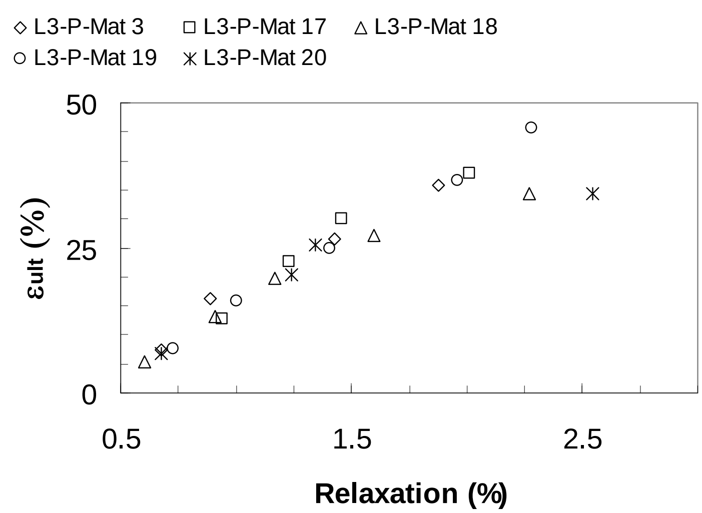

(c) Location 3 of Figure B9

Figure 3.6 - Strain Relaxation Behavior for Geometry 9 (Pine)

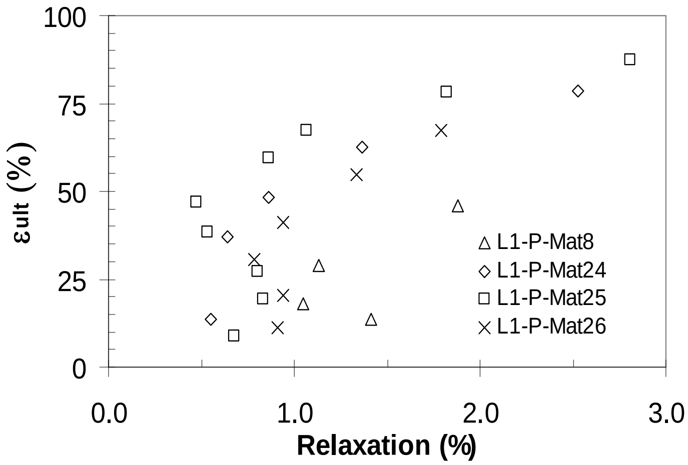

(a) Location 1 of Figure B10

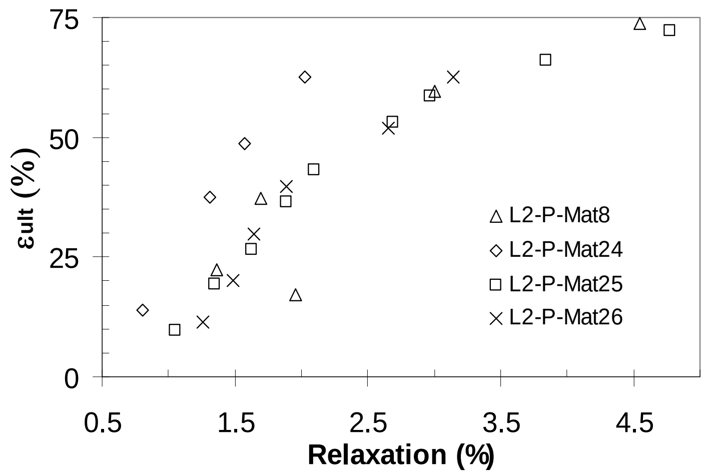

(b) Location 2 of Figure B10

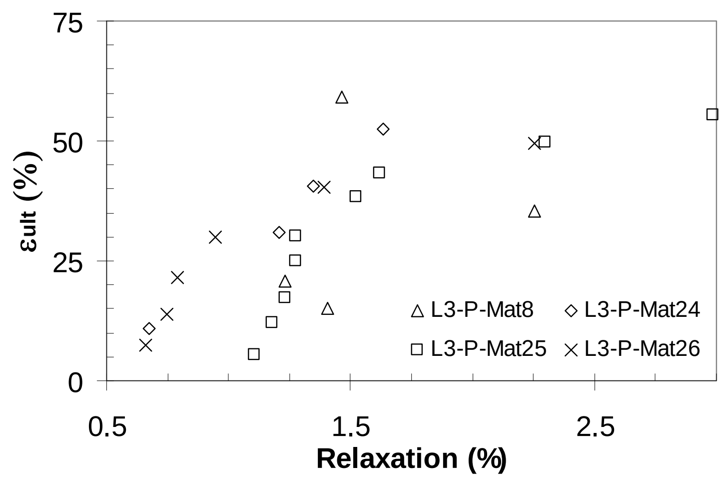

(c) Location 3 of Figure B10

Figure 3.7 - Strain Relaxation Behavior for Geometry 10 (Pine)

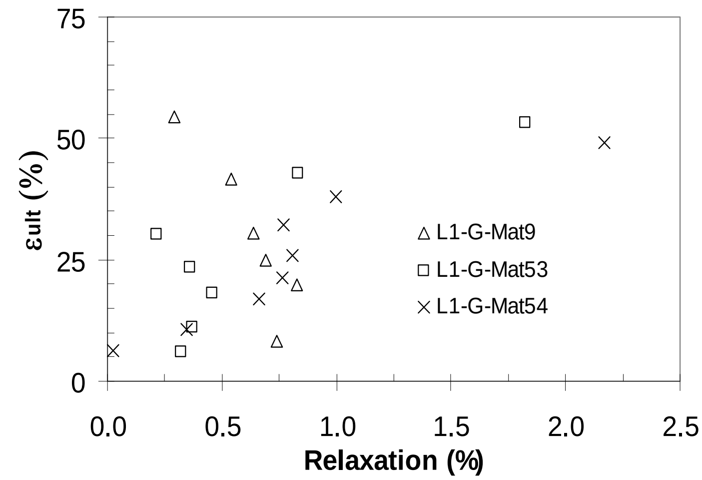

(a) Location 1 of Figure B11

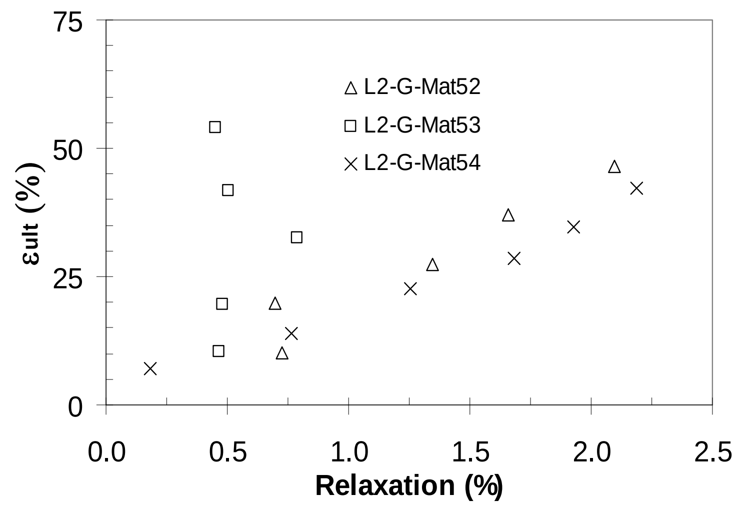

(b) Location 2 of Figure B11

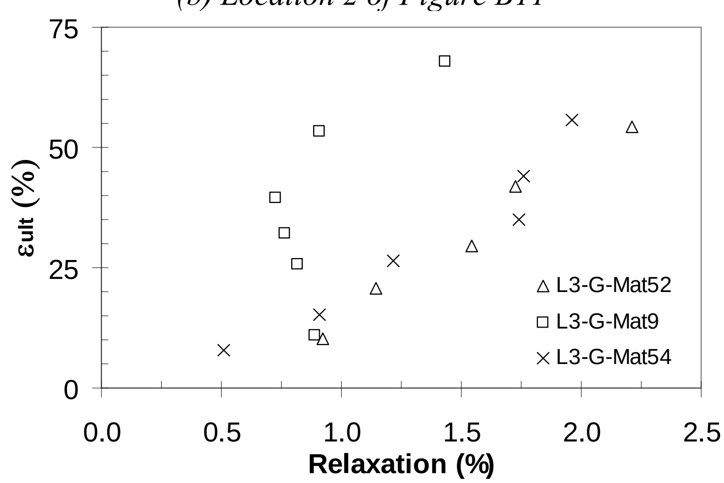

(c) Location 3 of Figure B11

Figure 3.8 - Strain Relaxation Behavior for Geometry 10 (Gum)

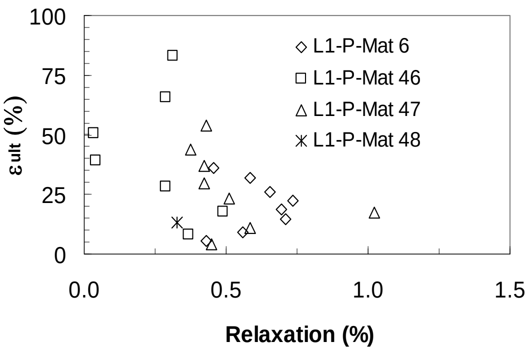

(a) Location 1 of Figure B12

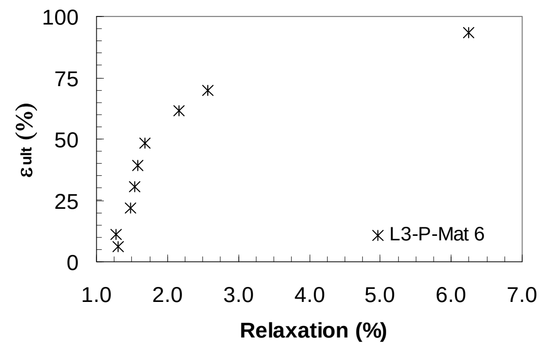

(b) Location 3 of Figure B12

Figure 3.9 - Strain Relaxation Behavior for Geometry 11 (Pine)

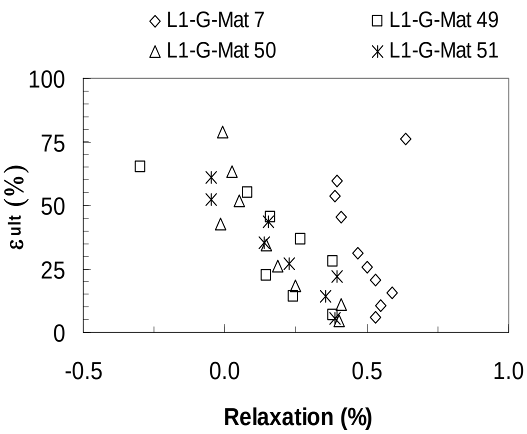

(a) Location 1 of Figure B13

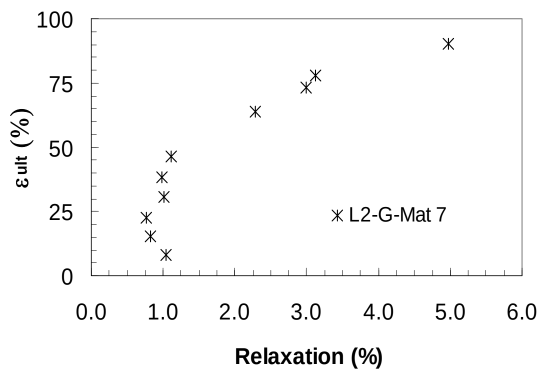

(b) Location 2 of Figure B13

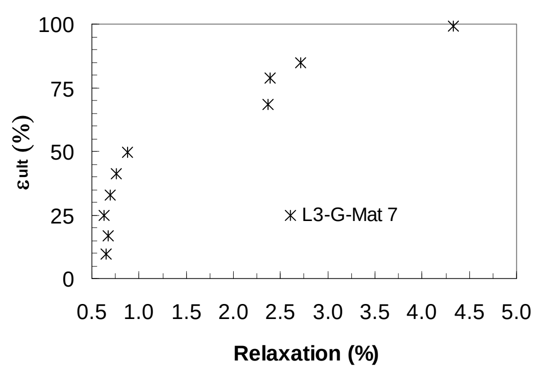

(c) Location 3 of Figure B13

Figure 3.10 - Strain Relaxation Behavior for Geometry 11 (Gum)

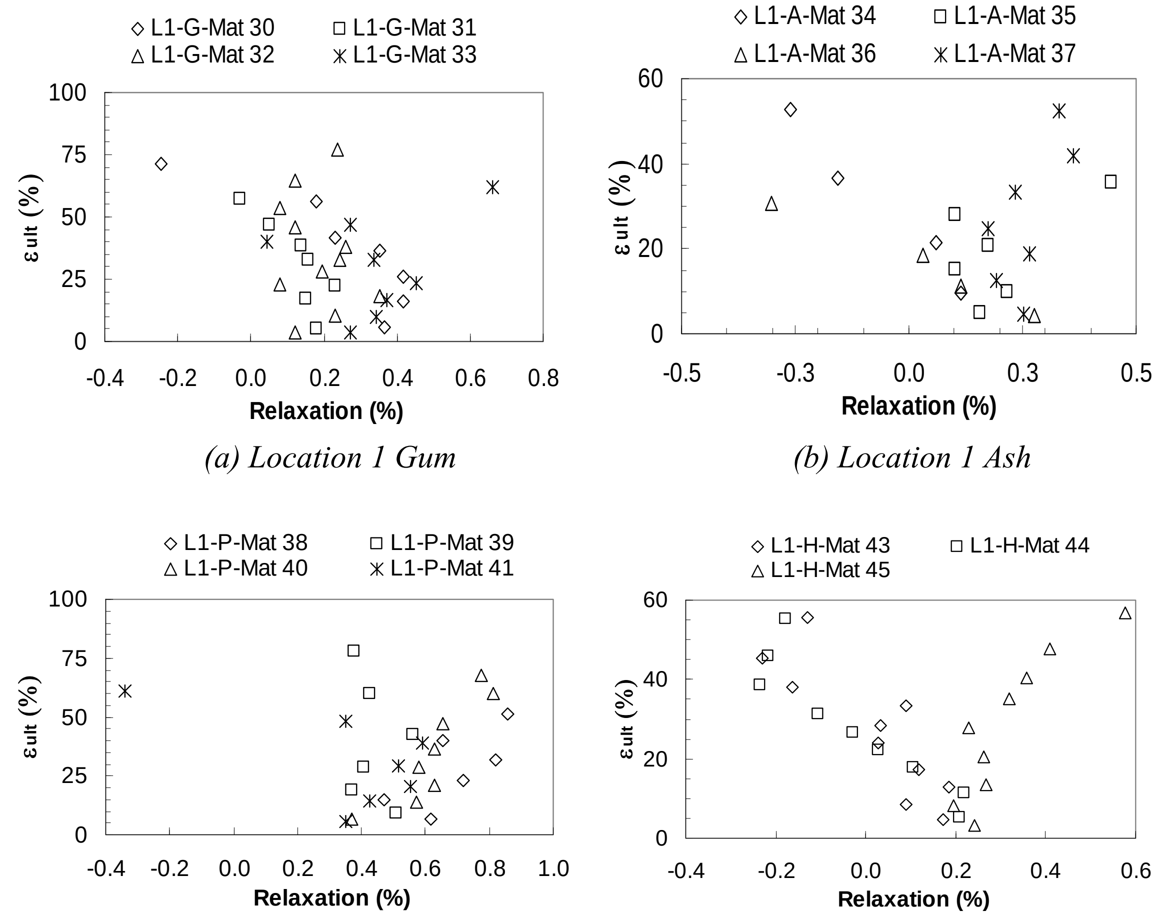

(a) Location 1 Gum *(b) Location 1 Ash*

(c) Location 1 Pine *(d)Location 1 Hickory*

Figure 3.11 - Strain Relaxation Behavior for Geometry 12

3.4.2 Full Scale Strain Results

Complete strain plots can be found in Appendix D. Table 3.10 provides the peak strains recorded during full scale testing. Note that recording a true peak strain is often difficult since malfunction (particularly delamanation) is very likely as failure approaches. The values were recorded in the center of the mat at the bottom.

Table 3.10 - Summary of Full Scale Maximum Strain Results

G*	Wood	Mats	Maximum Strain
14	Pine	55	7275
15	Pine	56, 57	6034
16	Pine	58, 59, 60, 61	4595
17	Pine	62	6819
18	Pine	63	1776

** G = Geometry*

The strain relaxation of the full scale mats when held at a fixed position for 1 min was performed in the same manner as with the prototype mats discussed previously. Since the strain plots were reasonably repeatable and measured strain in practically the same location, all data from a given mat geometry were averaged and used to develop the plot. The results can be seen in Figure 3.12. As seen, two distinct zones of data are observed. Geometries 16 and 18 relaxed significantly more than the others. Note that both are of the stacked ply configuration seen in Appendix A. Based on the limited information in the report, Geometry 18 does not appear to be a highly performing design.

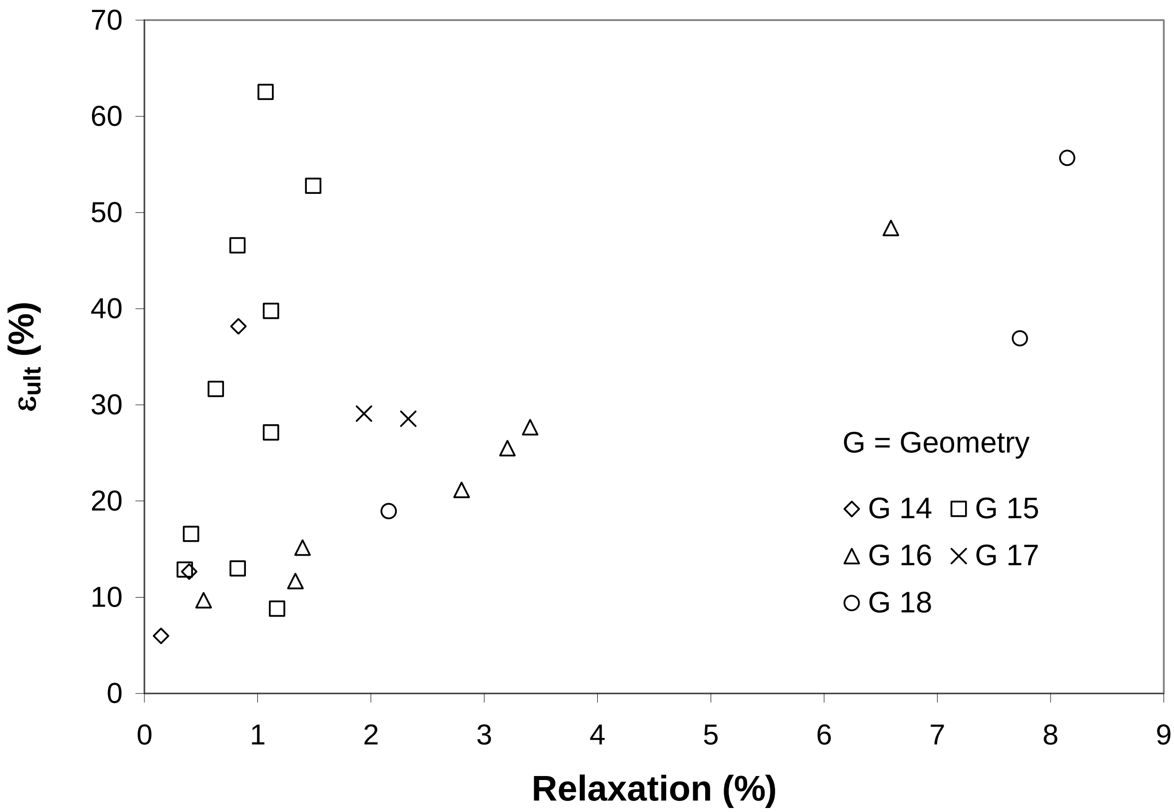

Figure 3.12 – Strain Relaxation for Full Scale Mats

3.5 Load Relaxation Results

3.5.1 Prototype Load Relaxation Behavior

Load relaxation of the prototype mats was calculated in the same manner as strain relaxation except that load versus time plots of Appendix C were used instead of strain versus time plots of Appendix D. The procedure is straightforward and is therefore not repeated. Note that geometries 1 and 13 have no relaxation data. The results can be seen in Figures 3.13 through 3.22.

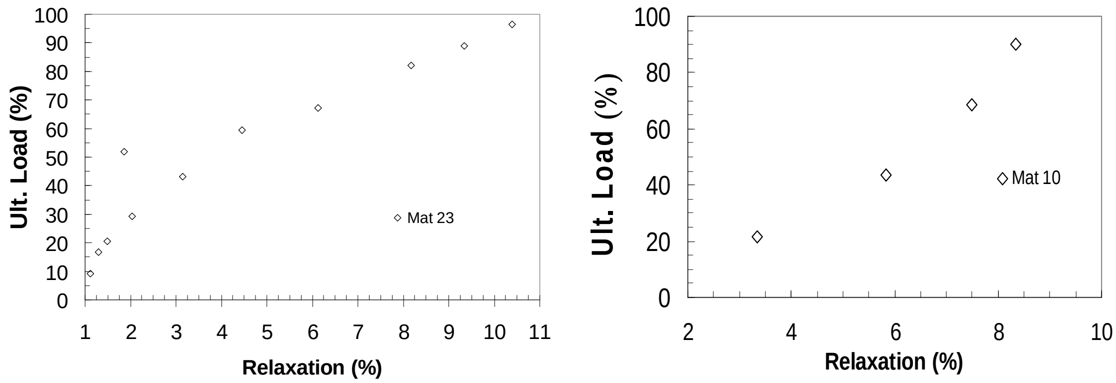

(a) Mat 23

(b) Mat 10

Figure 3.13 - Load Relaxation Behavior for Pine Mats Tested Without Replication

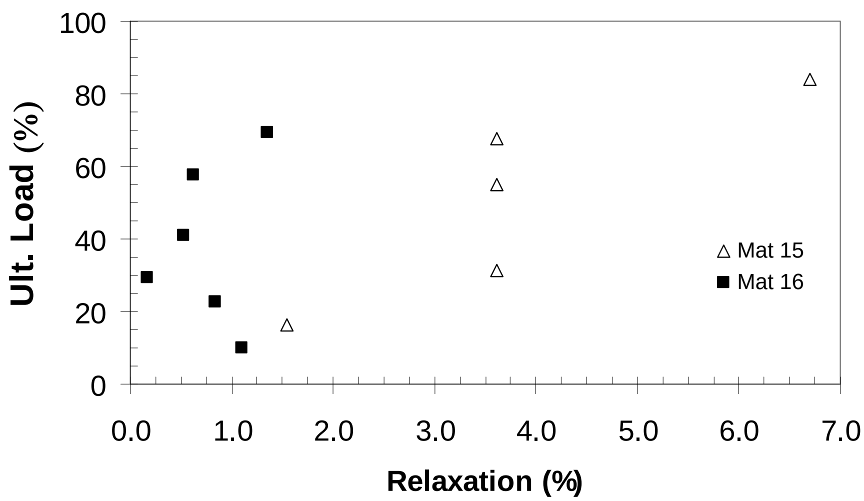

Figure 3.14 - Load Relaxation Behavior for Geometry 4

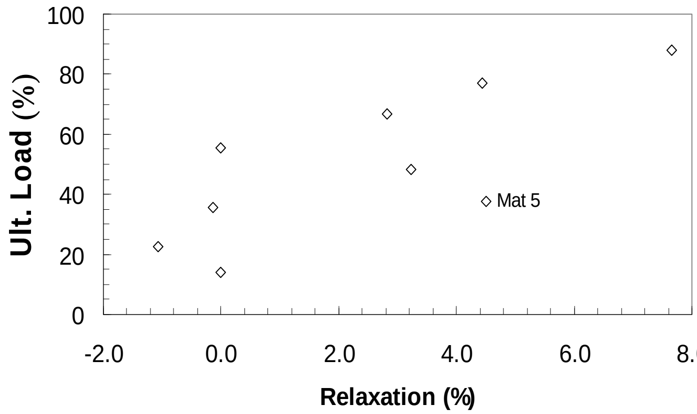

Figure 3.15 - Load Relaxation Behavior for Geometry 5

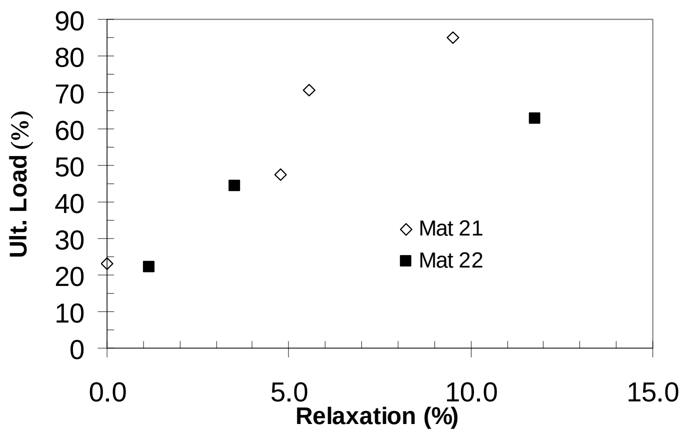

Figure 3.16 - Load Relaxation Behavior for Geometry 6

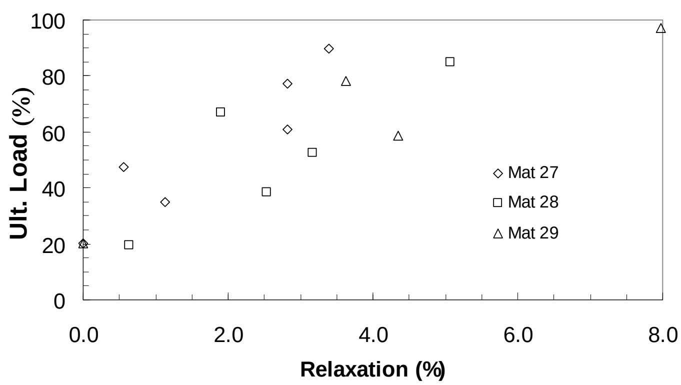

Figure 3.17 - Load Relaxation Behavior for Geometry 7

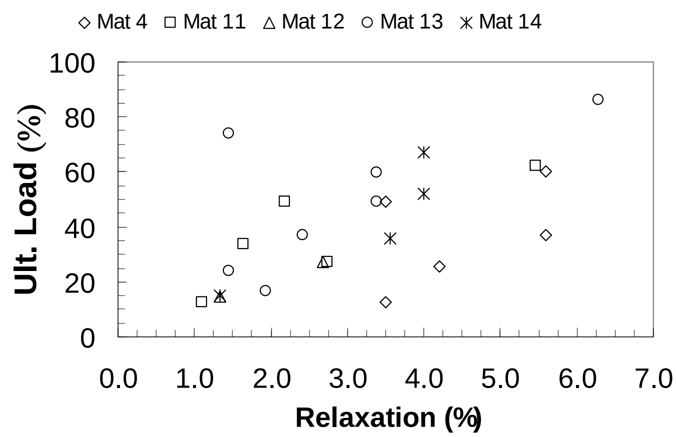

Figure 3.18 - Load Relaxation Behavior for Geometry 8

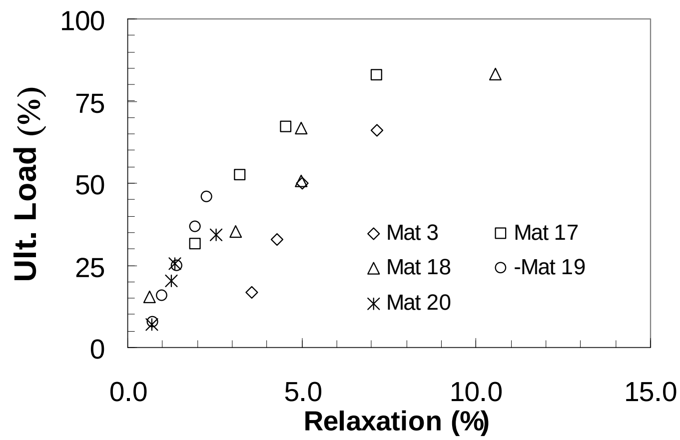

Figure 3.19 - Load Relaxation Behavior for Geometry 9

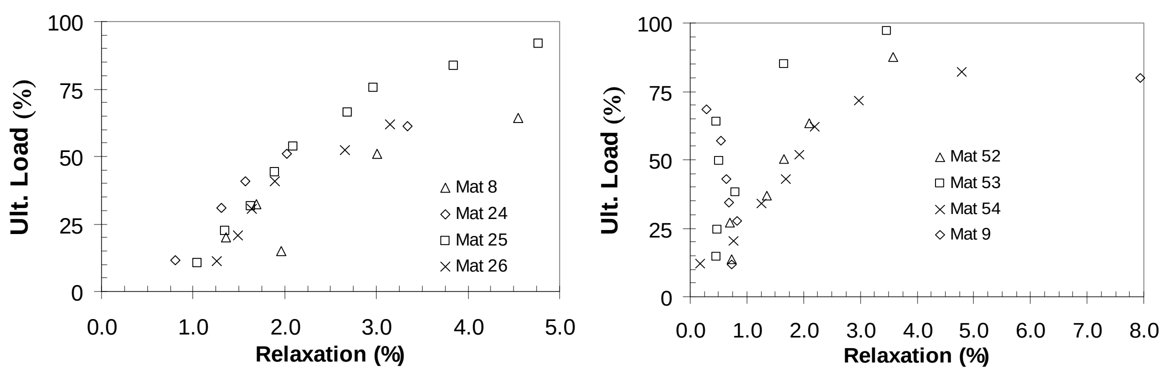

(a) Pine *(b) Gum*

Figure 3.20 - Load Relaxation Behavior for Geometry 10

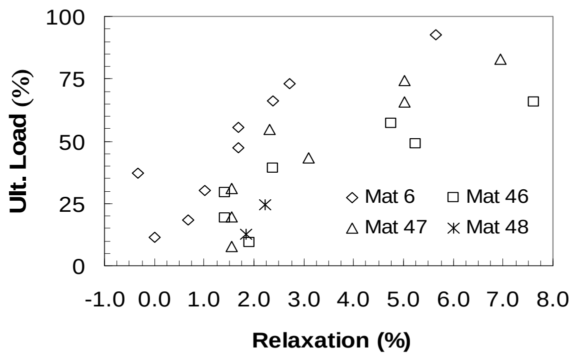

(a) Pine

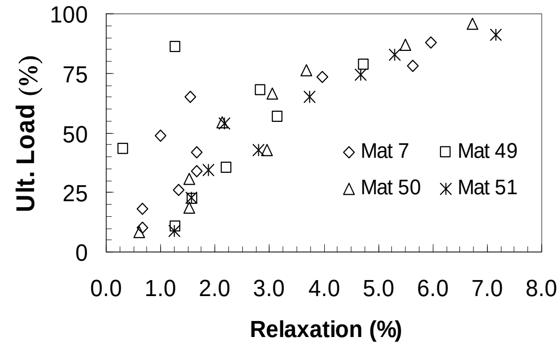

(b) Gum

Figure 3.21 - Load Relaxation Behavior for Geometry 11

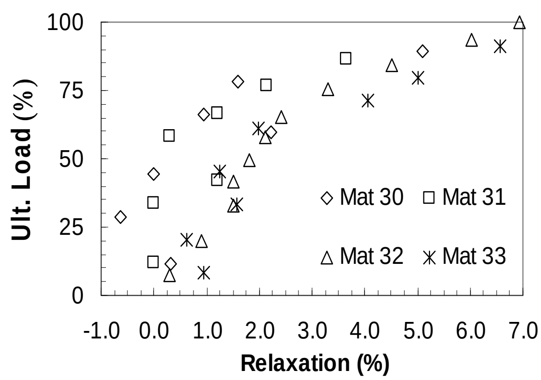

(a) Pine

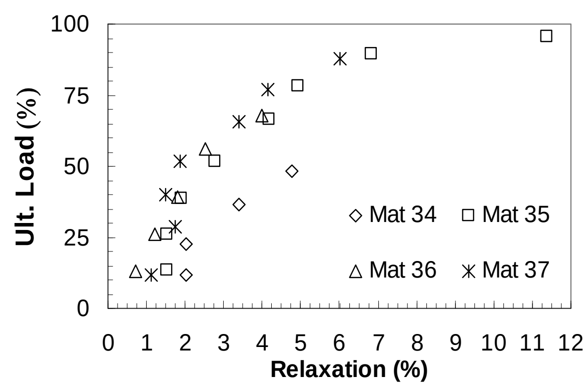

(b) Gum

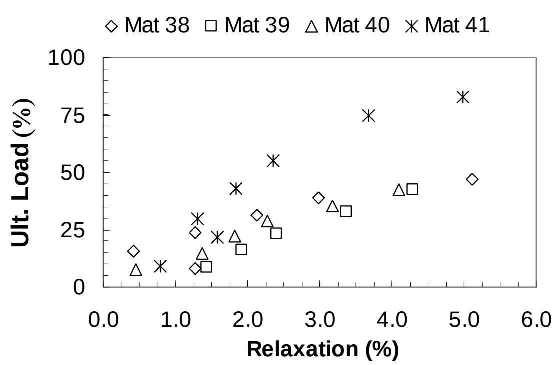

(a) Ash

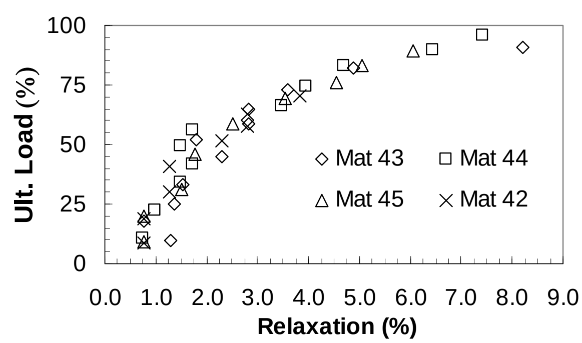

(b) Hickory

Figure 3.22 - Load Relaxation Behavior for Geometry 12

3.5.2 Full Scale Load Relaxation Results

No data was obtained pertaining to full scale load relaxation behavior. Logistics during testing, schedules of testing equipment, and similar made this impractical. However, the load relaxation behavior of the prototype mats appears reasonable.

3.6 Discussion of Failure Mechanisms and Mechanics Calculations

3.6.1 Prototype Stress and Strain Calculations

Standard bending theory was used to determine if it were capable of predicting the failure location of the mats by adjusting the geometric properties with position along the mat. The standard equation of flexural bending is seen in Eq. 3.3.

$$\sigma = \frac{Mc}{I} \tag{3.3}$$

Where,

σ = bending stress
c = distance from outermost fiber to neutral axis
I = moment of inertia at cross section being evaluated

The results of the calculations can be seen in Tables 3.11 to 3.13. Terminology used in the tables is as follows: $\boldsymbol{\sigma_c}$ is the maximum calculated stress at any location within the mat; $\boldsymbol{\sigma_f}$ is the stress calculated at the location of failure of the mat. Note the location of failure was determined by visual observation at the conclusion of testing and by ascertaining where the most damage occurred. This should be considered somewhat approximate since failure could initiate at on location and subsequently cause failure to progress throughout the mat.

As seen in the tables, the surface slats were accounted for in one set of calculations as fully resisting bending, while they were neglected entirely in the other set of calculations for mats that contained surface slats. Neither condition is true, rather the result would be expected to lie between the two extremities. With the information available, the approach was adequate for the current needs.

It can be seen that in many cases the mats broke at precisely the location predicted by Eq. 3.3. On other occasions, there was a difference in maximum stress and the failure location. In general, the results indicate that a combination of bending theory and testing of mats constructed with the target materials and procedures to be used is desirable. This is much more pronounced for mats constructed with surface slats. The mats constructed without surface slats, in general, were more accurately predicted using standard bending theory.

Geometry 12 provides a good set of data with which to analyze in terms of bending theory. The gum mats exceeded the Table 2.4 *MOR* values, the pine mats were below their *MOR* values, the ash mats were substantially below their *MOR* values, and the hickory mats exceeded their *MOR* values by noticeable amounts. The data also shows that the surface slats appeared to have a noticeable effect on the bending resistance. Take, for example, geometry 11 and 12 gum mats. The values of geometry 11 with slats considered in the calculations had $\boldsymbol{\sigma_c}$ values on the order of the geometry 12 mats. A reasonable, yet more sporadic, trend also exists in the pine mats. Finally, it should be noted that when surface slats are not considered on the mats that contain the slats, the $\boldsymbol{\sigma_c}$ values are often much higher than *MOR* and do not align with the geometry 12 findings were there was a moderate amount of repetition. Based on limited data, it appears the slats provide noticeable bending resistance.

Table 3.11 - Calculated Maximum Stress vs. Stress at Failure Location, US Units

Geometry	Wood	Mat	σ_c (ksi) w/ slats	σ_c (ksi) w/o slats	σ_f (ksi) w/ slats	σ_f (ksi) w/o slats
1	Pine	1	8.1	11.7	7.8	11.2
2	Pine	23	----	10.1	----	6.1
3	Pine	10	5.1	20.6	4.5	17.8
4	Pine	15	9.5	16.9	8.2	14.6
		16	9.0	16.0	6.5	11.5
5	Pine	5	10.5	18.6	5.2	9.3
6	Pine	21	8.9	15.8	5.3	9.5
		22	6.0	10.7	5.1	9.0
7	Pine	27	12.5	22.2	12.5	22.2
		28	11.2	19.8	11.2	19.8
		29	9.9	17.6	9.9	17.6
8	Pine	4	6.0	10.7	6.0	10.7
		11	6.4	11.4	6.4	11.4
		12	9.6	17.0	9.6	17.0
		13	8.7	15.5	8.7	15.5
		14	9.6	17.1	9.6	17.1
9	Pine	3	8.4	14.9	5.9	10.5
		17	9.3	16.5	6.1	10.9
		18	9.7	17.2	6.4	11.3
		19	9.7	17.3	6.9	12.2
		20	9.1	16.2	6.4	11.4
10	Pine	8	10.8	19.3	5.9	10.5
		24	11.2	19.9	6.1	10.8
		25	15.7	27.8	8.5	15.1
		26	10.8	19.3	5.9	10.5
10	Gum	9	11.4	20.2	11.4	20.2
		52	12.7	22.5	6.9	12.2
		53	13.1	23.2	7.1	12.6
		54	13.1	23.3	7.1	12.6
11	Pine	6	12.4	22.1	10.8	19.2
		46	8.6	15.7	3.2	5.8
		47	10.9	19.4	7.7	13.7
		48	11.5	20.4	11.5	20.4
11	Gum	7	12.8	22.7	12.8	22.7
		49	13.4	23.8	13.4	23.8
		50	13.8	24.5	13.8	24.5
		51	13.5	24.1	13.5	24.1
12	Pine	38	----	9.9	----	9.9
		39	----	8.8	----	8.2
		40	----	9.4	----	8.8
		41	----	16.1	----	16.1
12	Gum	30	----	13.2	----	11.5
		31	----	13.9	----	12.9
		32	----	14.8	----	13.8
		33	----	13.5	----	6.8
12	Ash	34	----	6.2	----	6.2
		35	----	10.8	----	9.4
		36	----	11.6	----	10.9
		37	----	11.2	----	10.4
12	Hickory	42	----	16.5	----	15.4
		43	----	16.5	----	15.4
		44	----	17.3	----	16.1
		45	----	16.7	----	15.6
13	Pine	2	7.8	13.8	7.763	13.8

Table 3.12 - Calculated Maximum Stress vs. Stress at Failure Location, SI Units

			σ_c (MPa)		σ_f (MPa)	
Geometry	**Wood**	**Mats**	**w/ slats**	**w/o slats**	**w/ slats**	**w/o slats**
1	Pine	1	56.0	80.7	53.6	77.2
2	Pine	23	----	69.6	----	41.8
3	Pine	10	35.5	141.9	30.7	122.9
4	Pine	15	65.7	116.8	56.7	100.8
		16	62.0	110.2	44.6	79.2
5	Pine	5	72.1	128.2	36.0	64.1
6	Pine	21	61.3	109.0	36.6	65.1
		22	41.4	73.6	35.0	62.2
7	Pine	27	86.2	153.1	86.2	153.2
		28	76.9	136.7	76.9	136.7
		29	68.1	121.2	68.1	121.2
8	Pine	4	41.6	73.9	41.6	73.8
		11	44.1	78.4	44.1	78.4
		12	65.9	117.3	65.9	117.3
		13	60.2	106.9	60.2	106.9
		14	66.3	117.8	66.3	117.8
9	Pine	3	57.7	102.5	40.7	72.3
		17	63.8	113.5	42.1	74.7
		18	66.7	118.6	43.9	78.1
		19	67.1	119.4	47.4	84.2
		20	62.6	111.3	44.2	78.5
10	Pine	8	74.9	133.3	40.6	72.1
		24	77.0	136.9	41.7	74.1
		25	107.9	191.8	58.4	103.7
		26	74.9	133.3	40.6	72.1
10	Gum	9	78.3	139.1	78.3	139.1
		52	87.3	155.2	47.2	83.9
		53	90.1	160.1	48.7	86.6
		54	90.2	160.4	48.8	86.7
11	Pine	6	85.7	152.4	74.3	132.1
		46	61.0	108.5	22.4	39.8
		47	75.3	133.8	52.9	94.0
		48	78.9	140.4	78.9	140.4
11	Gum	7	87.9	156.4	87.9	156.4
		49	92.1	163.8	92.1	163.8
		50	95.0	168.9	95.0	168.9
		51	93.3	165.9	93.3	165.9
12	Pine	38	----	68.3	----	68.3
		39	----	60.5	----	56.4
		40	----	64.8	----	60.5
		41	----	110.7	----	110.7
12	Gum	30	----	91.3	----	79.1
		31	----	95.6	----	89.3
		32	----	102.0	----	95.2
		33	----	93.0	----	46.5
12	Ash	34	----	42.7	----	42.7
		35	----	74.4	----	64.5
		36	----	80.2	----	74.8
		37	----	77.0	----	71.9
12	Hickory	42	----	113.9	----	106.3
		43	----	113.4	----	105.8
		44	----	118.8	----	110.9
		45	----	115.1	----	107.4
13	Pine	2	53.5	95.1	53.5	95.1

Table 3.13 - Difference in Calculated Maximum Stress and Failure Location Stress

			$\sigma_c - \sigma_f$ (ksi)		$\sigma_c - \sigma_f$ (MPa)	
Geometry	**Wood**	**Mats**	**w/ slats**	**w/o slats**	**w/ slats**	**w/o slats**
1	Pine	1	0.35	0.51	2.44	3.51
2	Pine	23	----	4.04	----	27.85
3	Pine	10	0.69	2.75	4.73	18.91
4	Pine	15	1.31	2.33	9.03	16.07
		16	2.53	4.50	17.44	31.01
5	Pine	5	5.23	9.30	36.05	64.08
6	Pine	21	3.59	6.38	24.71	43.93
		22	0.92	1.64	6.36	11.31
7	Pine	27	0	0	0	0
		28	0	0	0	0
		29	0	0	0	0
8	Pine	4	0	0	0	0
		11	0	0	0	0
		12	0	0	0	0
		13	0	0	0	0
		14	0	0	0	0
9	Pine	3	2.46	4.38	16.98	30.17
		17	3.16	5.62	21.79	38.74
		18	3.31	5.88	22.78	40.49
		19	2.87	5.10	19.76	35.13
		20	2.67	4.76	18.42	32.76
10	Pine	8	4.99	8.88	34.40	61.17
		24	5.13	9.12	35.35	62.84
		25	7.19	12.78	49.53	88.05
		26	4.99	8.88	34.40	61.17
10	Gum	9	0	0	0	0
		52	5.82	10.34	40.08	71.25
		53	6.00	10.67	41.33	73.50
		54	6.01	10.68	41.40	73.60
11	Pine	6	1.66	2.95	11.43	20.33
		46	5.61	9.98	38.66	68.73
		47	3.25	5.78	22.39	39.79
		48	0	0	0	0
11	Gum	7	0	0	0	0
		49	0	0	0	0
		50	0	0	0	0
		51	0	0	0	0
12	Pine	38	----	0	----	0
		39	----	0.59	----	4.03
		40	----	0.63	----	4.32
		41	----	0	----	0
12	Gum	30	----	1.77	----	12.17
		31	----	0.93	----	6.38
		32	----	0.99	----	6.80
		33	----	6.75	----	46.51
12	Ash	34	----	0	----	0
		35	----	1.44	----	9.92
		36	----	0.78	----	5.35
		37	----	0.75	----	5.14
12	Hickory	42	----	1.10	----	7.60
		43	----	1.10	----	7.56
		44	----	1.15	----	7.93
		45	----	1.11	----	7.67
13	Pine	2	0	0	0	0

Hooke's Law (Eq. 3.4) was used to determine if the measured strains at failure resembled the predicted values using the properties of Table 2.4.

$$\varepsilon = \frac{\sigma}{\mathrm{E}} \tag{3.4}$$

Where,

ε = strain
σ = stress
E = Young's Modulus

Substitution of Table 2.4 *MOR* values for σ and *MOE* values for E results in the $\boldsymbol{\varepsilon_f}$ values in Table 3.14. They are determined for a material that behaves Hooke's law until failure. Note wood does not typically perform in this fashion to failure, but the assumption was made for this analysis. The maximum strain recorded for the given wood type was extracted from Table 3.9 and shown as $\boldsymbol{\varepsilon_{max}}$.

Table 3.14 – Estimated Failure Strains

Material	ε_f	ε_{max}	$\varepsilon_{max}/\varepsilon_f$
White Ash	8,620	16,586	1.92
Sweetgum	7,620	13,925	1.83
Hickory-Pecan	7,920	17,876	2.26
Southern Pine	7,470	13,379	1.79

It is evident from Table 3.14 that the materials do not remain linear until failure, at least at some locations within the mats. Information of this nature can be used to set acceptable limits of loading to avoid plastic strains from occurring. This should be used in conjunction with probabilistic analysis procedures.

3.6.2 Full Scale Stress and Strain Calculations

All full scale mats with the exception of 56 and 57 experienced glue line failures due to shear forces. The modulus of rupture of the full scale mats can be seen in Table 3.15. As can be clearly seen, most of the mats did not come close to the *MOR* of pine seen in Table 2.4. This indicates an inefficient use of material in many of the mats for bending applications.

Table 3.15 – Full Scale Modulus of Rupture (*MOR*) Results

G*	Wood	Mats	***MOR*-MPa** (***Mean Value***)	***MOR*-10^3*psi** (***Mean Value)***
14	Pine	55	18.23 ***(18.3)***	2.65 ***(2.65)***
15	Pine	56, 57	58.1, 60.5 ***(59.3)***	8.43, 8.78 ***(8.61)***
16	Pine	58, 59, 60, 61	18.3, 22.1, 16.0, 17.8 ***(18.6)***	2.65. 3.20, 2.32, 2.59 ***(2.69)***
17	Pine	62	10.3 ***(10.3)***	1.50 ***(1.50)***
18	Pine	63	10.1 ***(10.1)***	1.46 ***(1.46)***

** G = Geometry*

CHAPTER 4-CONCLUSIONS AND RECOMMENDATIONS

4.1 Summary and Conclusions

Table 4.1 summarizes all prototype data collected during testing. The strain and load relaxation plots were summarized by a single range of values as seen in Table 4.1. For strain, the location where the maximum value was measured was used in the assessment. Note this is not a comprehensive evaluation of the data. Much more information could be learned by additional analysis of the plots.

Table 4.1 - Summary of Prototype Mat Properties

			Mean and/or Representative Values Used						
G[1]	**Wood**	**Mats**	**Strength kN (lb)**	**Density kN/m^3 (pcf)**	***S/D*** **m^3 (ft^3)**	**Def (Δ)[2] mm (in^{-3})**	**Strain (ε)[2]**	**ε_R[3]**	**L_R[4]**
7	Pine	27,28,29	10.56 (2375)	4.85 (30.8)	2.18 (77.0)	11.5 (452)	7436	(1) 1.5-9.0	0.0-5.0
8	Pine	4,11,12,13,14	12.77 (2870)	5.35 (34.0)	2.39 (84.5)	13.0 (512)	13294	(2) 1.0-25.0	1.0- 6.3
9	Pine	3,17,18,19,20	10.30 (2316)	4.91 (31.2)	2.10 (74.3)	14.1 (555)	10388	(1) 10-37.0	0.8-10.5
10	Pine	8,24,25,26	13.56 (3049)	5.24 (33.3)	2.59 (91.6)	13.3 (524)	6970	(2) 1.0-4.5	0.8- 4.8
10	Gum	9,52,53,54	14.01 (3149)	5.32 (33.8)	2.63 (93.1)	15.1 (593)	12733	(2) 0.3-2.3	0.3-5.0
11	Pine	6,46,47,48	17.28 (3884)	6.15 (39.1)	2.81 (99.3)	13.8 (545)	12515	(3) 1.3-6.3	0.0-7.8
11	Gum	7,49,50,51	21.15 (4754)	6.51 (41.4)	3.25 (115.0)	14.8 (584)	12406	(2) 1.0-5.0	0.3-7.3
12	Pine	38,39,40,41	17.46 (3926)	5.91 (37.5)	2.96 (104.6)	13.2 (519)	10843	(1) -0.4-0.8	0.0-7.0
12	Gum	30,31,32,33	21.92 (4928)	6.57 (41.8)	3.33 (117.9)	13.5 (530)	13925	(1) -0.3-0.7	0.8-7.0
12	Ash	34,35,36,37	15.75 (3540)	6.45 (41.0)	2.44 (86.3)	12.2 (480)	16586	(1) -0.3-0.5	0.5 -5.0
12	Hickory	42,43,44,45	26.47 (5951)	7.96 (50.6)	3.32 (87.0)	17.5 (688)	17876	(1) -0.2-0.6	0.8-8.0

1: G = Geometry
*2: Maximum Strain (**ε**) and Deflection (Δ) Values Shown.*
3: Maximum Relaxation (R) Range for Strain (ε). The Location Used in Shown in Parenthesis.
4: Maximum Relaxation (R) Range for Load (L).

Geometries 7 to 12 were the only prototype mats tested with sufficient repetition to make comparative assessments. As a result, they are the only values shown in Table 4.1. Table 4.2 ranks these mat geometry configurations in terms of each property evaluated.

As seen the solid geometries (11 and 12) out performed the others in terms of S/D ratio. For very high strength applications where the majority of loading is along the primary direction, this configuration appears superior in terms of the properties evaluated. However, additional analysis where material is removed from the solid configuration while still allowing acceptable strength and stiffness could be valuable. Adaptations of geometries 7 to 10 would be worthwhile for lower strength applications, while geometry (11 or 12) would appear superior in high strength and stiffness applications. Having two configurations similar in overall manufacture yet having different end uses would seem desirable.

Based on availability and performance, gum and pine appear to be the most promising materials. Ash did not perform well and based on these limited results should be abandoned. Supply of hickory could be a concern and its properties were not such that gun couldn't be used instead.

Note that deflection, strain, and relaxation behaviors were ranked from the highest to the lowest value. This would be application dependent. For example, working over soft soil would be an application where less deflection would be more desirable. However, in any application more deflection to mat failure (for a given stiffness) is a desirable behavior (i.e.

ductility), and was used in the ranking. The reader is cautioned not to confuse deflection to failure with stiffness. At any given load, less deflection is almost always desirable, but for a given stiffness additional deflection to failure provides more ductility. Prototype stiffness was not evaluated in this report.

Table 4.2 - Rankings of Prototype Performance in Terms of All Properties

			Ranking (1 = Best Ranking)						
G[1]	Wood	Mats	Strength	Density[2]	*S/D*	Deflection (Δ)[3]	Strain (ε)[3]	ε_R[4]	L_R[5]
7	Pine	27, 28, 29	10	1	10	11	10	3	8
8	Pine	4, 11,12, 13, 14	9	5	9	9	4	2	7
9	Pine	3, 17, 18, 19, 20	11	2	11	4	9	1	1
10	Pine	8, 24, 25, 26	8	3	7	7	11	6	11
10	Gum	9, 52, 53, 54	7	4	6	2	5	7	9
11	Pine	6, 46, 47, 48	5	7	5	5	6	4	2
11	Gum	7, 49, 50, 51	3	9	3	3	7	5	4
12	Pine	38, 39, 40, 41	4	6	4	8	8	8	5
12	Gum	30, 31, 32, 33	2	10	1	6	3	9	6
12	Ash	34, 35, 36, 37	6	8	8	10	2	11	10
12	Hickory	42, 43, 44, 45	1	11	2	1	1	10	3

1: G = Geometry
2: Lowest Density Ranked 1
3: Maximum Deflection Ranked 1. Maximum Strain Also Ranked 1. Could vary with application
4: Relaxation (R) Ranking for Strain (ε). Table 4.1 Ranges Used for Ranking
5: Relaxation (R) Ranking for Load (L). Table 4.1 Ranges Used for Ranking

The glue lines in the prototype materials, in general, performed very well. Geometry 3 experienced shear failure. Prototype mats with glue lines on the exterior members showed no signs of initiating failure and based on the testing performed in this program it is not recommended to take special precautions to ensure the but joints are interior to the mat. Failures of the prototype mats were, in general, observed to occur across a large portion of the transverse direction. This indicates the mats were carrying load in a relatively uniform fashion and did not fail as a result of an isolated area that was defective. The two most common areas of failure were the specimen centerline and the intersection of continuous lateral wooden area and slotted lateral wooden area. These two locations are not surprising. Full scale mats failed either in tension at the center of the mat (geometry 15) or due to shear failure at the glue lines (all other geometries).

No adverse behaviors were observed adjacent to butt joints in prototype testing. However, no but joints existed without surface slats. As seen in full scale testing, butt joints can cause problems as evidenced by the very low strength of geometry 17. Provided no financial, logistical, or other advantages can be obtained this behavior should be avoided at several locations in the same cross section (even when initial strength is not compromised).

Full scale strength, stiffness, and *S/V* ratios were far superior in geometry 15, which was similar in design to prototype geometry 12. For general use, geometry 16 appears to have promise provided increased shear resistance can be obtained. Evaluating versions of geometry 15 with material removed could prove worthwhile for operations moving primarily in the longitudinal direction (i.e. pipeline construction). Geometry 16 has conceptual application for light duty work where loads could be applied in both directions.

In general, the proportional limit of many woods is on the order of two thirds of the ultimate stress. Stress is proportional to strain below proportional limit and as a result the lower the strain the further from the proportional limit. Wood is much more prone to time dependent creep behavior above the proportional limit. All other parameters being equal, the more relaxation that occurs per unit time the lower the strain (and stress), and consequently a reduced creep potential. However, in an actual mat all parameters do not necessarily remain equal. Mats that are prone to high relaxation could also be prone to higher creep than a mat prone to low relaxation. These behaviors are likely driven by the properties of the glue and the geometry/construction of the mat.

The relaxation data included in the report should be interpreted in the context in which it was created, especially above the proportional limit. Typically, wood will increase its deflection under a sustained and constant load. The sustained testing portion of this current program, however, was performed by maintaining a constant load head position for a relatively short period of time. Note that continued deformation would occur if creep behaviors exceeded relaxation behaviors over the same period of time. During the initial periods tested, the materials relaxed, but more test durations over sustained periods of time are needed to fully capture the time dependent behaviors. The data provided is, in no way, a creep test.

4.2 Recommendations

Testing of mats that have been aged by a combination of temperature and moisture is recommended to establish durability and sustainability of the materials and geometric configurations. Testing of the creep and relaxation behavior of the mats over soft soils for prolonged periods of time is also recommended. Instrumenting the subgrade with pressure cells and the mats with strain gages would provide an excellent means to assess the ability of the full scale mats to handle loads such as a crane being parked on a mat overnight.

Numerical simulations of the mats would be an excellent mechanism to extend the results of testing and provide design guidance. Finite element or finite difference techniques would be excellent choices. Finally, using the data in the report alongside additional information to develop design procedures would be worthwhile. The design could then be tested and/or tweaked with products developed to meet the material and loading specifications.

CHAPTER 5 – REFERENCES

Anon. (1961). "*Chloe* Pipeline Laid in Louisiana," *Petroleum Management,* Vol. 33, No. 9, pp. 248-249.

Beavers, J.E., Moore, J.R., Rinehart, R., and Schriver, W.R. (2006). "Crane-Related Fatalities in the Construction Industry," *Journal of Construction Engineering and Management,* Vol. 132, No. 9, pp. 901-910.

Franklin, J.M., Taylor, S.E., Morgan, P.A., and Ritter, M.A. (1999). "Design Criteria for Portable Timber Bridge Systems: Static versus Dynamic Loads," Presented July 18-21 in Toronto, Canada, Paper No. 99-4208 ASAE, pp. 21.

Hislop, L.E. (1996). *Improving Access and Environmental Sensitivity With Portable Surfaces on Low Volume Roads*. United States Department of Agriculture, 9624 1211-SDTDC.

Hislop, L.E. (1996a). "Portable Surfaces for Crossing Unstable Roadbeds," *National Conference on Wood Transportation Structures,* Oct 23-25, Madison, WI, pp. 138-144.

Kestler, M.A., Shoop, S.A., Henry, K.S., Stark, J.A., and Affleck, R.T. (1999). *Rapid Stabilization of Thawing Soils for Enhanced Vehicle Mobility: A Field Demonstration Project.* US Army Corps of Eng., CRREL Report 99-3, pp. 80.

Mason, L.E., and Greenfield, P.H. (1995). "Portable Crossings for Weak Soil Areas and Streams," *Transportation Research Record, Journal of the Transportation Research Board,* No. 1504, pp. 118-124.

Wipf, T.J., Ritter, M.A., and Wood, D.L. (1996) "Dynamic Evaluation of Timber Bridges," *National Conference on Wood Transportation Structures,* Oct 23-25, Madison, WI, pp. 114-121.

Santoni, R.L., Smith, C.J., Tingle, J.S., and Webster, S.L. (2001). *Expedient Road Construction Over Soft Soils.* US Army Corps of Engineers, ERDC/GSL TR-01-7, pp. 107.

Schweitzer, L., and Marinello, S. (1996). "Do Heavy Construction in Fragile Wetland With Hardwood Mat Systems," *Electrical World*, Vol. 210, No. 12, pp. 25-26.

Wood Handbook (1999) *Wood Handbook: Wood as an Engineering Material.* General Technical Report 113, US Dept of Agriculture, Madison, WI, pp. 463.

APPENDIX A- PHOTOS OF MAT GEOMETRIES INSTRUMENTATION AND TESTING

Figure A1. Mat Geometry 1

Figure A2. Mat Geometry 2

Figure A3. Mat Geometry 3

Figure A4. Mat Geometry 4

Figure A5. Mat Geometry 5

Figure A6. Mat Geometry 6

Figure A7. Mat Geometry 7

Figure A8. Mat Geometry 8

Figure A9. Mat Geometry 9

Figure A10. Mat Geometry 10

Figure B11. Mat Geometry 11

Figure A12. Mat Geometry 12

Figure A.13. Mat Geometry 13

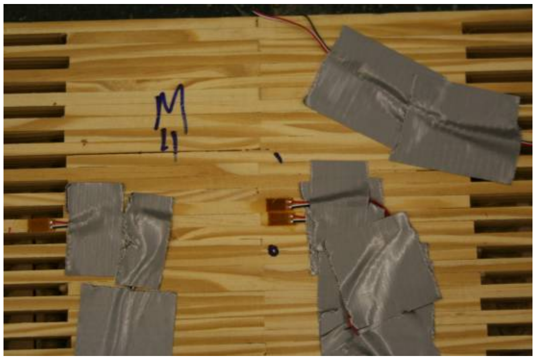

(a) Instrumentation Photo 1 of 3

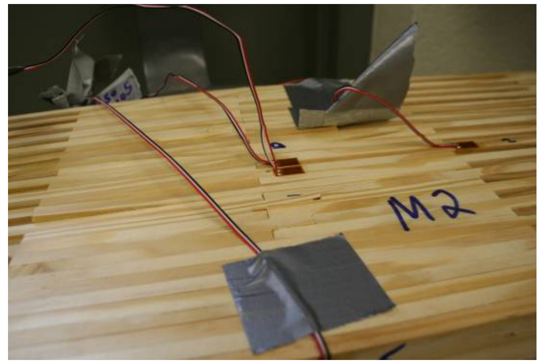

(b) Instrumentation Photo 2 of 3

(c) Instrumentation Photo 3 of 3

(d) Testing Photo 1 of 3

(e) Testing Photo 2 of 3

(f) Testing Photo 3 of 3

Figure A14. Instrumentation and Testing of Prototype Mats

Figure A.15. Photo of Mat Geometry 14

Figure A.16. Photo of Mat Geometry 15

Figure A.17. Photo of Mat Geometry 16

Figure A.18. Photo of Mat Geometry 17

Figure A.19. Photo of Mat Geometry 18

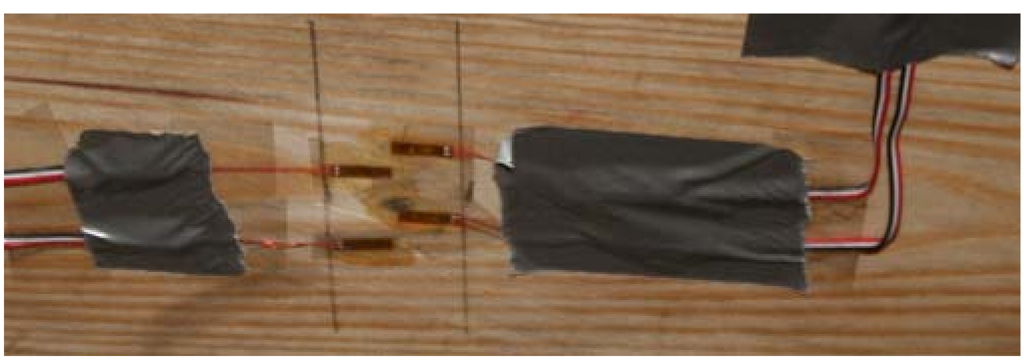

Figure A.20. Example Full Scale Instrumentation Layout

Figure A.21. Photo of Full Scale Testing: 1 of 2

Figure A.22. Photo of Full Scale Testing: 2 of 2

APPENDIX B- PROTOTYPE MAT DRAWINGS SHOWING INSTRUMENT LOCATIONS

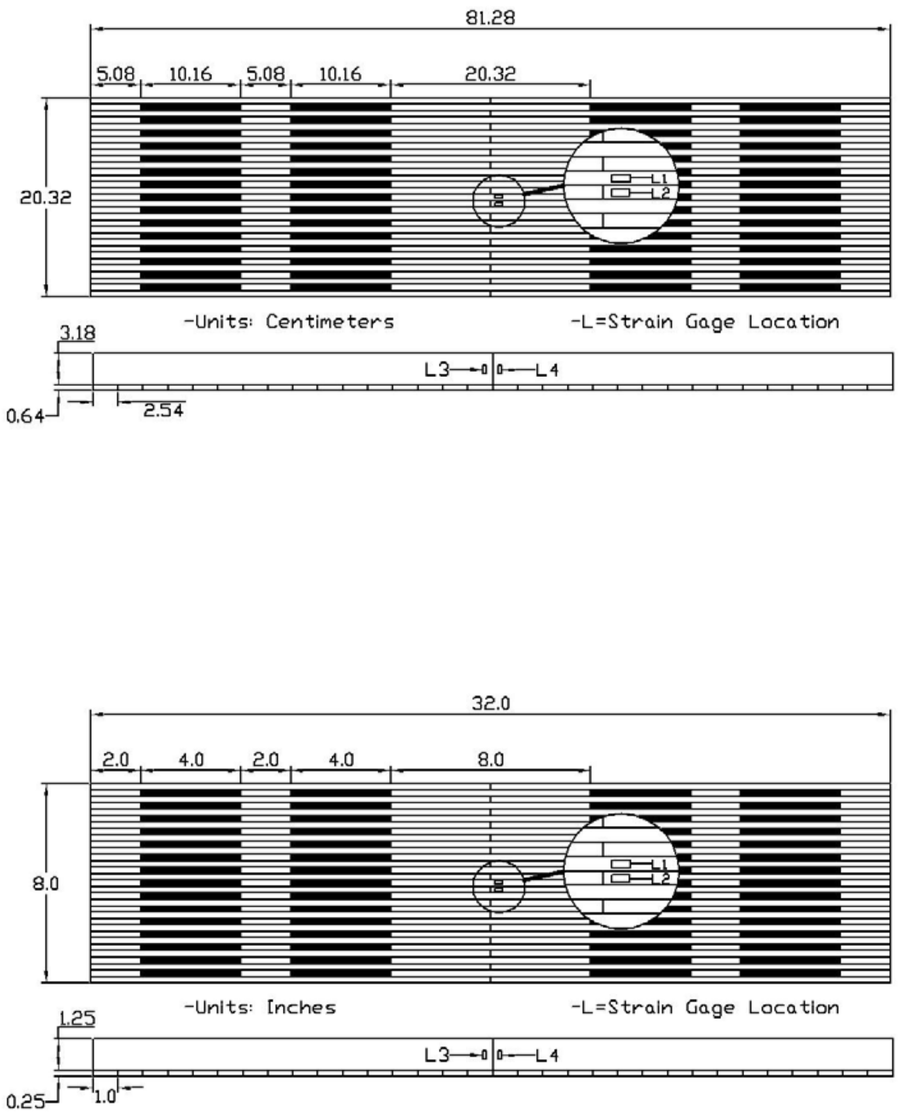

Figure B1. Mat Geometry 1

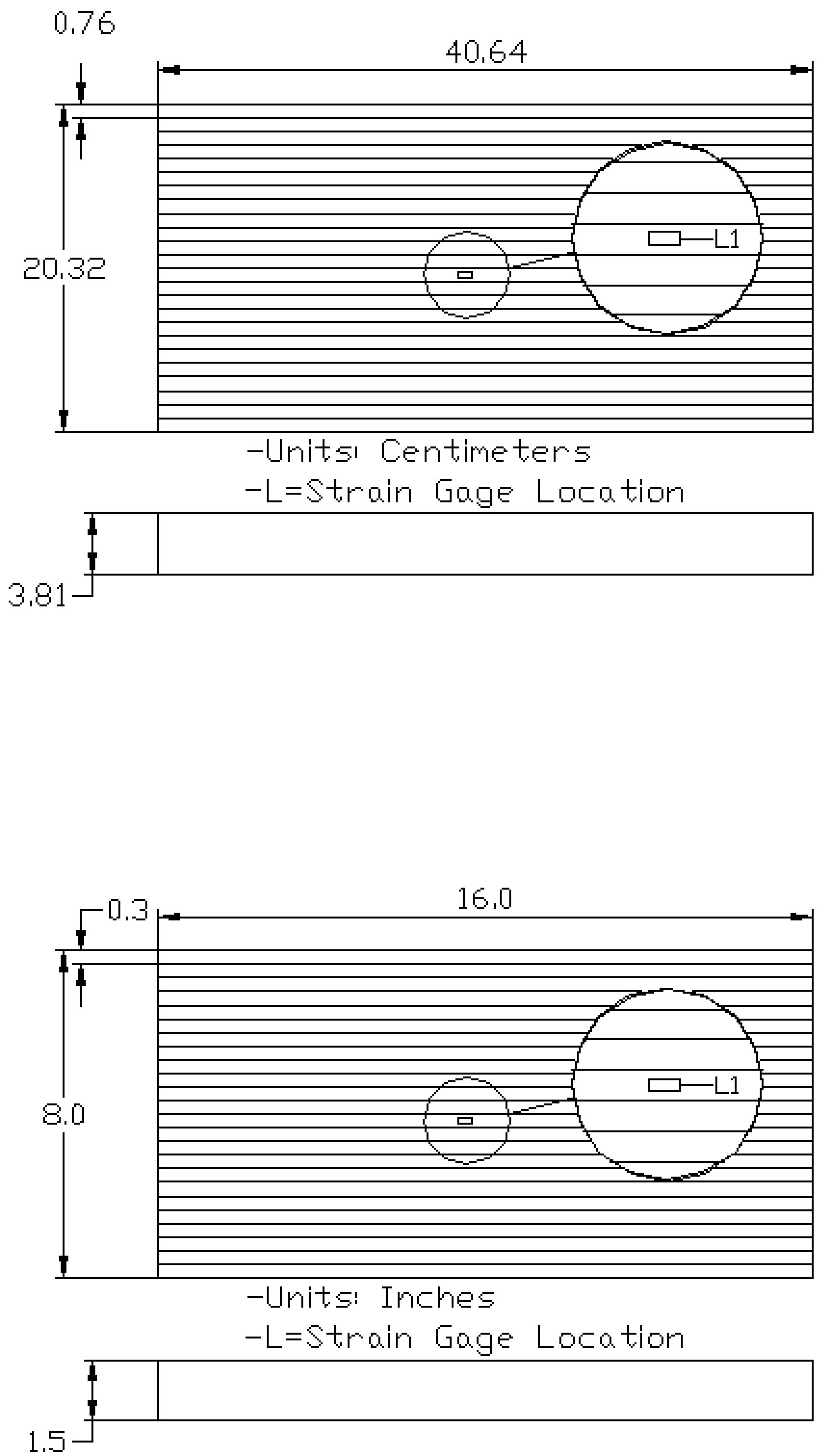

Figure B2. Mat Geometry 2

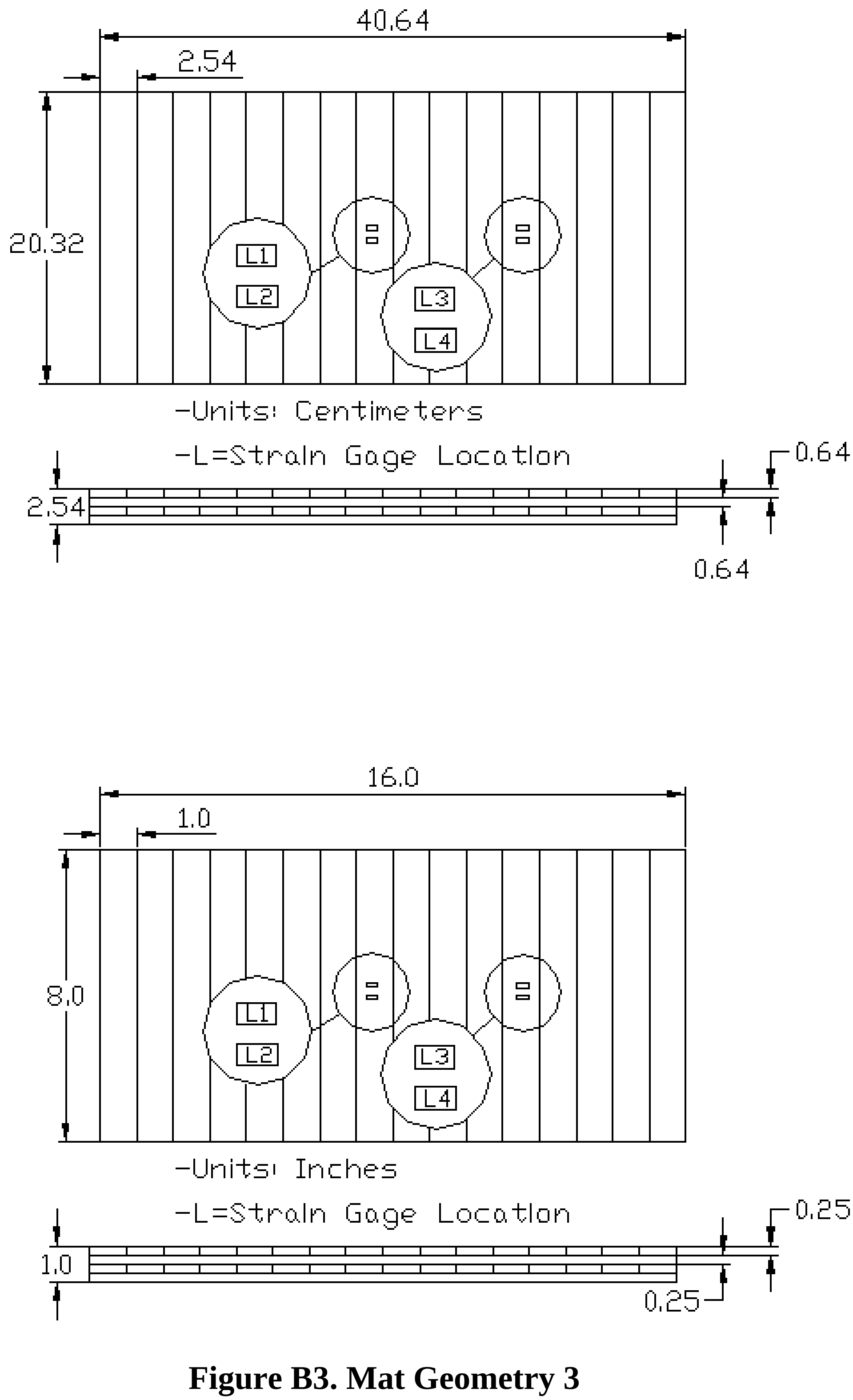

Figure B3. Mat Geometry 3

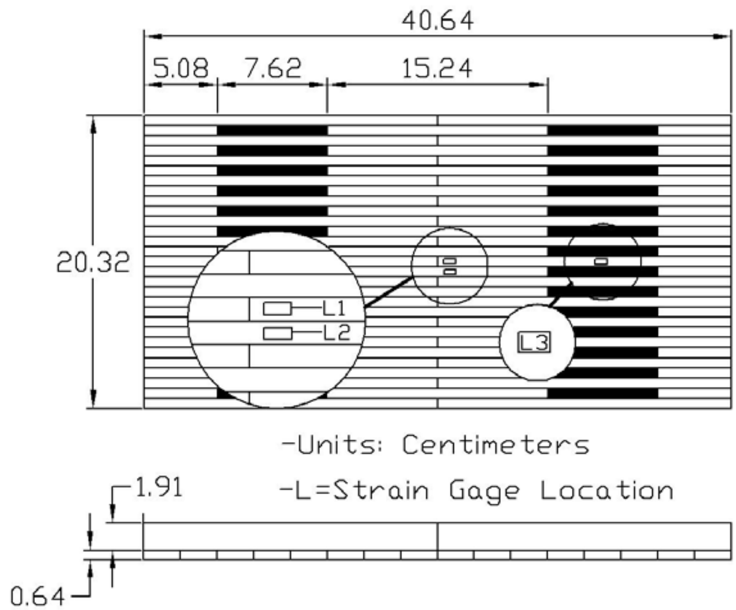

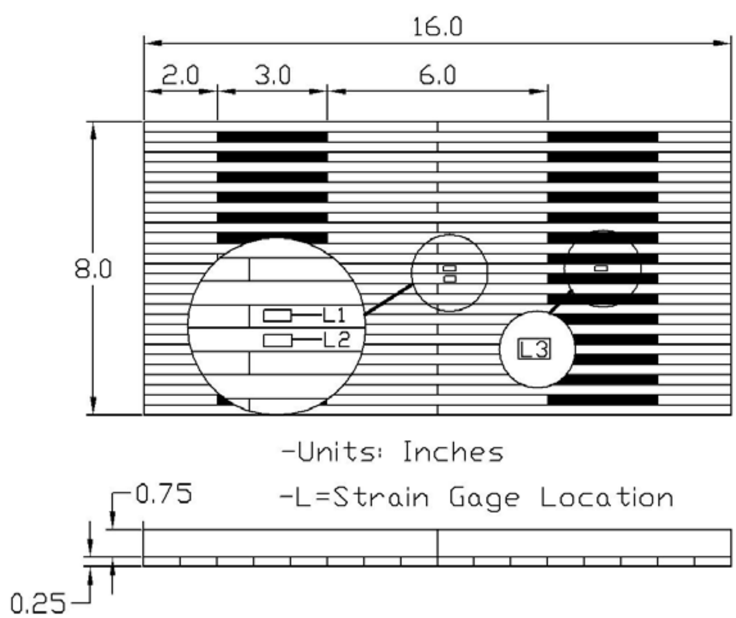

Figure B4. Mat Geometry 4

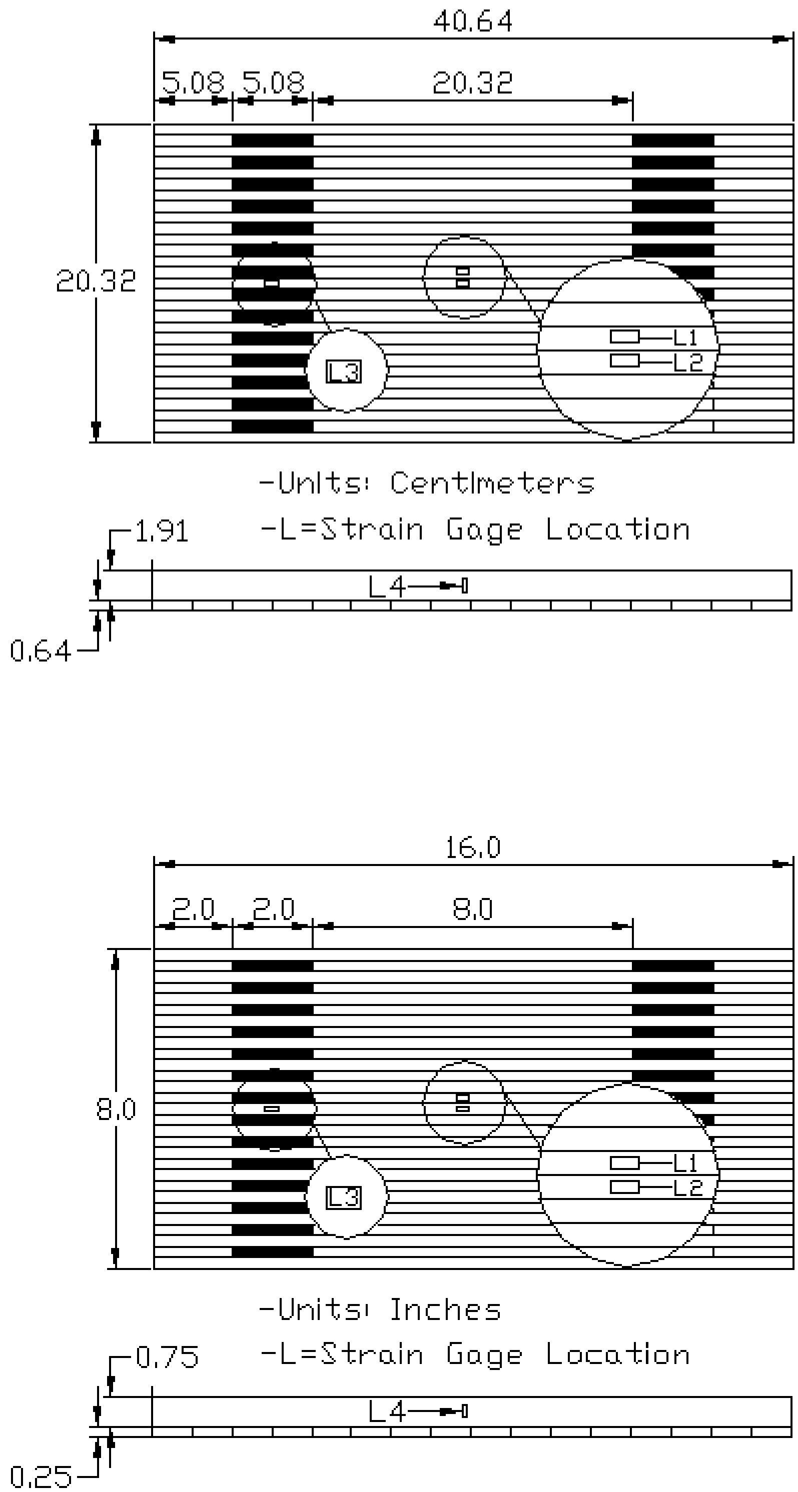

Figure B5. Mat Geometry 5

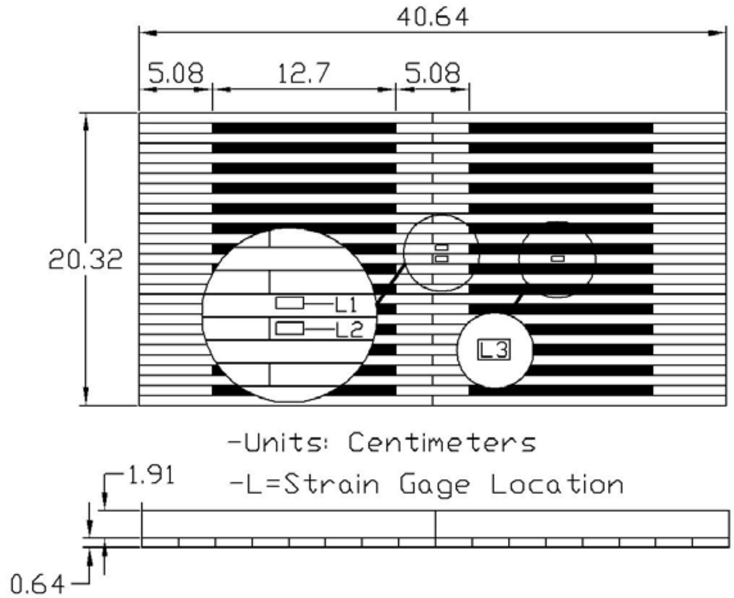

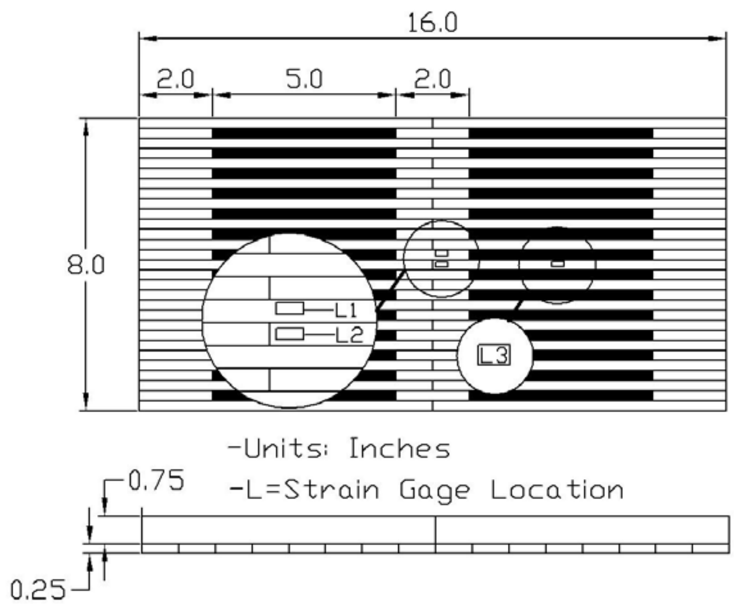

Figure B6. Mat Geometry 6

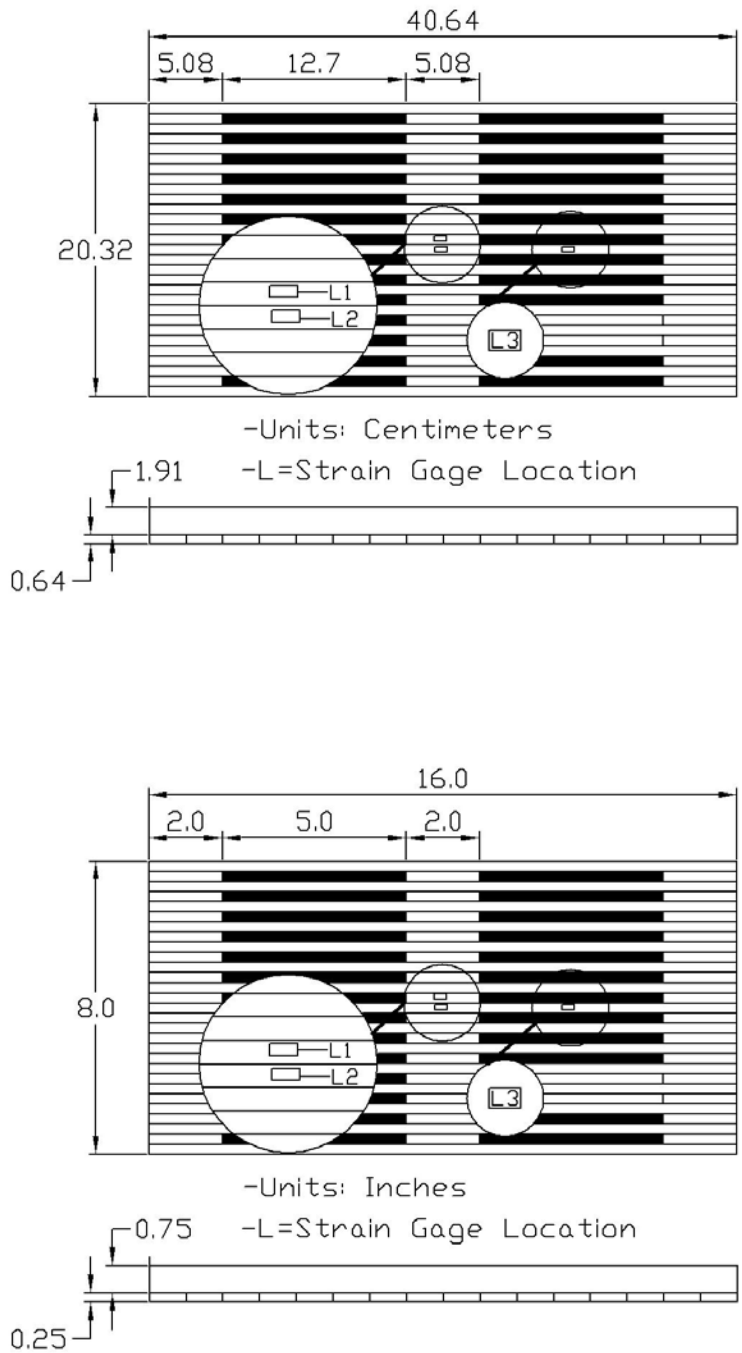

Figure B7. Mat Geometry 7

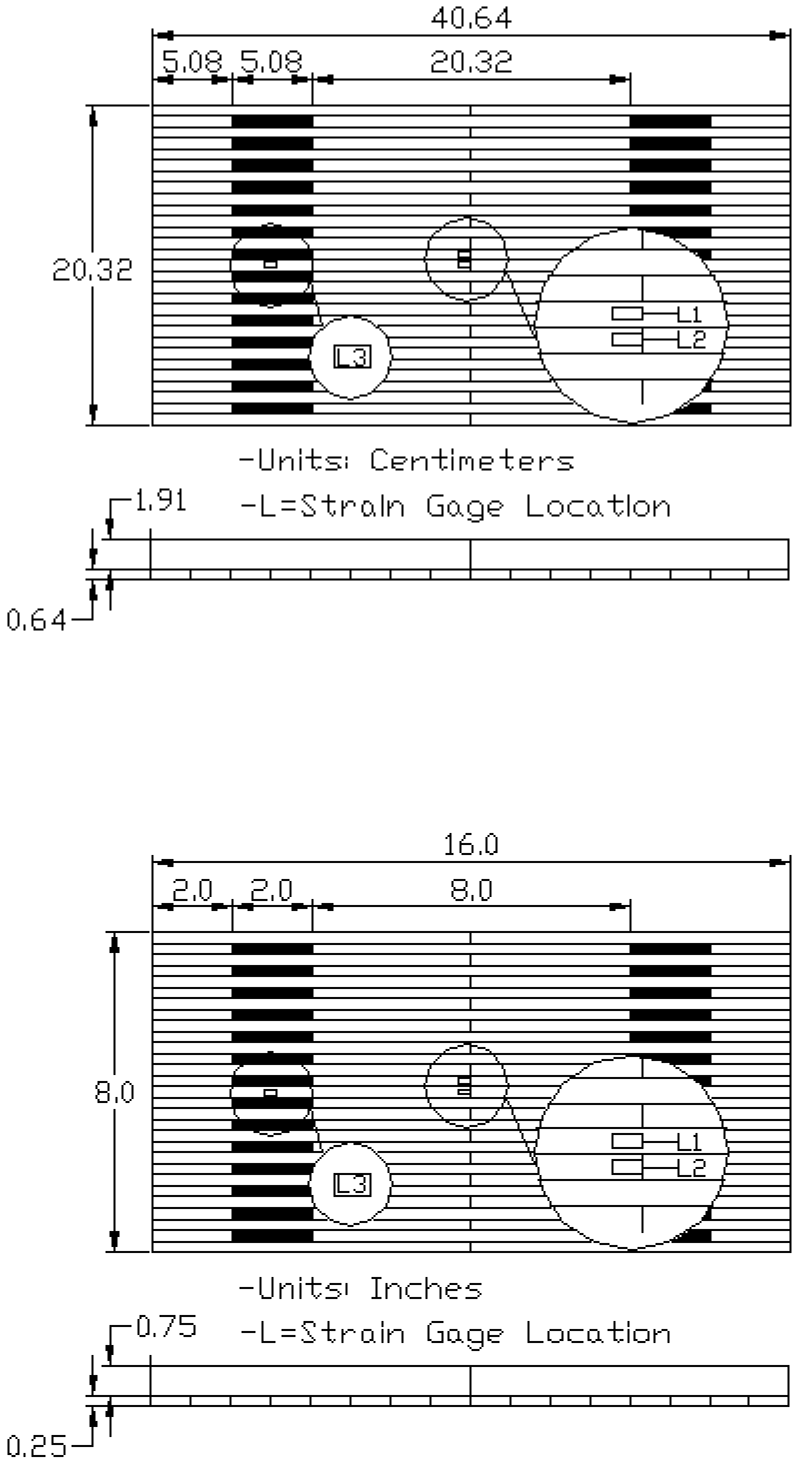

Figure B8. Mat Geometry 8

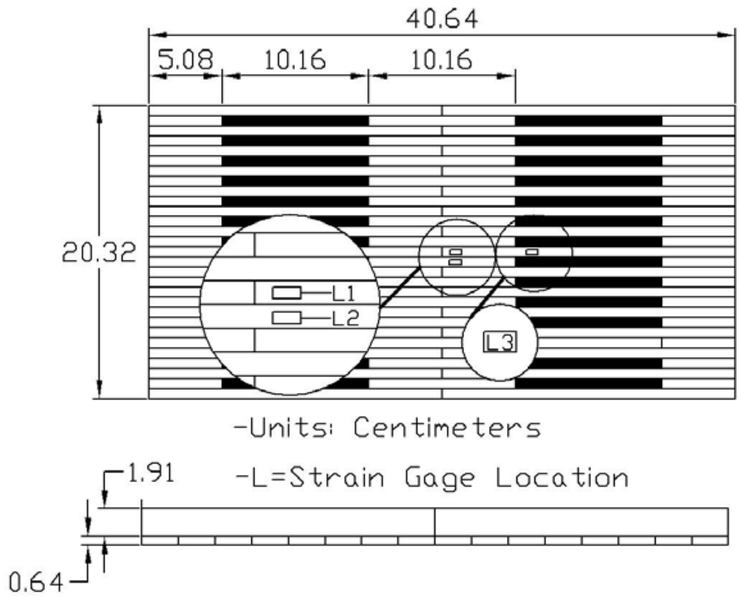

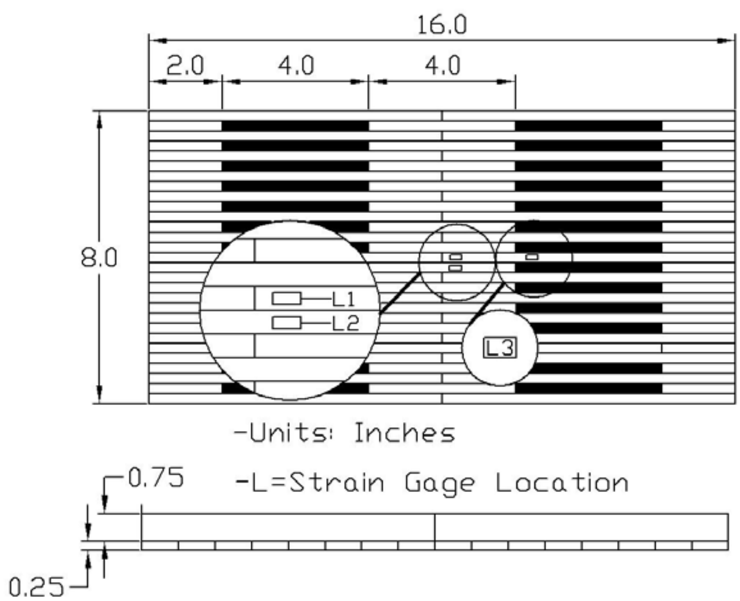

Figure B9. Mat Geometry 9

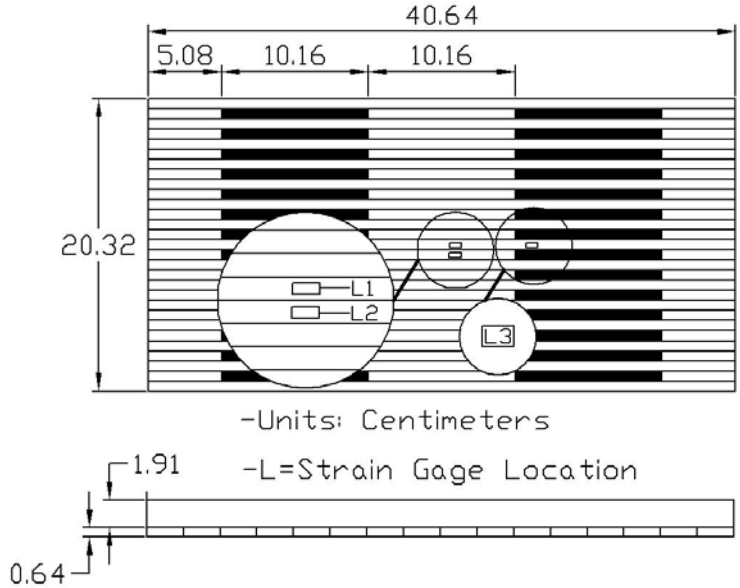

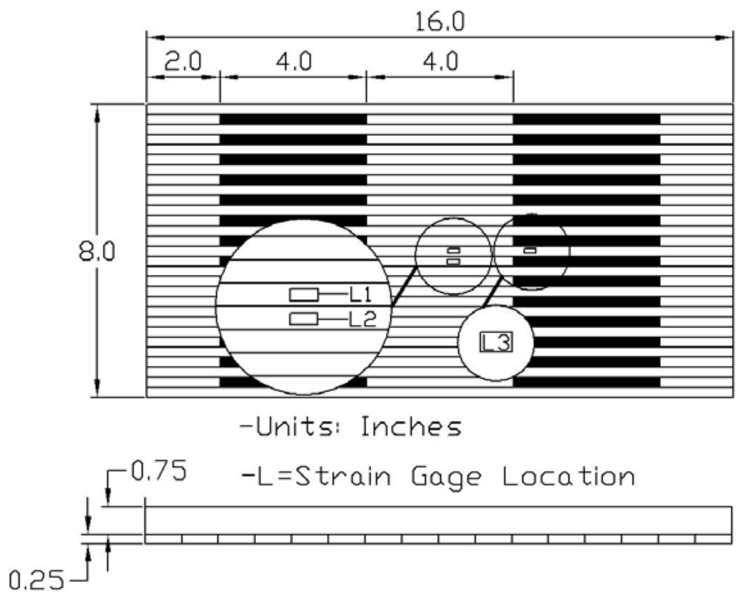

Figure B10. Mat Geometry 10

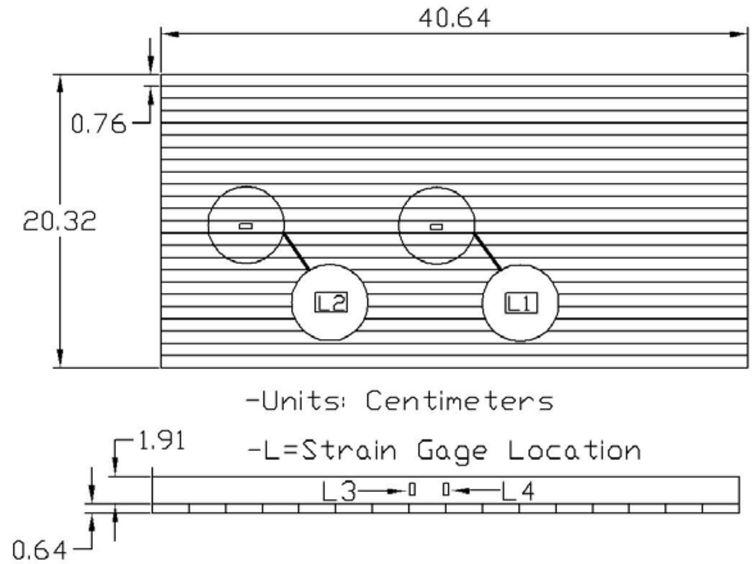

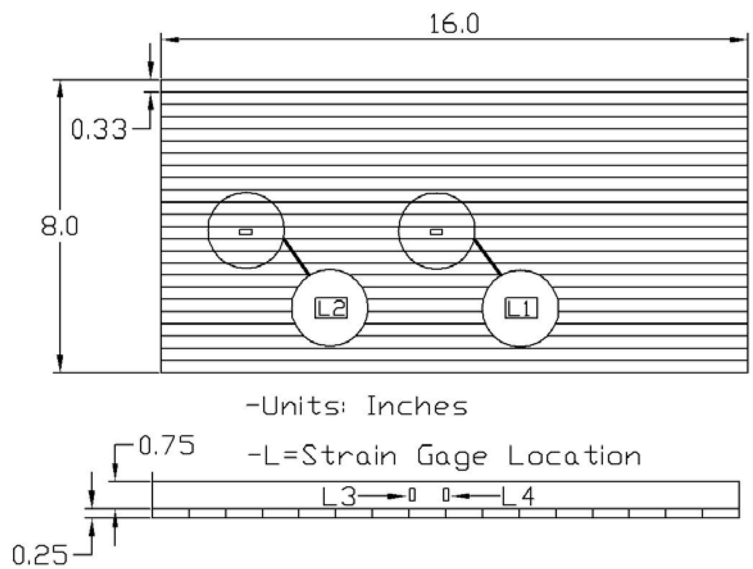

Figure B11. Mat Geometry 11

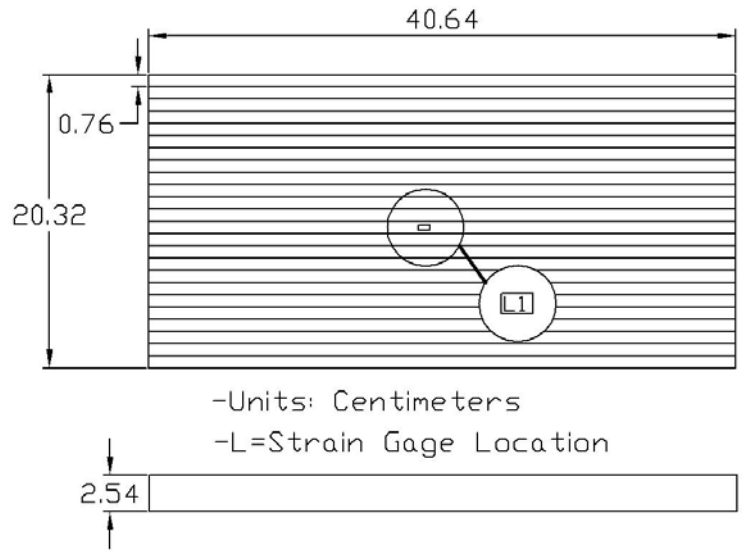

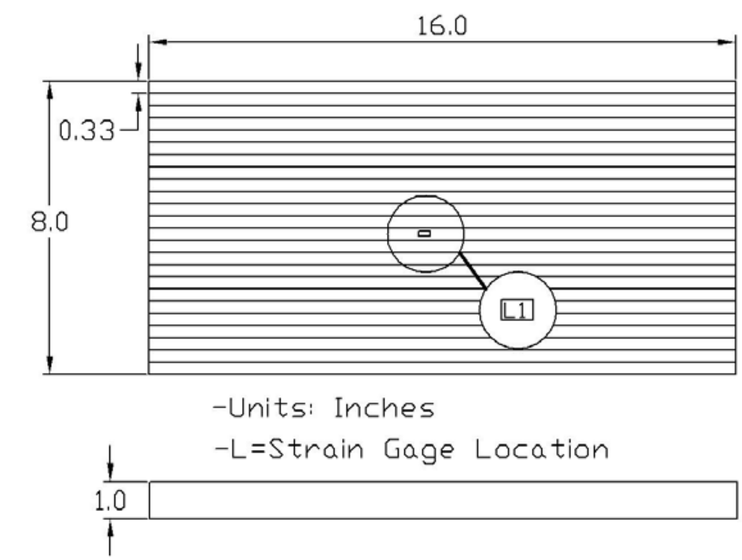

Figure B12. Mat Geometry 12

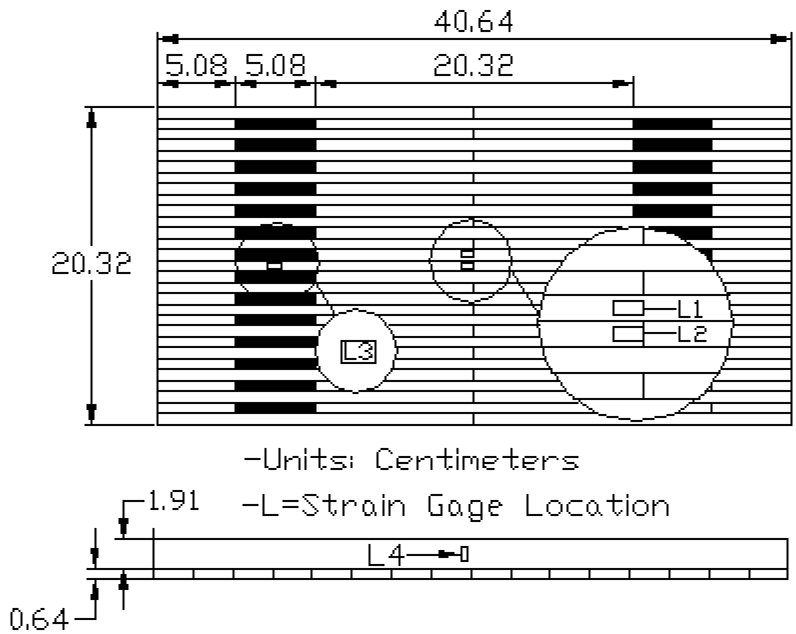

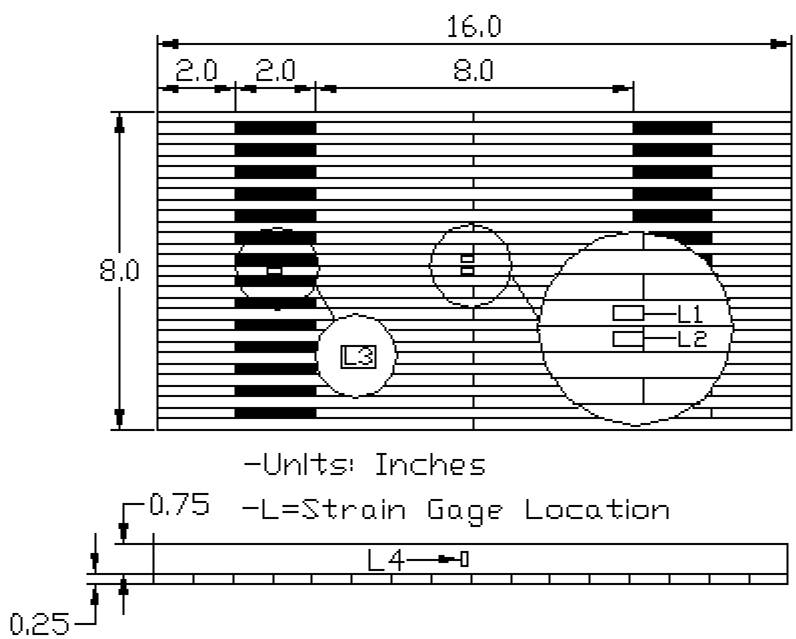

Figure B13. Mat Geometry 13

APPENDIX C-LOAD DEFLECTION PLOTS

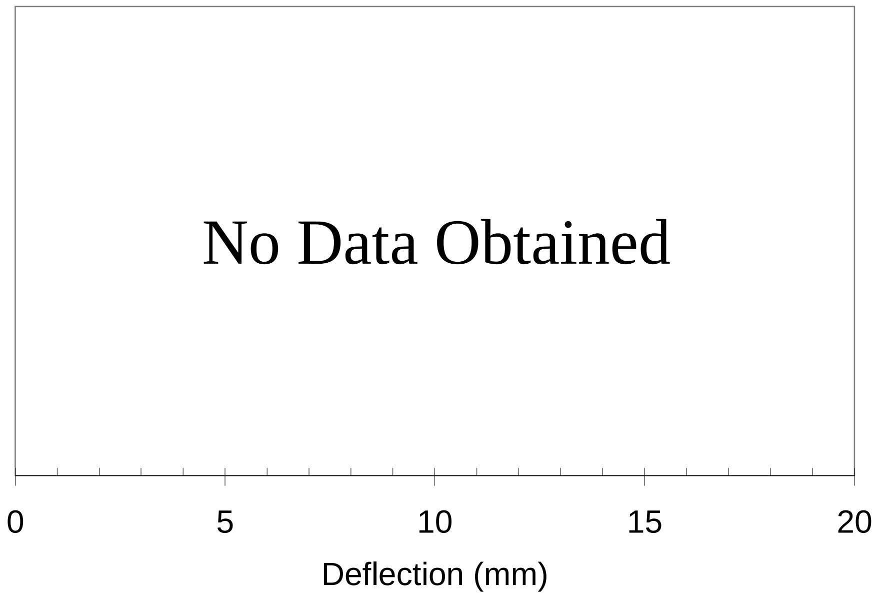

Figure C1. Deflection Behaviors for Mat 1: Geometry 1

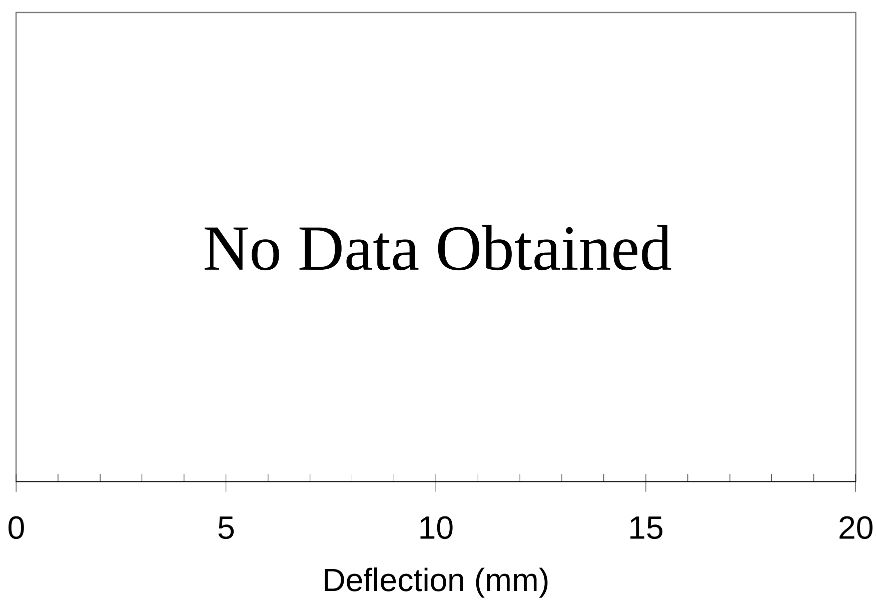

Figure C2. Deflection Behaviors for Mat 2: Geometry 13

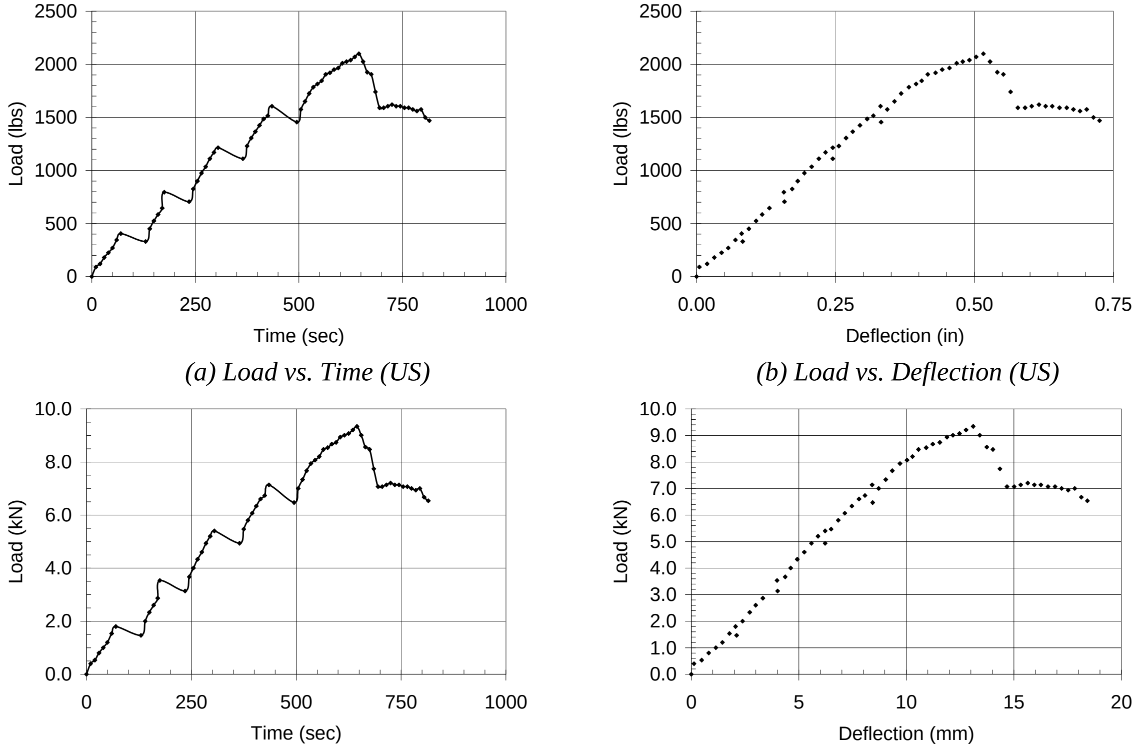

(a) Load vs. Time (US) *(b) Load vs. Deflection (US)*

(c) Load vs. Time (SI) *(d) Load vs. Deflection (SI)*

Figure C3. Deflection Behaviors for Mat 3: Geometry 9

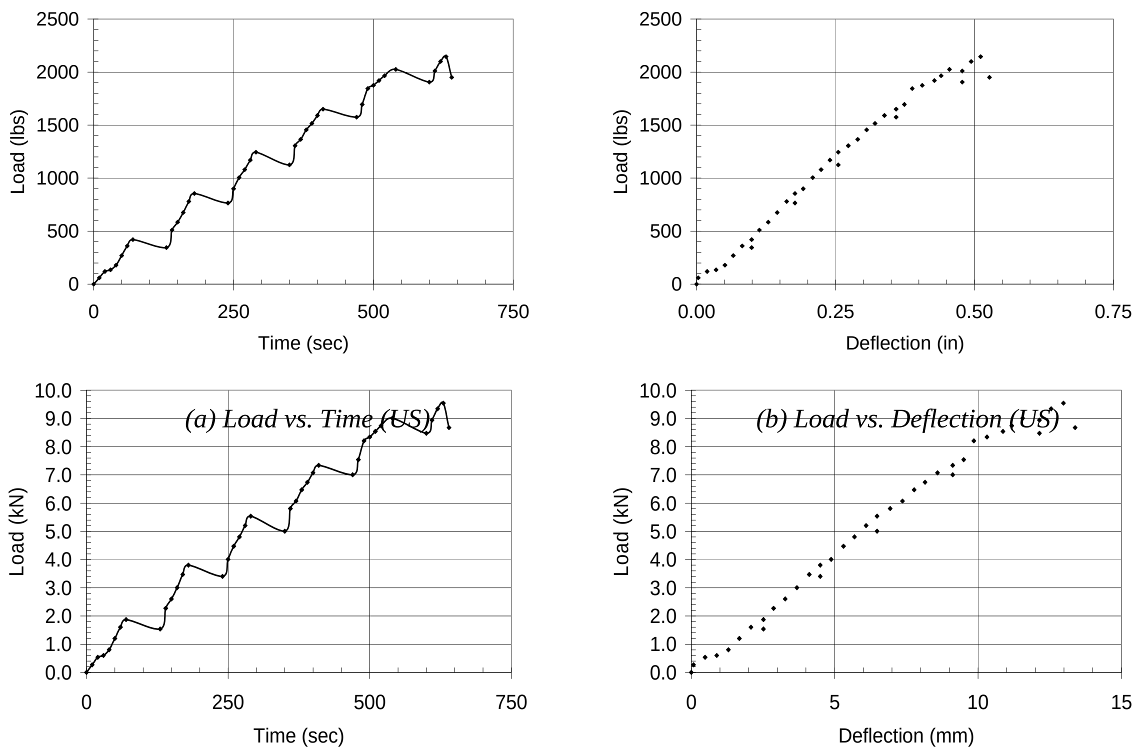

(c) Load vs. Time (SI) *(d) Load vs. Deflection (SI)*

Figure C4. Deflection Behaviors for Mat 4: Geometry 8

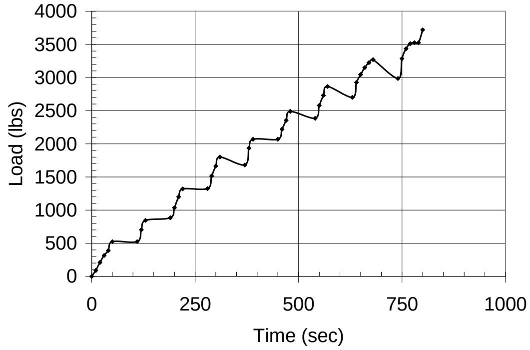

(a) Load vs. Time (US)

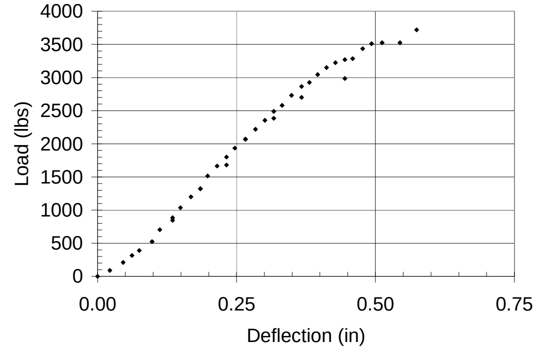

(b) Load vs. Deflection (US)

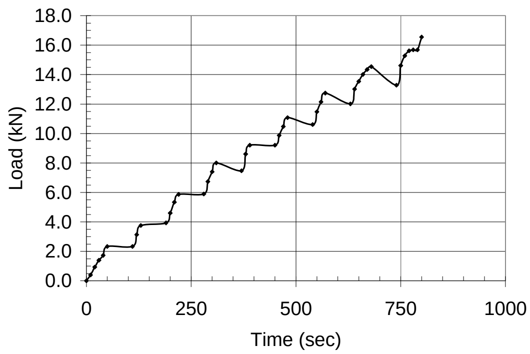

(c) Load vs. Time (SI)

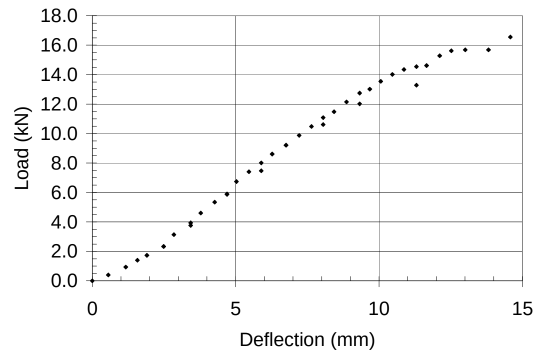

(d) Load vs. Deflection (SI)

Figure C5. Deflection Behaviors for Mat 5: Geometry 5

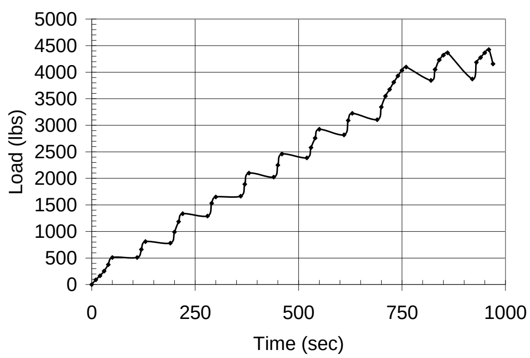

(a) Load vs. Time (US)

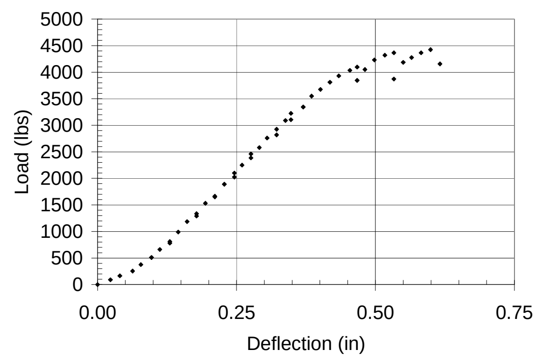

(b) Load vs. Deflection (US)

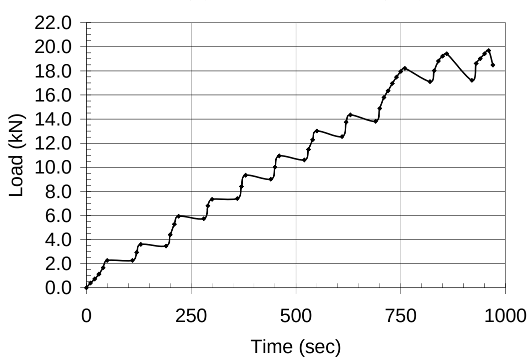

(c) Load vs. Time (SI)

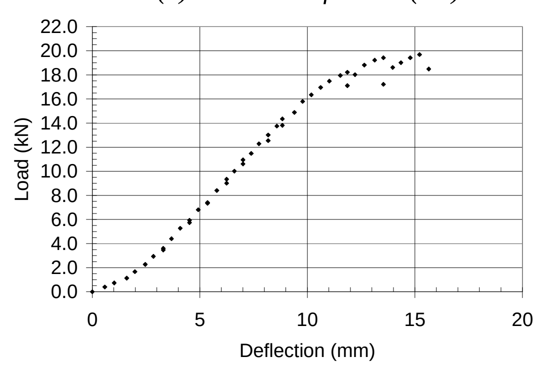

(d) Load vs. Deflection (SI)

Figure C6. Deflection Behaviors for Mat 6: Geometry 11

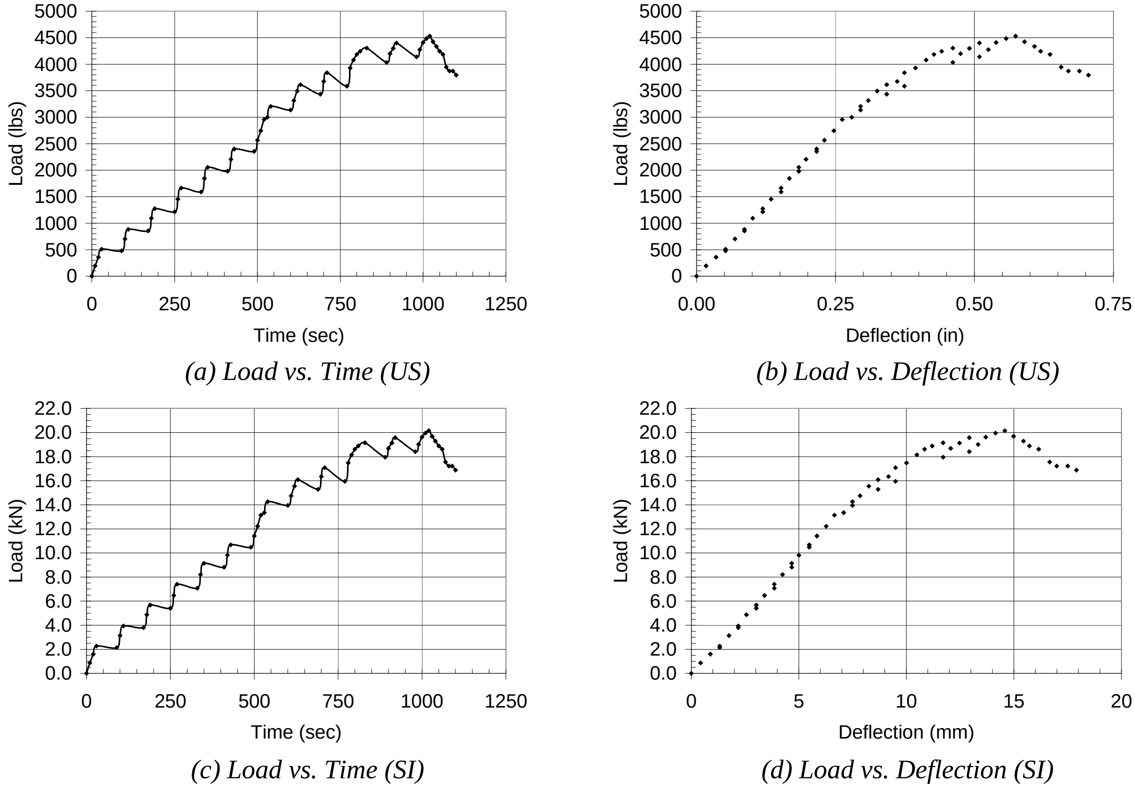

(a) Load vs. Time (US) (b) Load vs. Deflection (US)

(c) Load vs. Time (SI) (d) Load vs. Deflection (SI)

Figure C7. Deflection Behaviors for Mat 7: Geometry 11

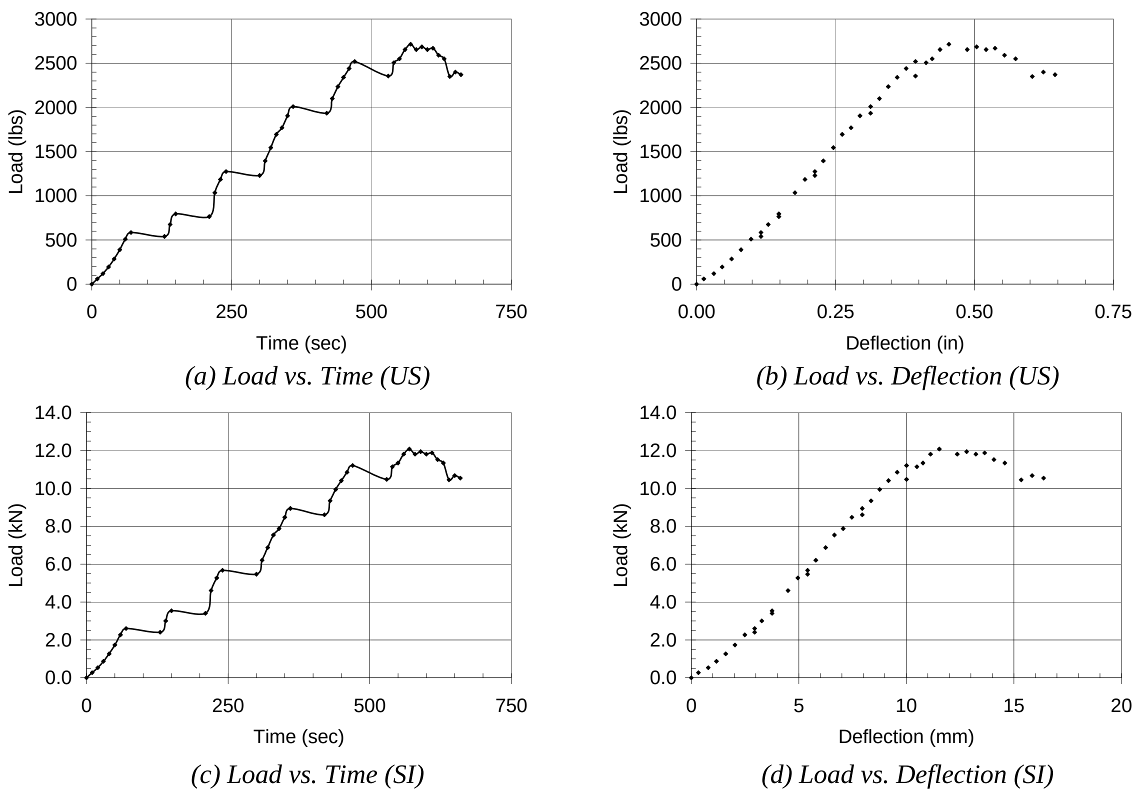

(a) Load vs. Time (US) (b) Load vs. Deflection (US)

(c) Load vs. Time (SI) (d) Load vs. Deflection (SI)

Figure C8. Deflection Behaviors for Mat 8: Geometry 10

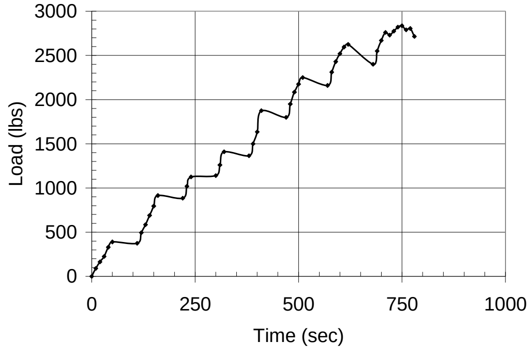

(a) Load vs. Time (US)

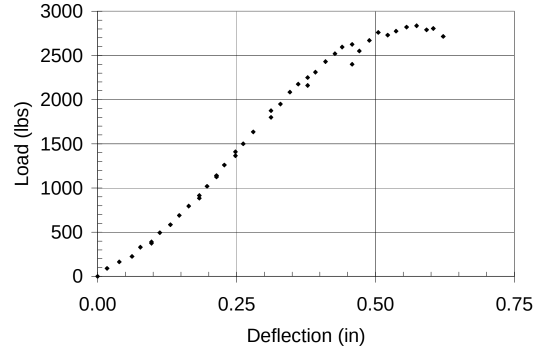

(b) Load vs. Deflection (US)

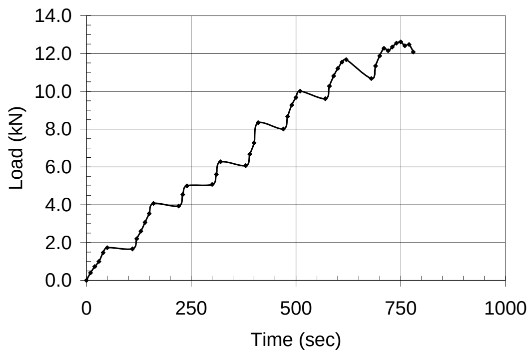

(c) Load vs. Time (SI)

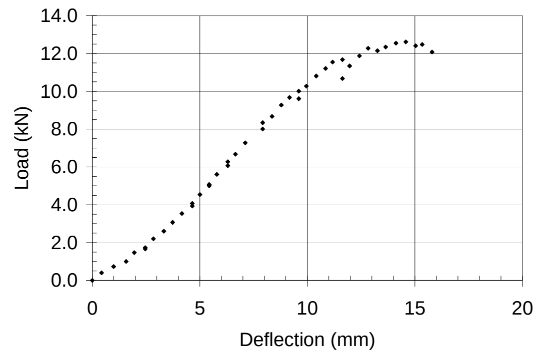

(d) Load vs. Deflection (SI)

Figure C9. Deflection Behaviors for Mat 9: Geometry 10

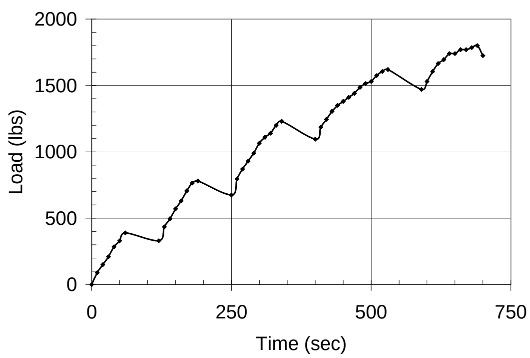

(a) Load vs. Time (US)

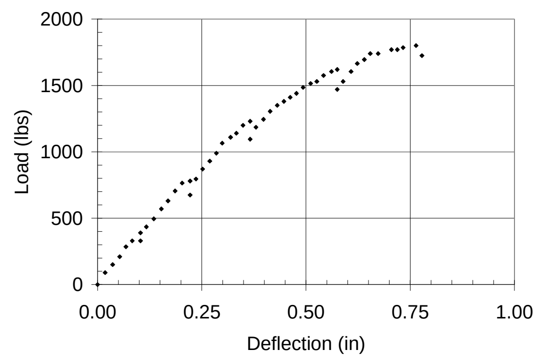

(b) Load vs. Deflection (US)

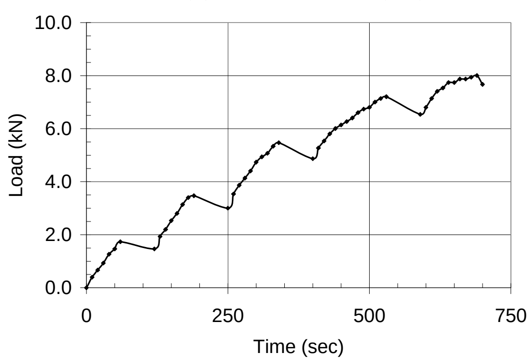

(c) Load vs. Time (SI)

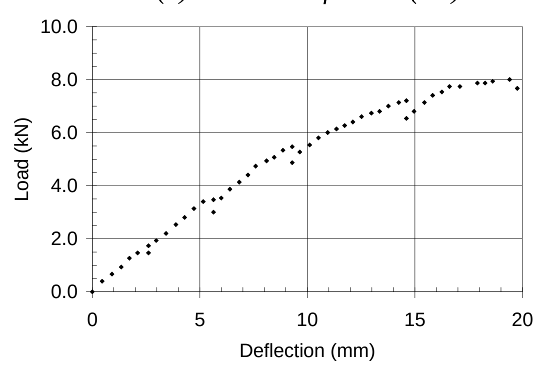

(d) Load vs. Deflection (SI)

Figure C10. Deflection Behaviors for Mat 10: Geometry 3

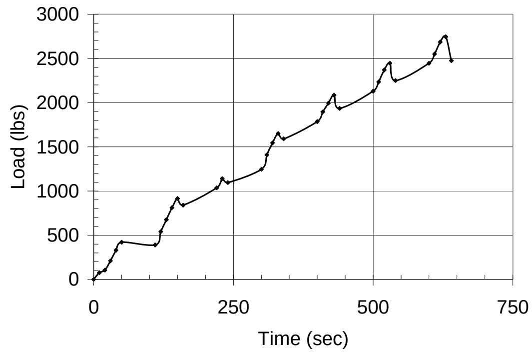

(a) Load vs. Time (US)

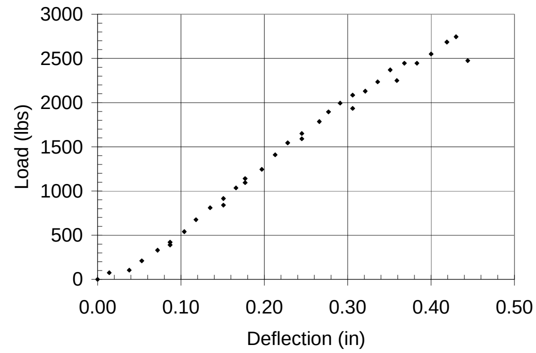

(b) Load vs. Deflection (US)

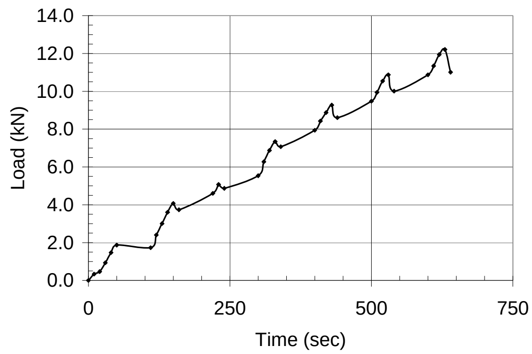

(c) Load vs. Time (SI)

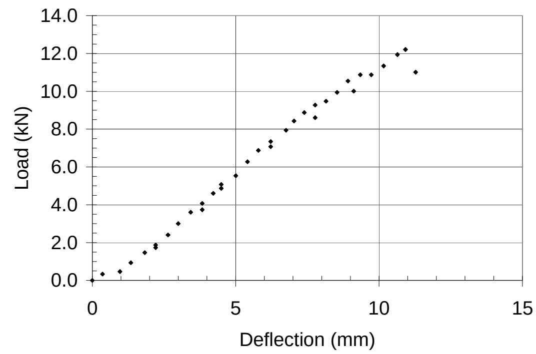

(d) Load vs. Deflection (SI)

Figure C11. Deflection Behaviors for Mat 11: Geometry 8

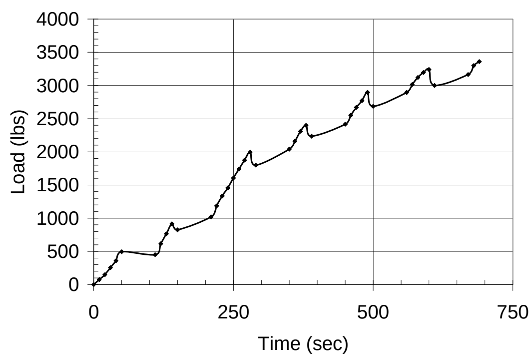

(a) Load vs. Time (US)

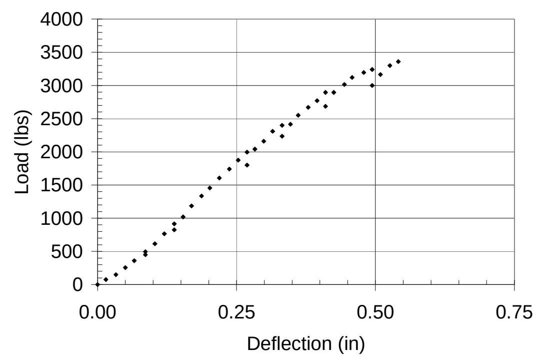

(b) Load vs. Deflection (US)

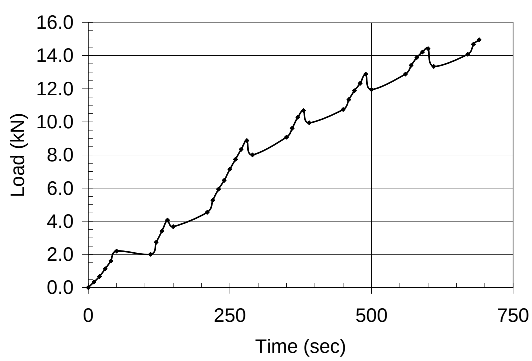

(c) Load vs. Time (SI)

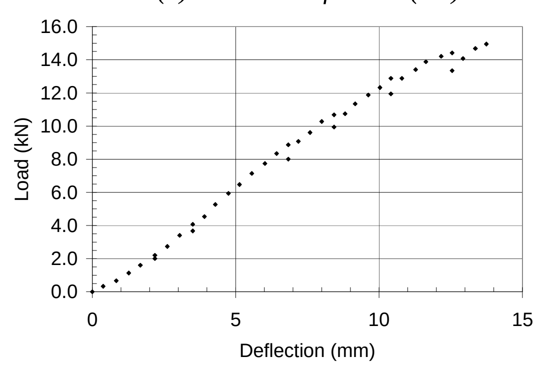

(d) Load vs. Deflection (SI)

Figure C12. Deflection Behaviors for Mat 12: Geometry 8

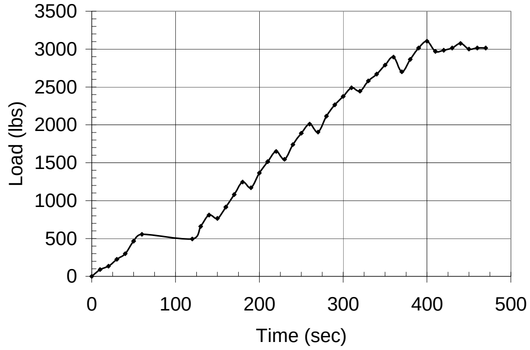

(a) Load vs. Time (US)

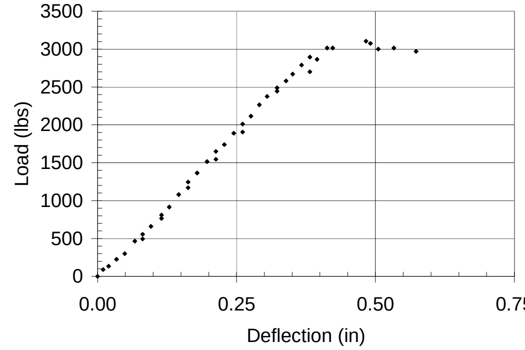

(b) Load vs. Deflection (US)

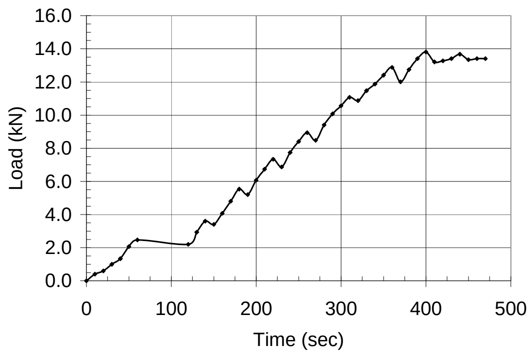

(c) Load vs. Time (SI)

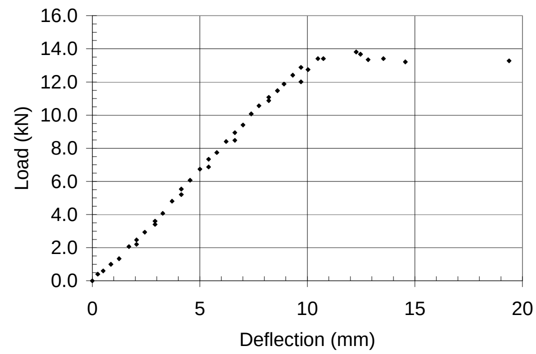

(d) Load vs. Deflection (SI)

Figure C13. Deflection Behaviors for Mat 13: Geometry 8

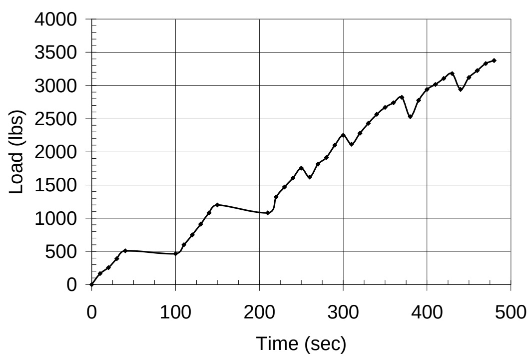

(a) Load vs. Time (US)

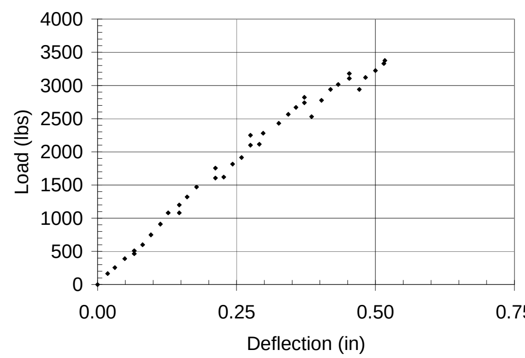

(b) Load vs. Deflection (US)

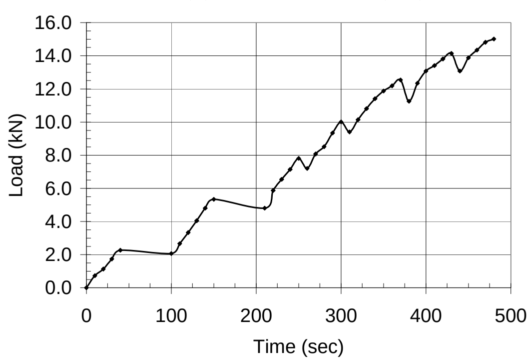

(c) Load vs. Time (SI)

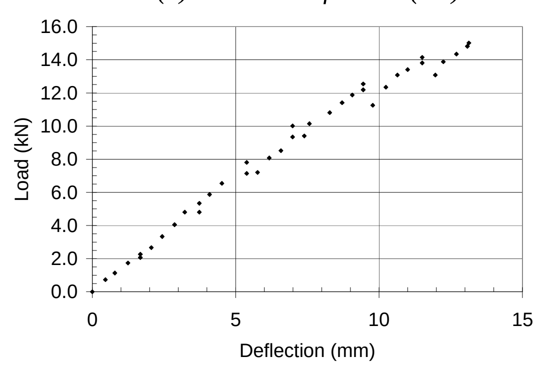

(d) Load vs. Deflection (SI)

Figure C14. Deflection Behaviors for Mat 14: Geometry 8

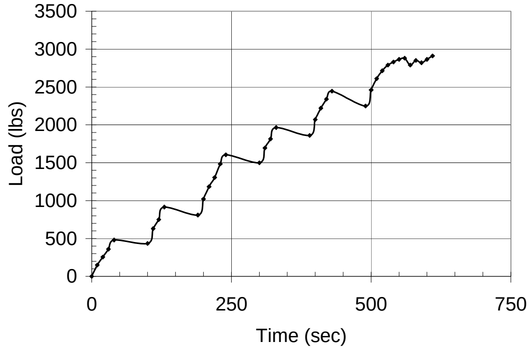

(a) Load vs. Time (US)

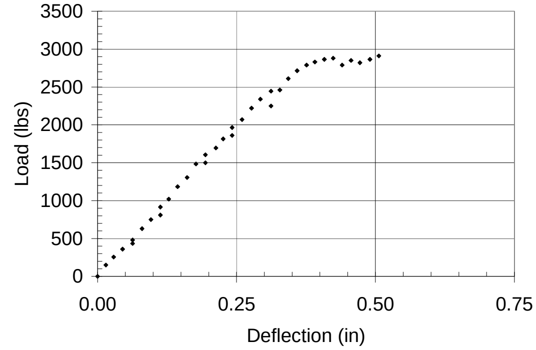

(b) Load vs. Deflection (US)

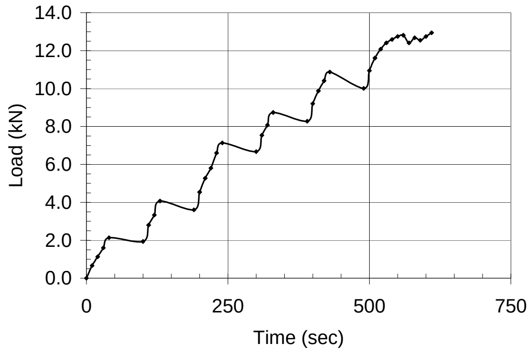

(c) Load vs. Time (SI)

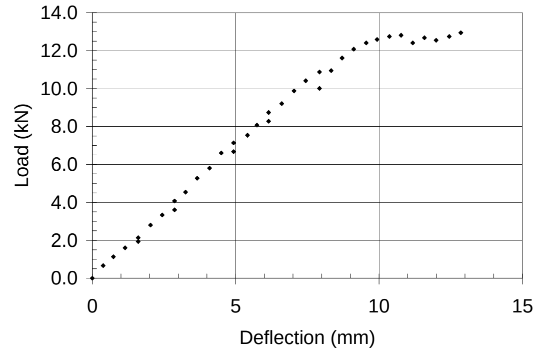

(d) Load vs. Deflection (SI)

Figure C15. Deflection Behaviors for Mat 15: Geometry 4

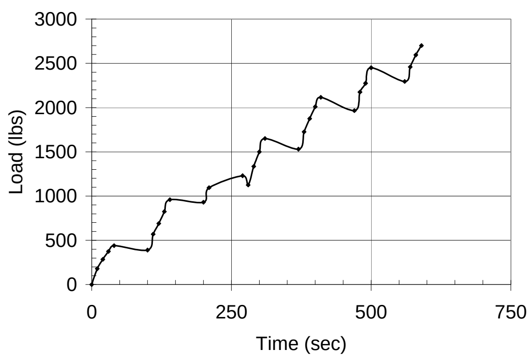

(a) Load vs. Time (US)

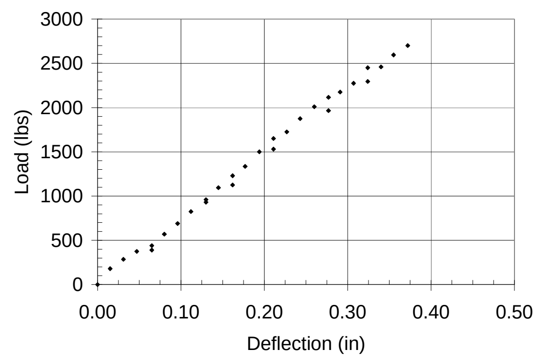

(b) Load vs. Deflection (US)

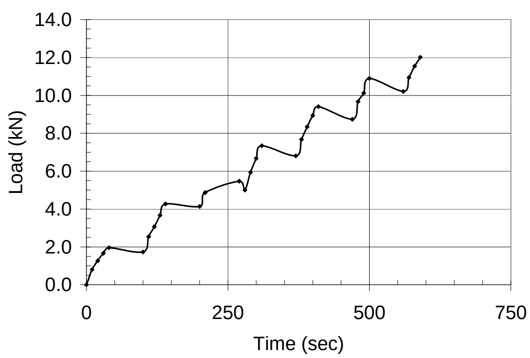

(c) Load vs. Time (SI)

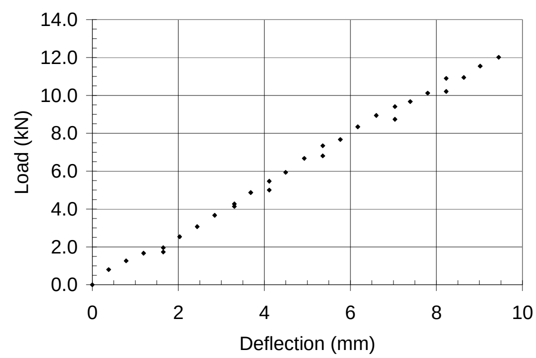

(d) Load vs. Deflection (SI)

Figure C16. Deflection Behaviors for Mat 16: Geometry 4

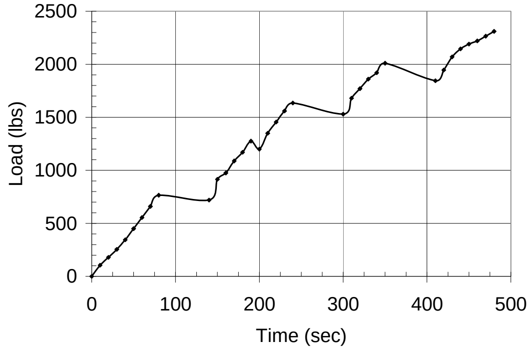

(a) Load vs. Time (US)

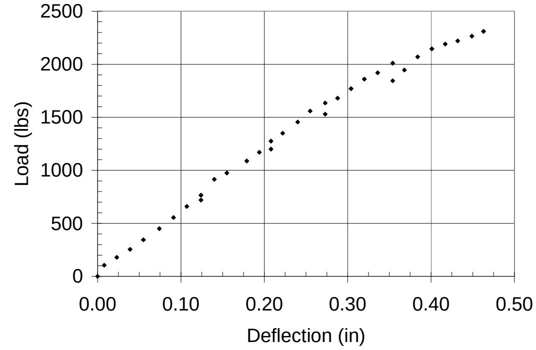

(b) Load vs. Deflection (US)

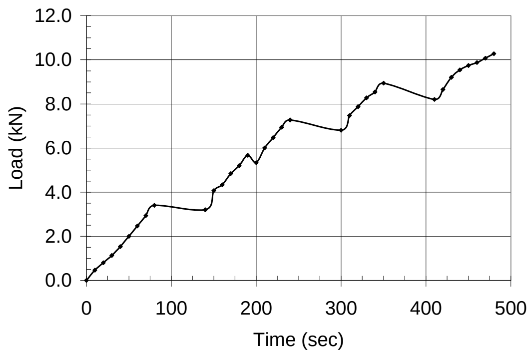

(c) Load vs. Time (SI)

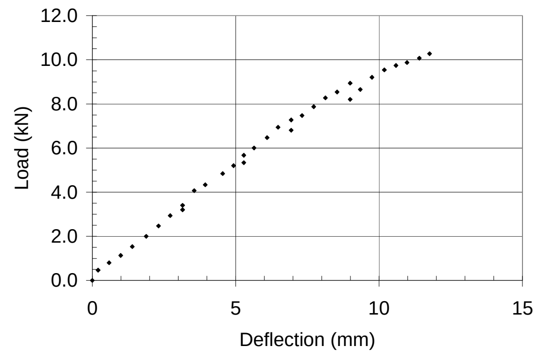

(d) Load vs. Deflection (SI)

Figure C17. Deflection Behaviors for Mat 17: Geometry 9

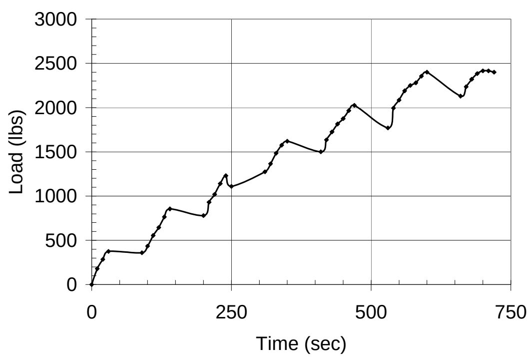

(a) Load vs. Time (US)

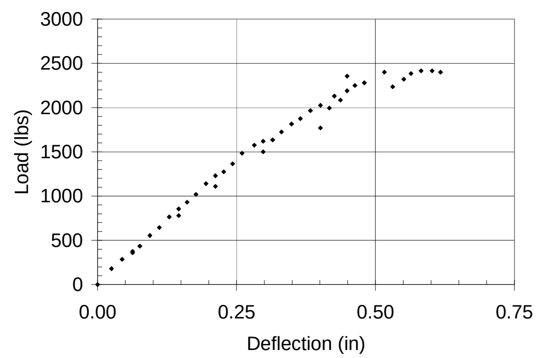

(b) Load vs. Deflection (US)

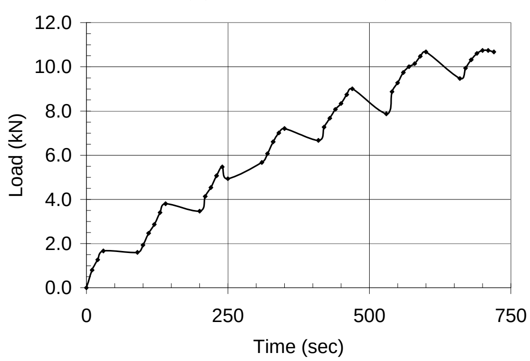

(c) Load vs. Time (SI)

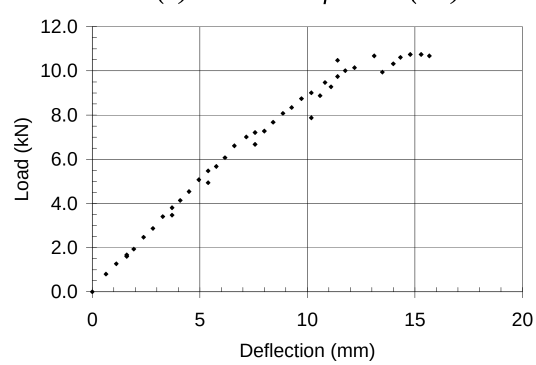

(d) Load vs. Deflection (SI)

Figure C18. Deflection Behaviors for Mat 18: Geometry 9

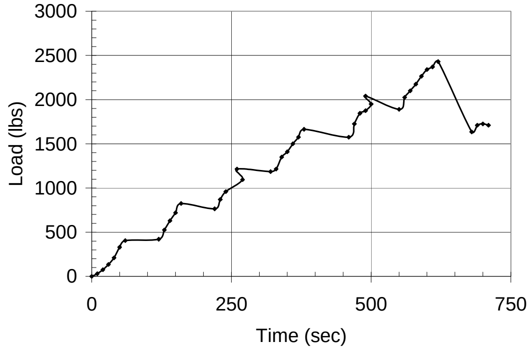

(a) Load vs. Time (US)

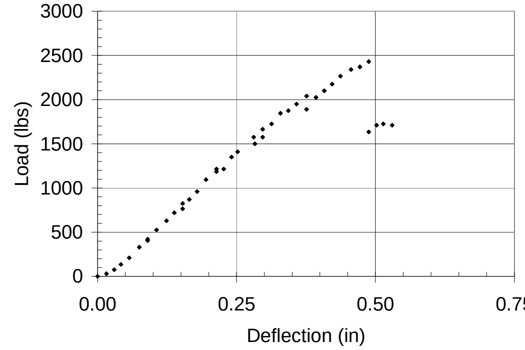

(b) Load vs. Deflection (US)

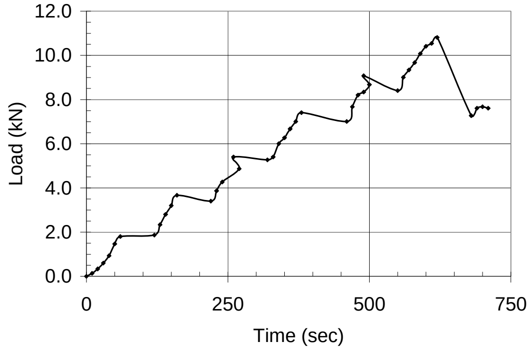

(c) Load vs. Time (SI)

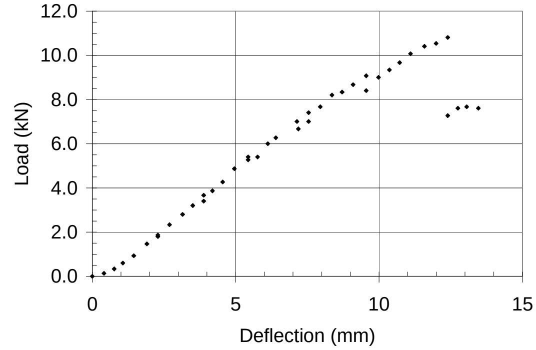

(d) Load vs. Deflection (SI)

Figure C19. Deflection Behaviors for Mat 19: Geometry 9

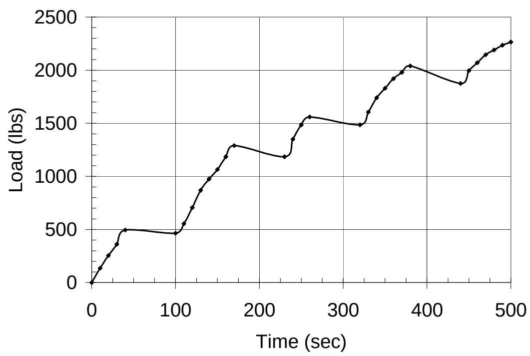

(a) Load vs. Time (US)

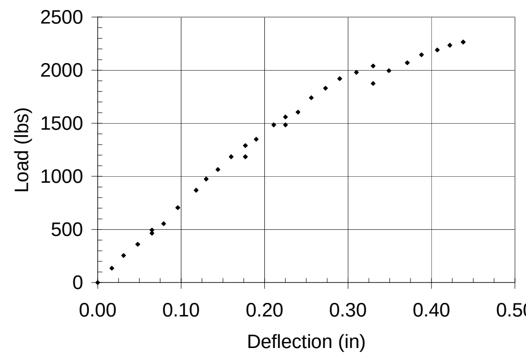

(b) Load vs. Deflection (US)

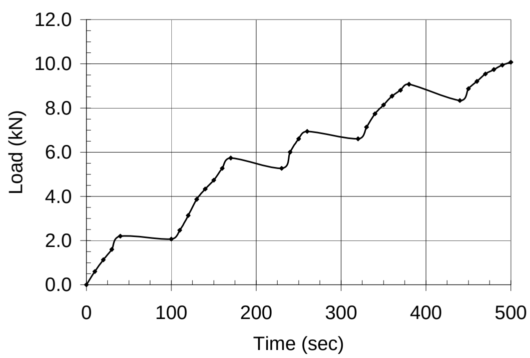

(c) Load vs. Time (SI)

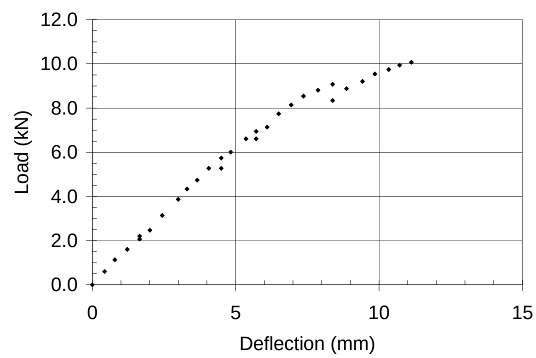

(d) Load vs. Deflection (SI)

Figure C20. Deflection Behaviors for Mat 20: Geometry 9

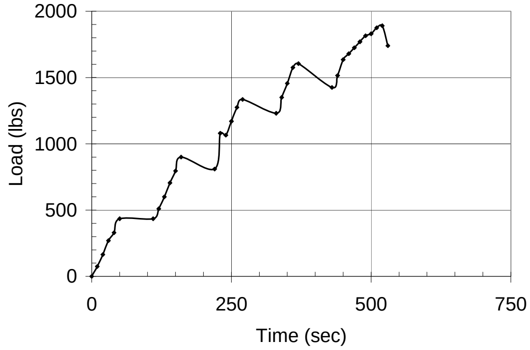

(a) Load vs. Time (US)

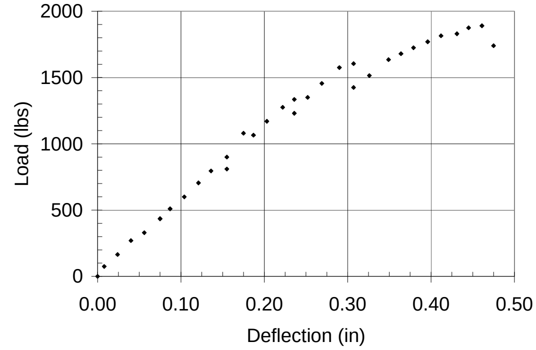

(b) Load vs. Deflection (US)

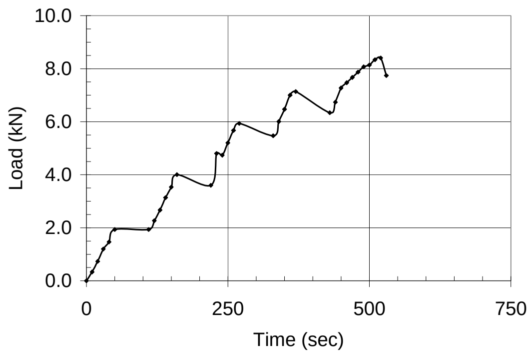

(c) Load vs. Time (SI)

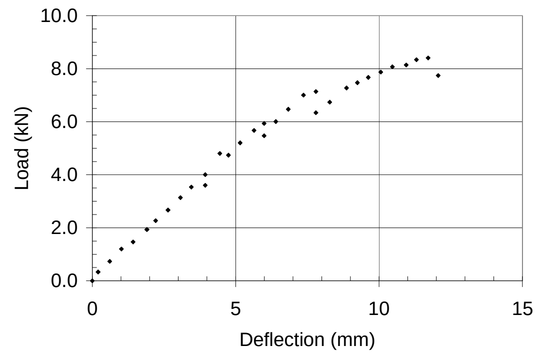

(d) Load vs. Deflection (SI)

Figure C21. Deflection Behaviors for Mat 21: Geometry 6

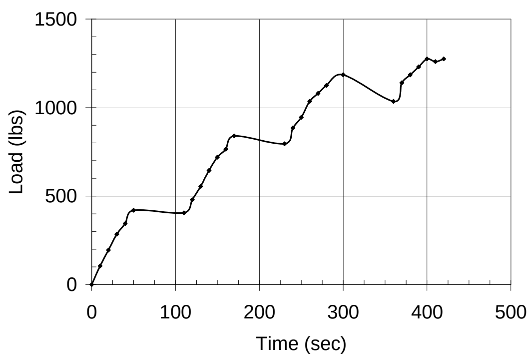

(a) Load vs. Time (US)

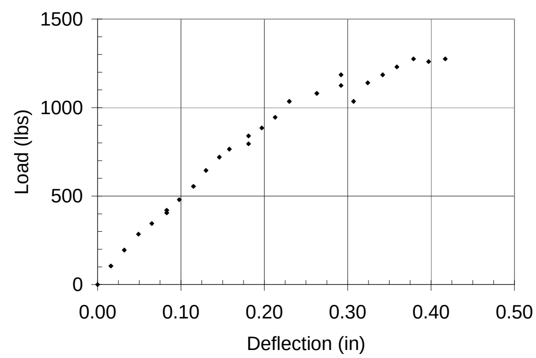

(b) Load vs. Deflection (US)

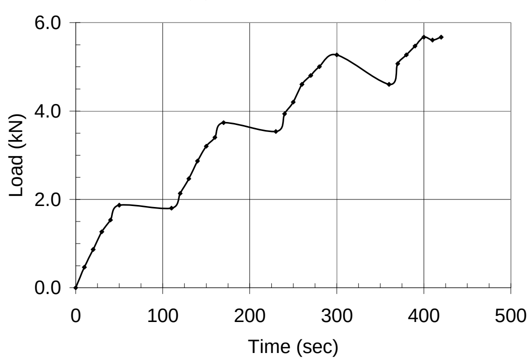

(c) Load vs. Time (SI)

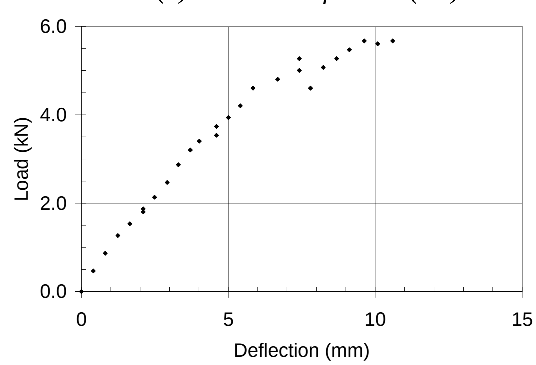

(d) Load vs. Deflection (SI)

Figure C22. Deflection Behaviors for Mat 22: Geometry6

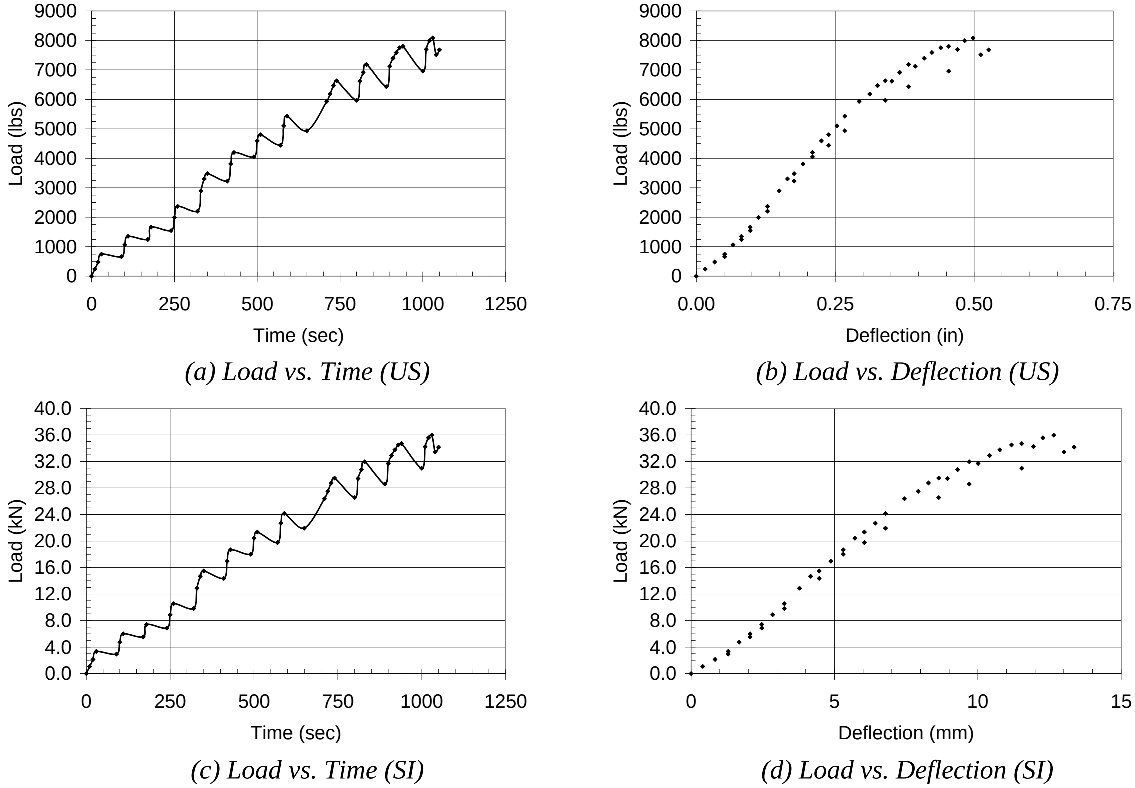

(a) Load vs. Time (US)
(b) Load vs. Deflection (US)
(c) Load vs. Time (SI)
(d) Load vs. Deflection (SI)

Figure C23. Deflection Behaviors for Mat 23: Geometry 2

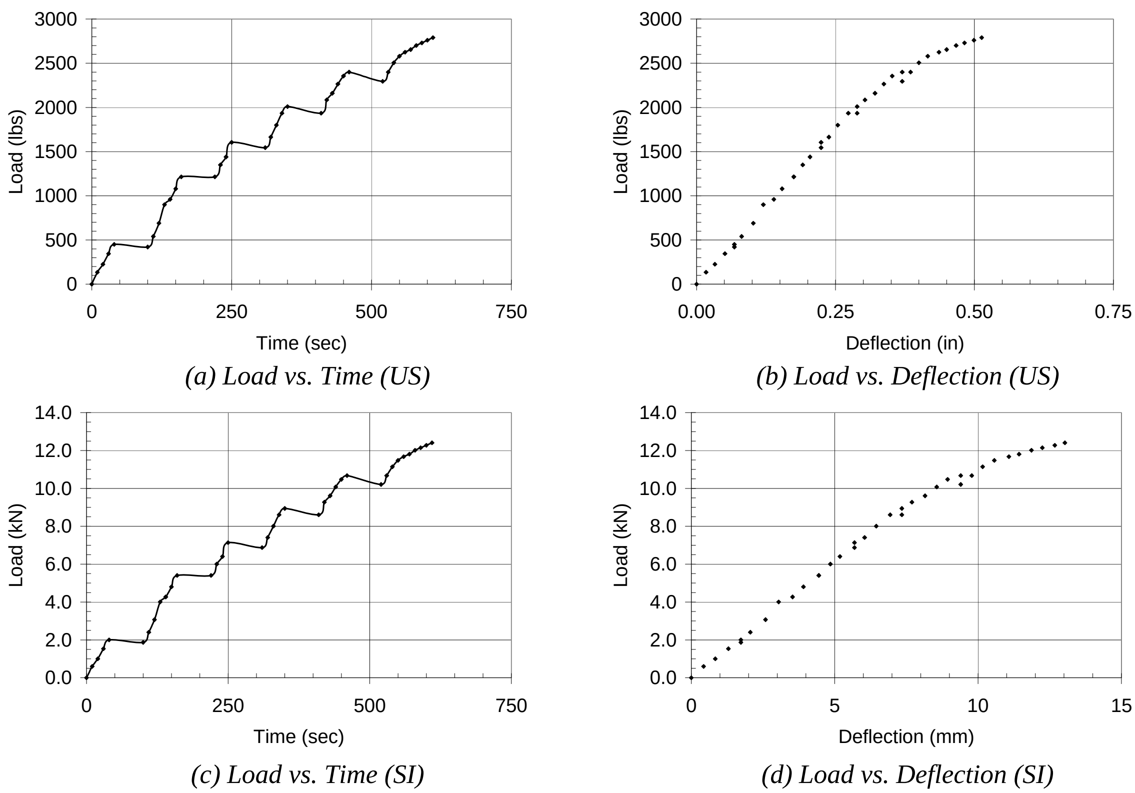

(a) Load vs. Time (US)
(b) Load vs. Deflection (US)
(c) Load vs. Time (SI)
(d) Load vs. Deflection (SI)

Figure C24. Deflection Behaviors for Mat 24: Geometry 10

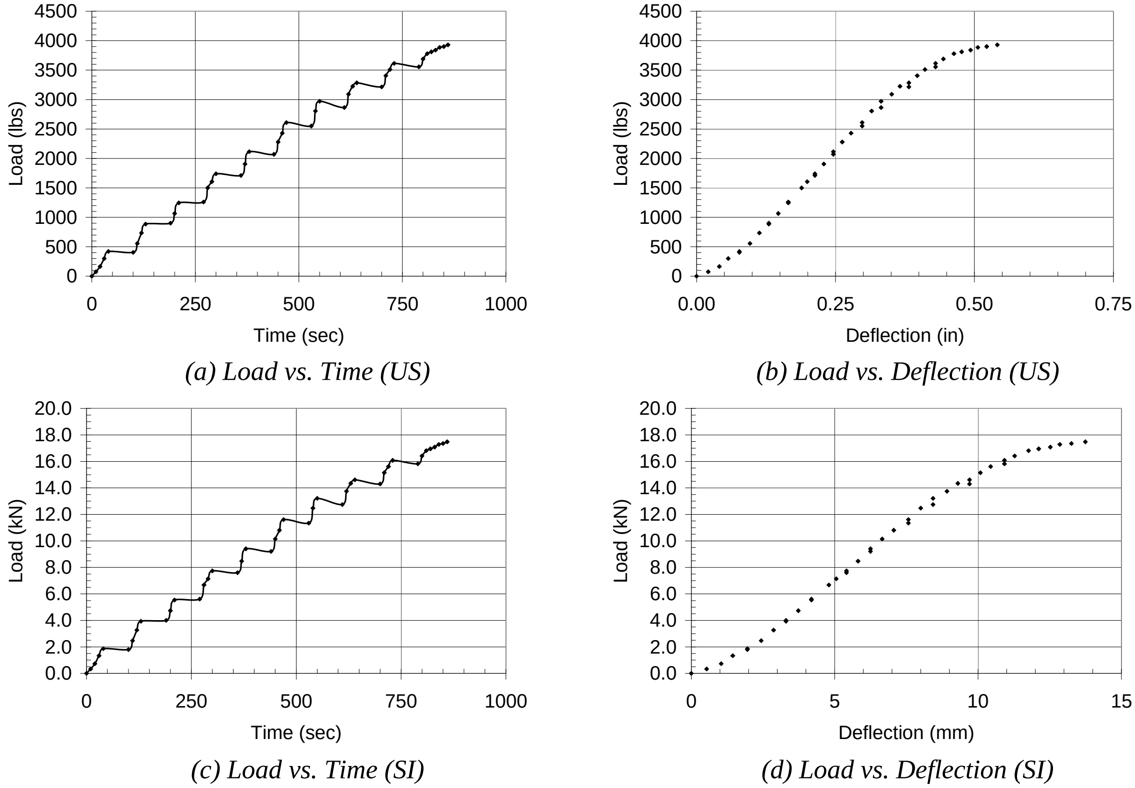

(a) Load vs. Time (US) *(b) Load vs. Deflection (US)*

(c) Load vs. Time (SI) *(d) Load vs. Deflection (SI)*

Figure C25. Deflection Behaviors for Mat 25: Geometry 10

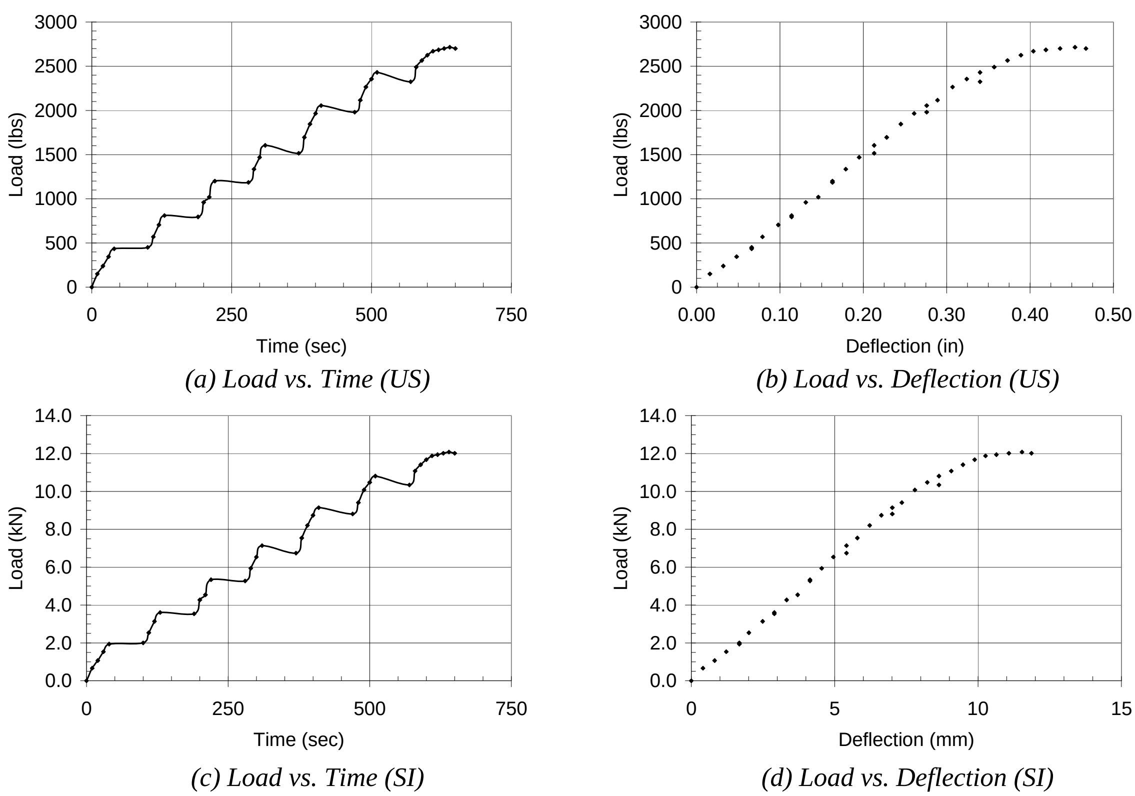

(a) Load vs. Time (US) *(b) Load vs. Deflection (US)*

(c) Load vs. Time (SI) *(d) Load vs. Deflection (SI)*

Figure C26. Deflection Behaviors for Mat 26: Geometry 10

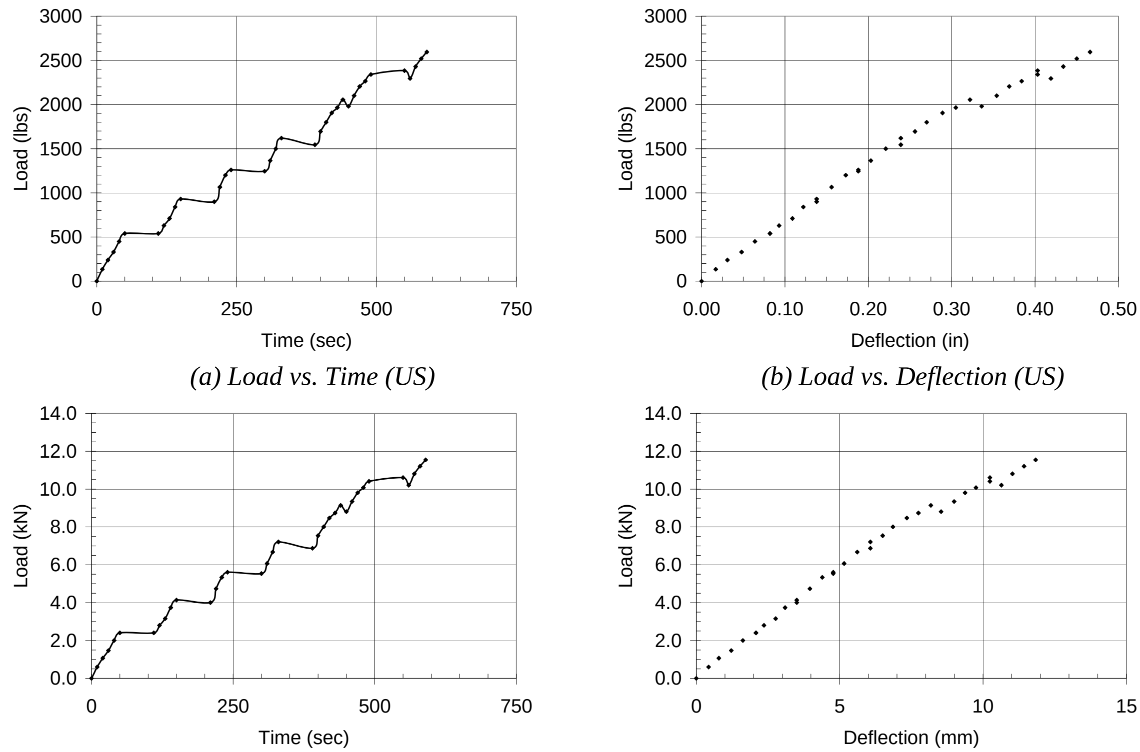

(a) Load vs. Time (US) *(b) Load vs. Deflection (US)*

(c) Load vs. Time (SI) *(d) Load vs. Deflection (SI)*

Figure C27. Deflection Behaviors for Mat 27: Geometry 7

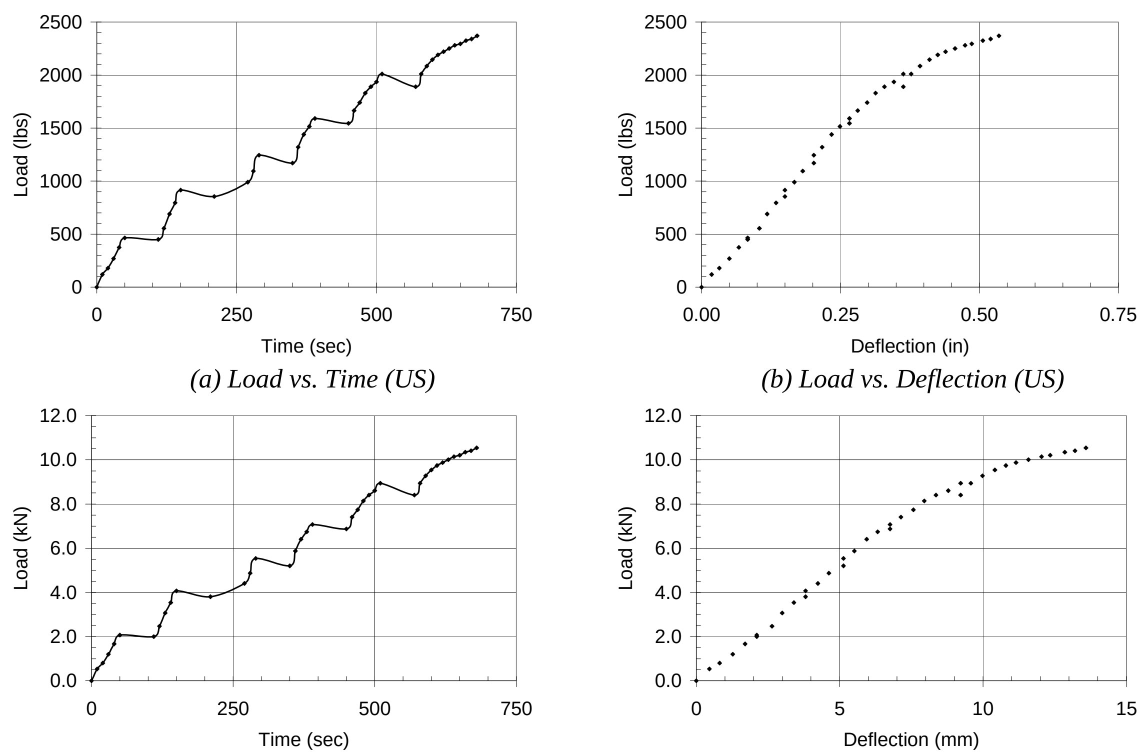

(a) Load vs. Time (US) *(b) Load vs. Deflection (US)*

(c) Load vs. Time (SI) *(d) Load vs. Deflection (SI)*

Figure C28. Deflection Behaviors for Mat 28: Geometry 7

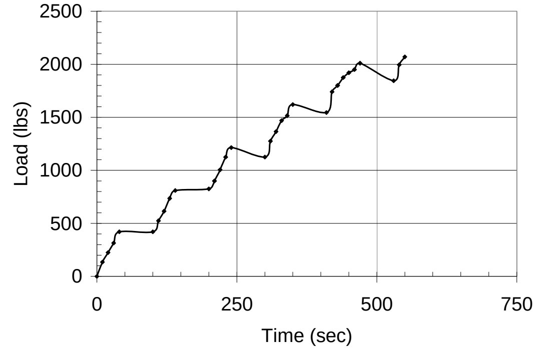

(a) Load vs. Time (US)

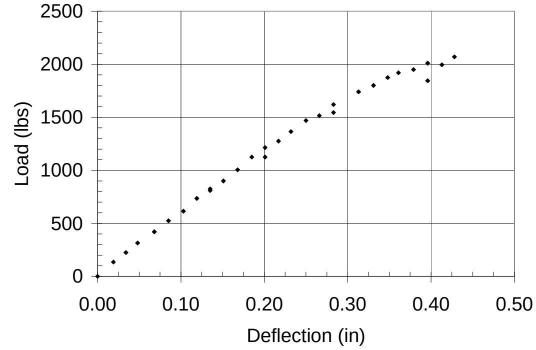

(b) Load vs. Deflection (US)

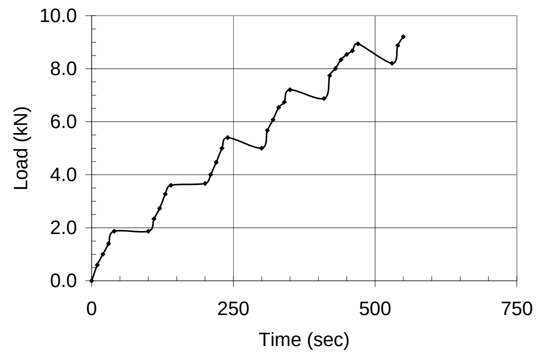

(c) Load vs. Time (SI)

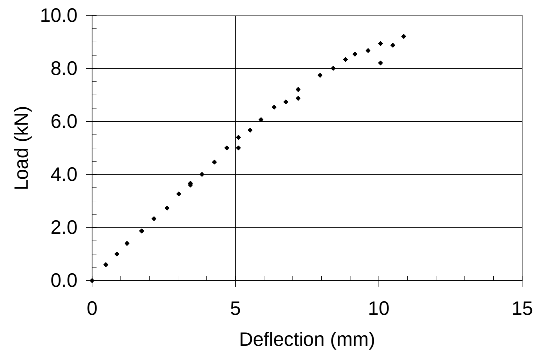

(d) Load vs. Deflection (SI)

Figure C29. Deflection Behaviors for Mat 29: Geometry 7

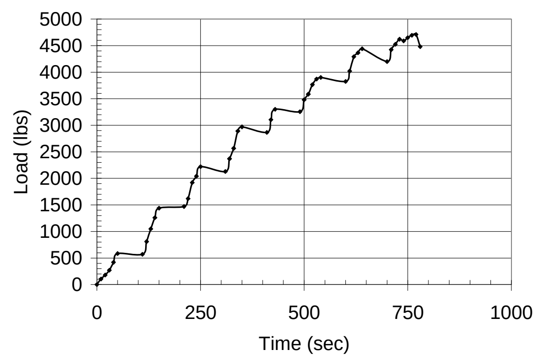

(a) Load vs. Time (US)

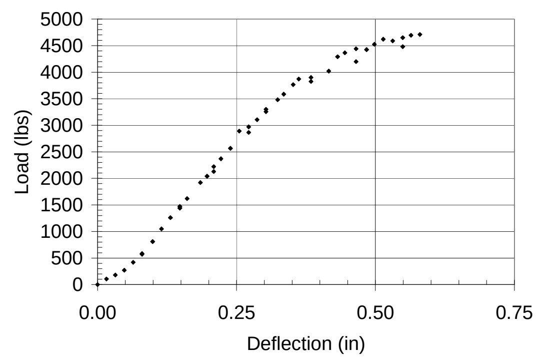

(b) Load vs. Deflection (US)

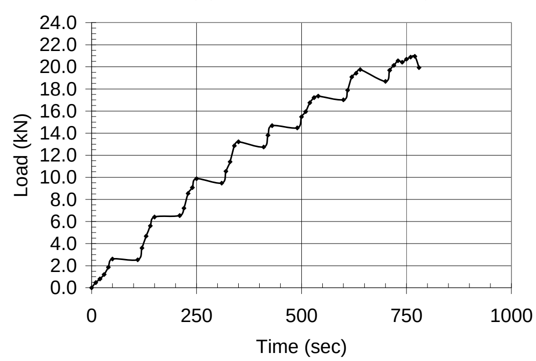

(c) Load vs. Time (SI)

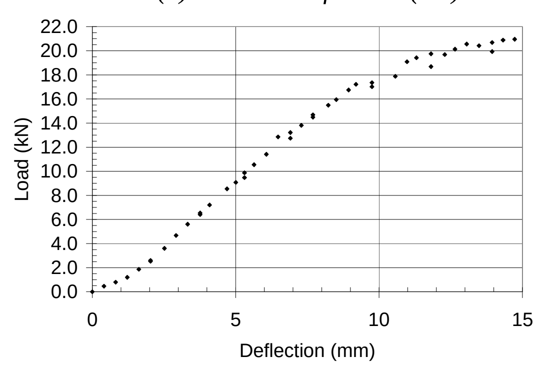

(d) Load vs. Deflection (SI)

Figure C30. Deflection Behaviors for Mat 30: Geometry 12

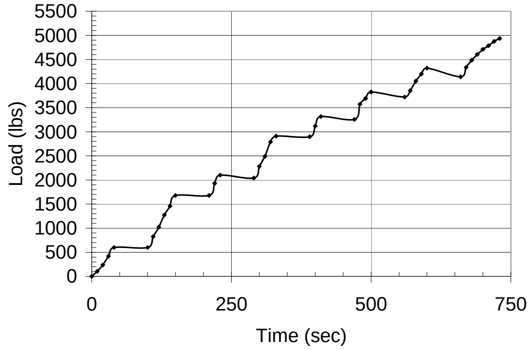

(a) Load vs. Time (US)

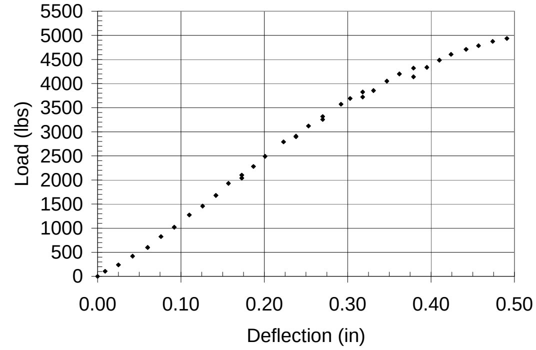

(b) Load vs. Deflection (US)

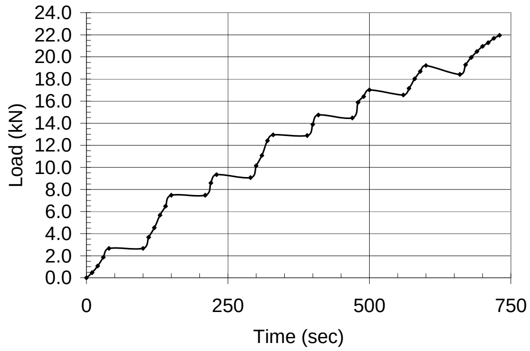

(c) Load vs. Time (SI)

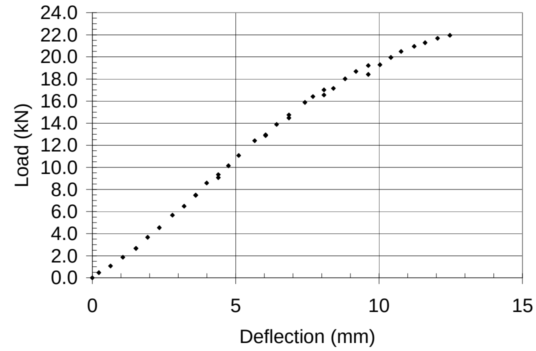

(d) Load vs. Deflection (SI)

Figure C31. Deflection Behaviors for Mat 31: Geometry 12

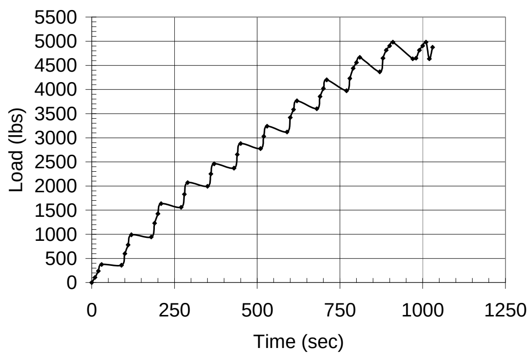

(a) Load vs. Time (US)

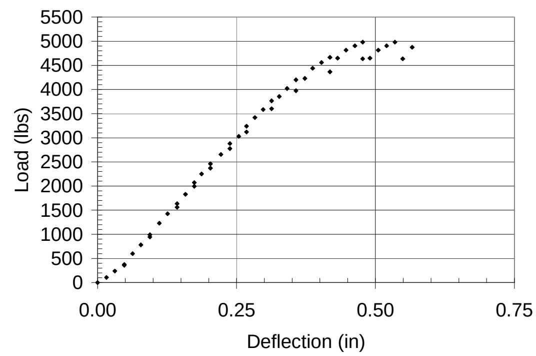

(b) Load vs. Deflection (US)

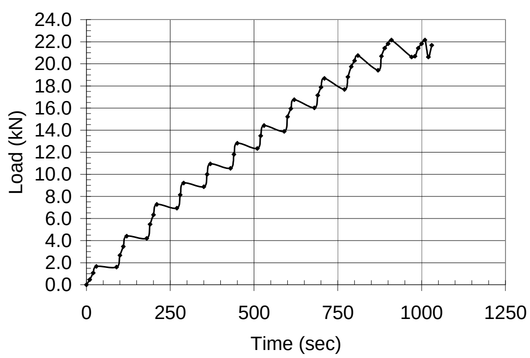

(c) Load vs. Time (SI)

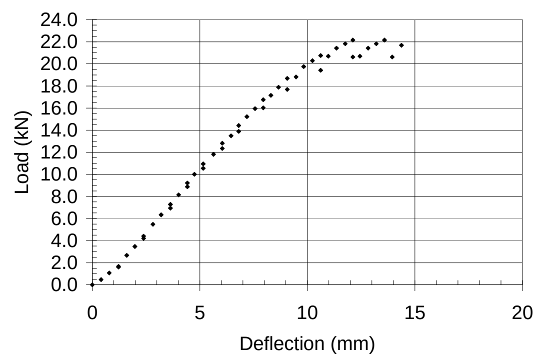

(d) Load vs. Deflection (SI)

Figure C32. Deflection Behaviors for Mat 32: Geometry 12

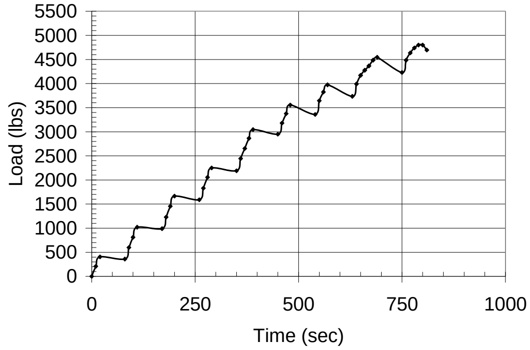

(a) Load vs. Time (US)

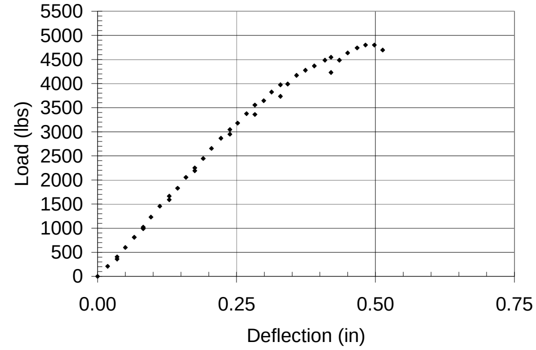

(b) Load vs. Deflection (US)

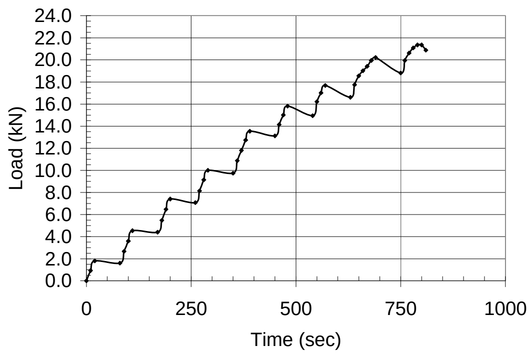

(c) Load vs. Time (SI)

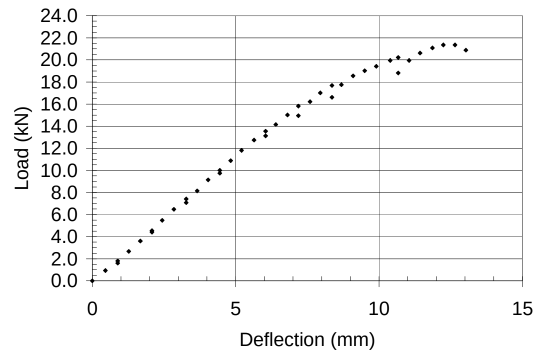

(d) Load vs. Deflection (SI)

Figure C33. Deflection Behaviors for Mat 33: Geometry 12

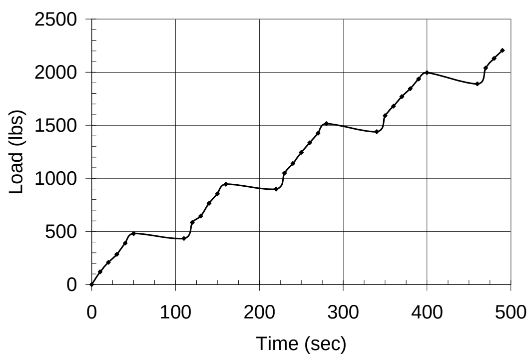

(a) Load vs. Time (US)

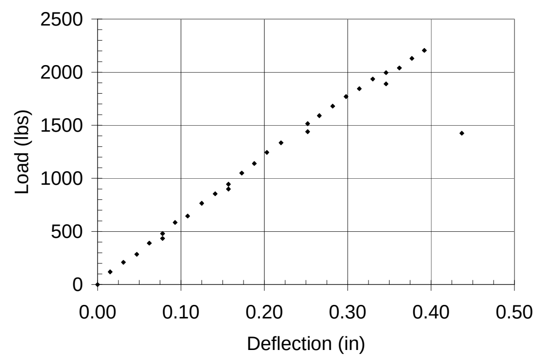

(b) Load vs. Deflection (US)

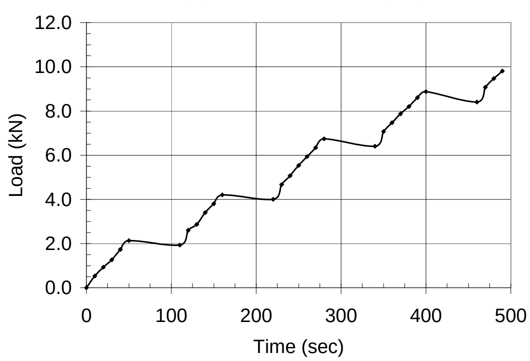

(c) Load vs. Time (SI)

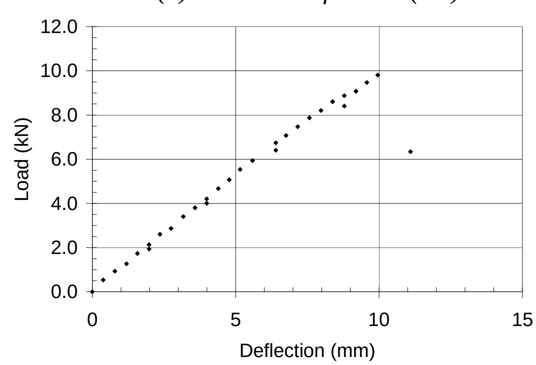

(d) Load vs. Deflection (SI)

Figure C34. Deflection Behaviors for Mat 34: Geometry 12

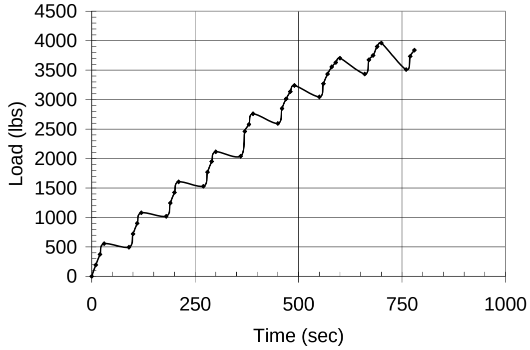

(a) Load vs. Time (US)

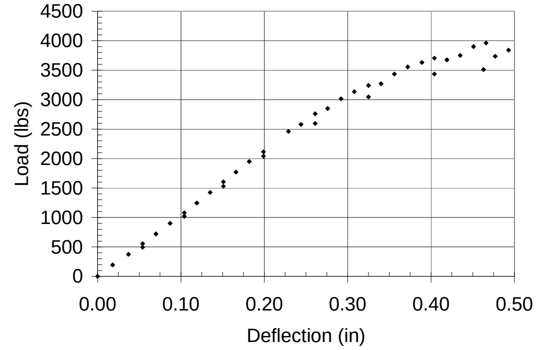

(b) Load vs. Deflection (US)

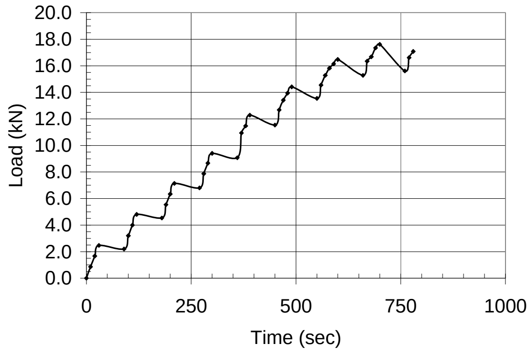

(c) Load vs. Time (SI)

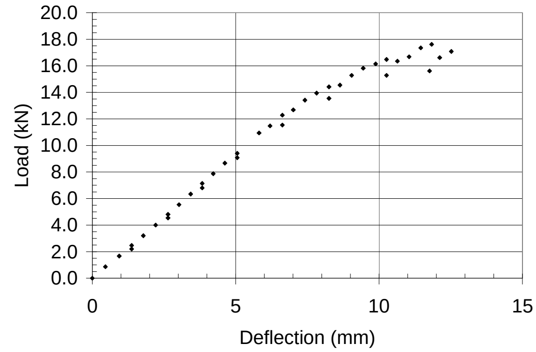

(d) Load vs. Deflection (SI)

Figure C35. Deflection Behaviors for Mat 35: Geometry 12

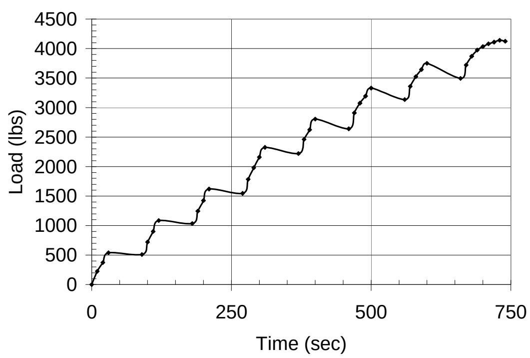

(a) Load vs. Time (US)

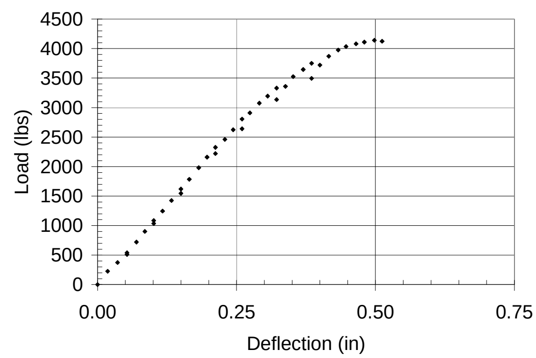

(b) Load vs. Deflection (US)

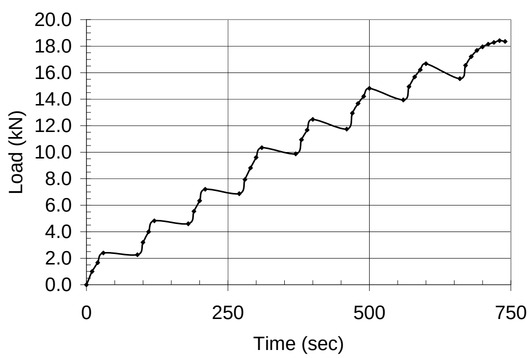

(c) Load vs. Time (SI)

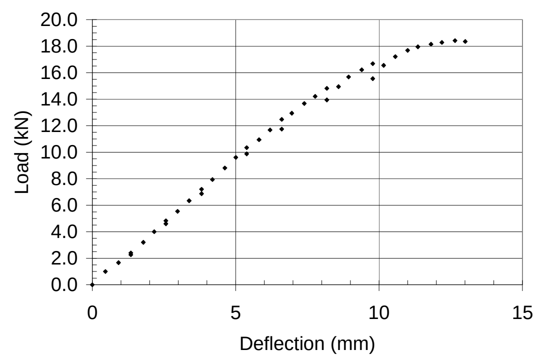

(d) Load vs. Deflection (SI)

Figure C36. Deflection Behaviors for Mat 36: Geometry 12

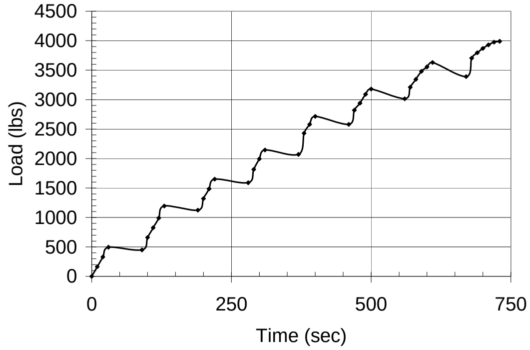

(a) Load vs. Time (US)

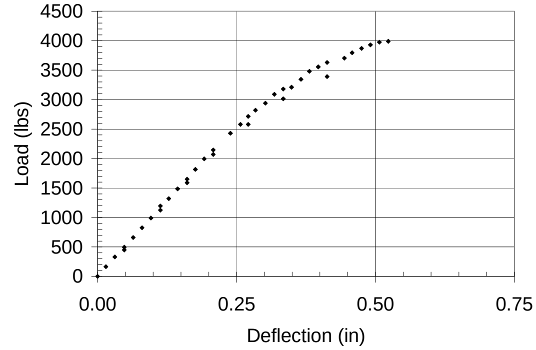

(b) Load vs. Deflection (US)

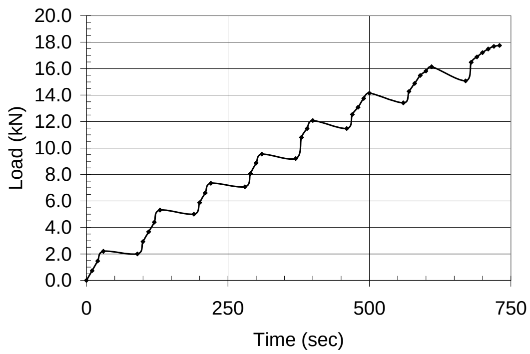

(c) Load vs. Time (SI)

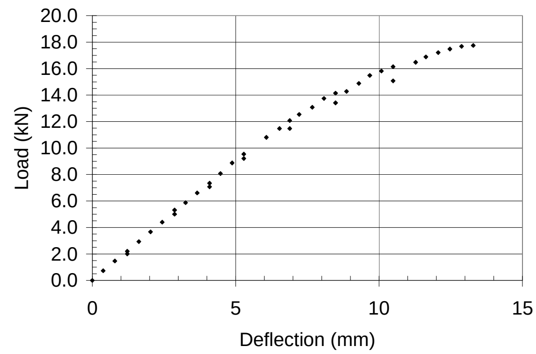

(d) Load vs. Deflection (SI)

Figure C37. Deflection Behaviors for Mat 37: Geometry 12

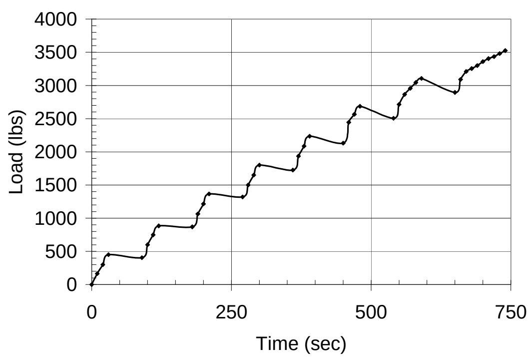

(a) Load vs. Time (US)

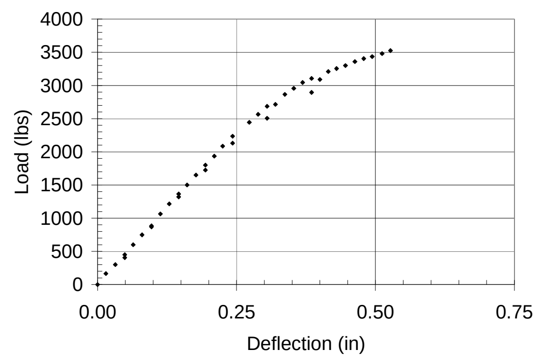

(b) Load vs. Deflection (US)

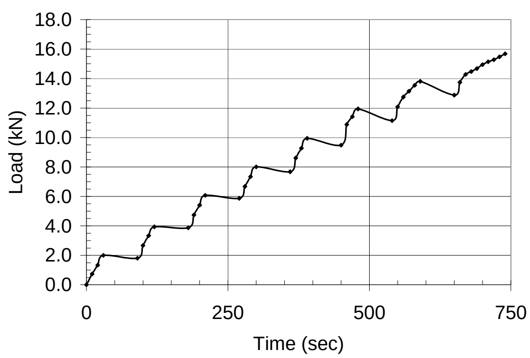

(c) Load vs. Time (SI)

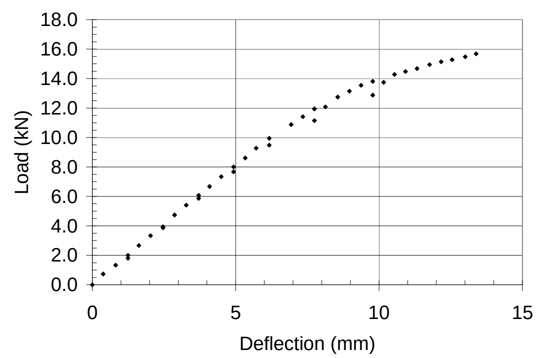

(d) Load vs. Deflection (SI)

Figure C38. Deflection Behaviors for Mat 38: Geometry 12

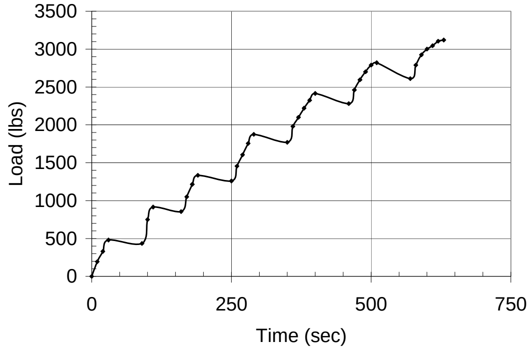

(a) Load vs. Time (US)

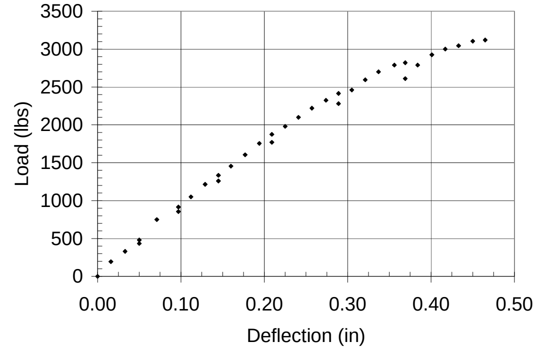

(b) Load vs. Deflection (US)

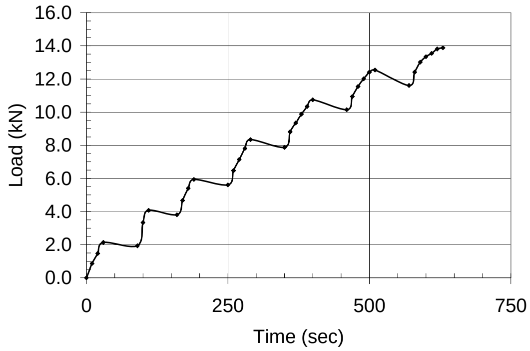

(c) Load vs. Time (SI)

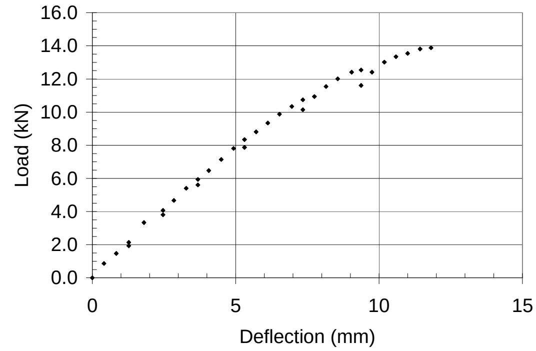

(d) Load vs. Deflection (SI)

Figure C39. Deflection Behaviors for Mat 39: Geometry 12

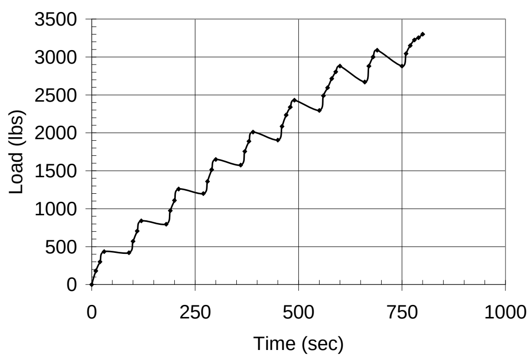

(a) Load vs. Time (US)

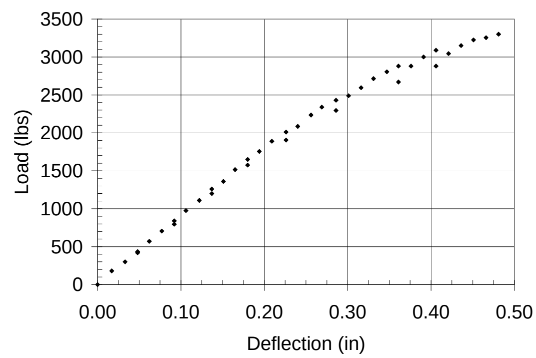

(b) Load vs. Deflection (US)

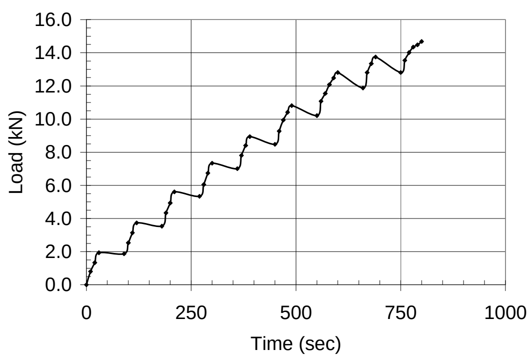

(c) Load vs. Time (SI)

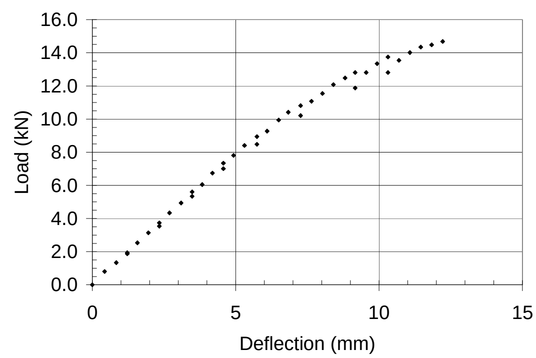

(d) Load vs. Deflection (SI)

Figure C40. Deflection Behaviors for Mat 40: Geometry 12

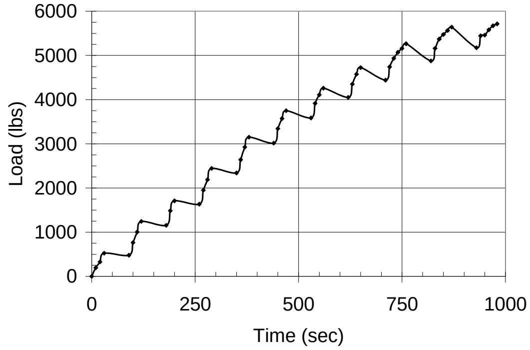

(a) Load vs. Time (US)

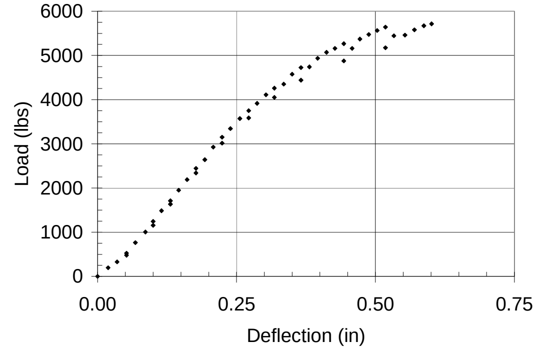

(b) Load vs. Deflection (US)

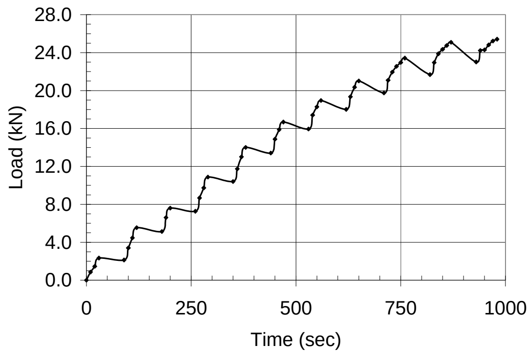

(c) Load vs. Time (SI)

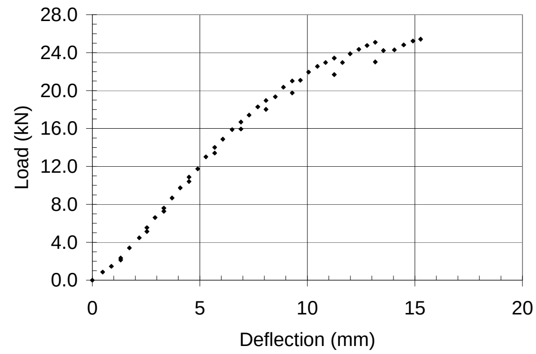

(d) Load vs. Deflection (SI)

Figure C41. Deflection Behaviors for Mat 41: Geometry 12

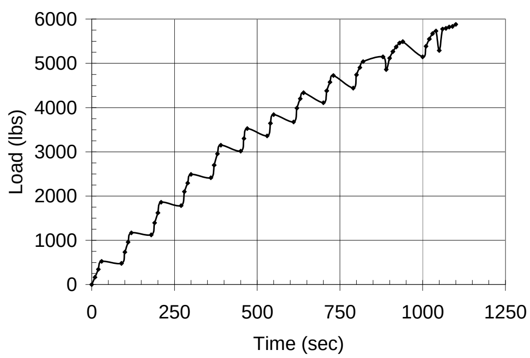

(a) Load vs. Time (US)

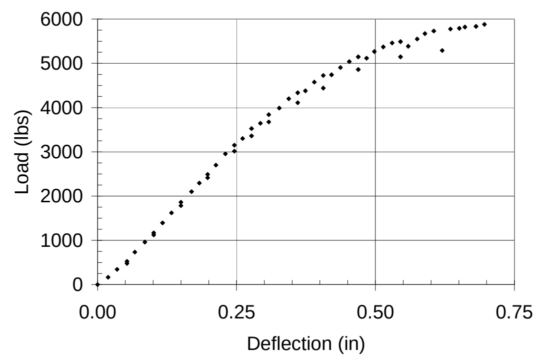

(b) Load vs. Deflection (US)

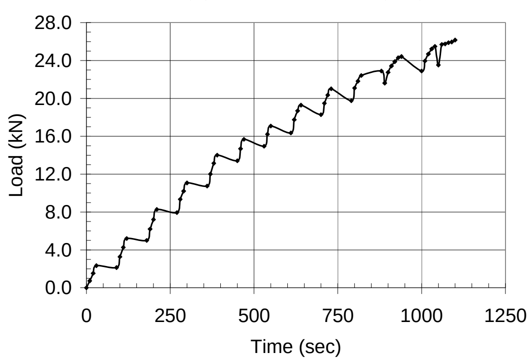

(c) Load vs. Time (SI)

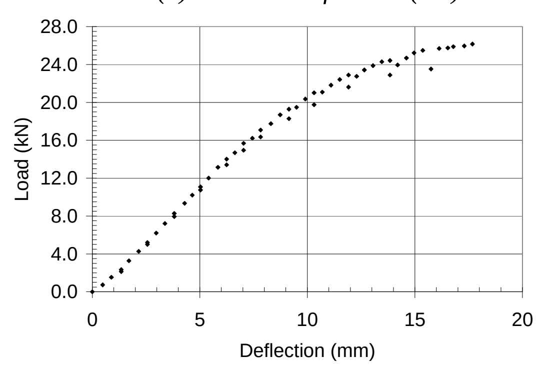

(d) Load vs. Deflection (SI)

Figure C42. Deflection Behaviors for Mat 42: Geometry 12

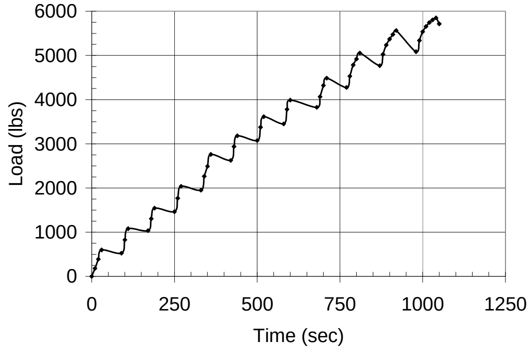

(a) Load vs. Time (US)

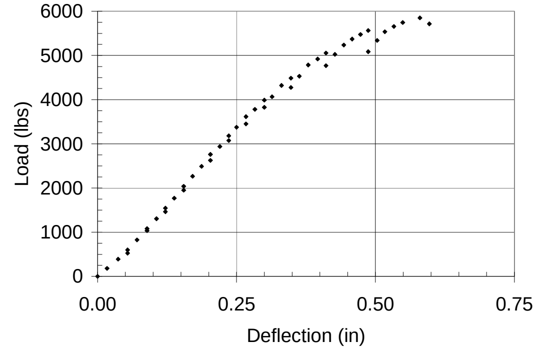

(b) Load vs. Deflection (US)

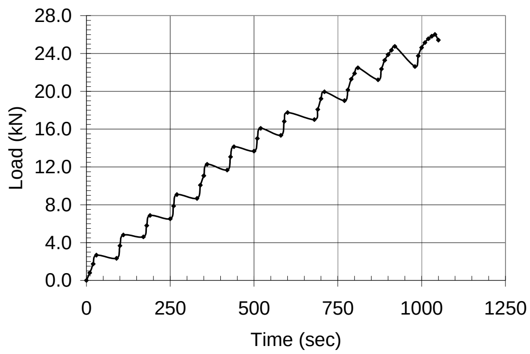

(c) Load vs. Time (SI)

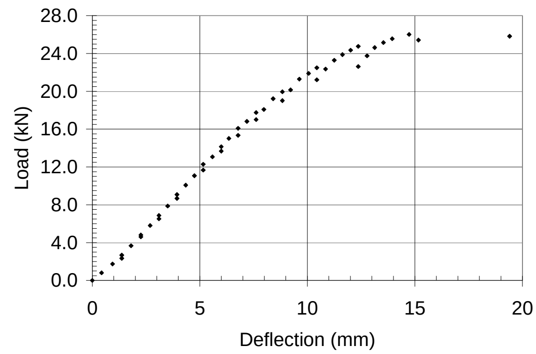

(d) Load vs. Deflection (SI)

Figure C43. Deflection Behaviors for Mat 43: Geometry 12

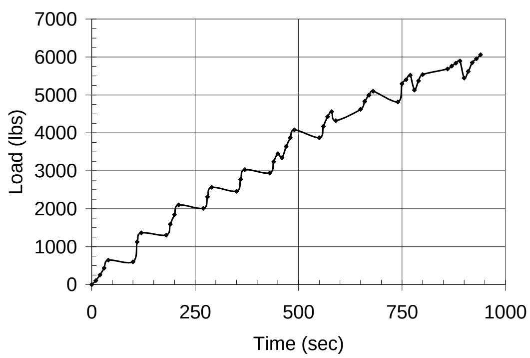

(a) Load vs. Time (US)

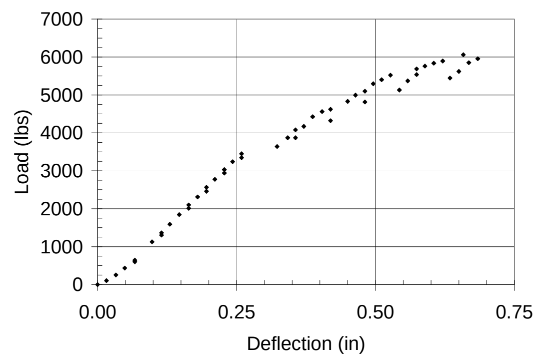

(b) Load vs. Deflection (US)

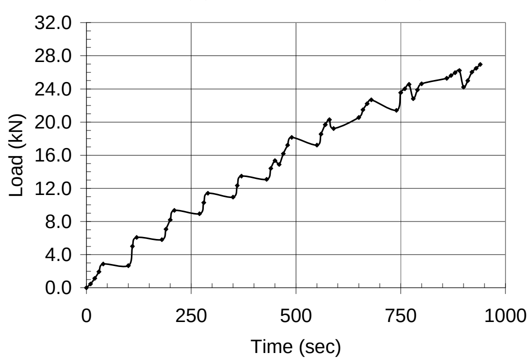

(c) Load vs. Time (SI)

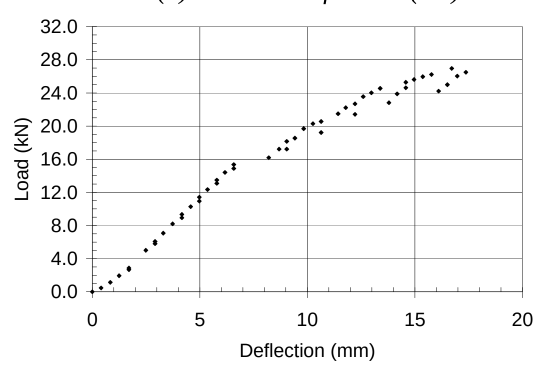

(d) Load vs. Deflection (SI)

Figure C44. Deflection Behaviors for Mat 44: Geometry 12

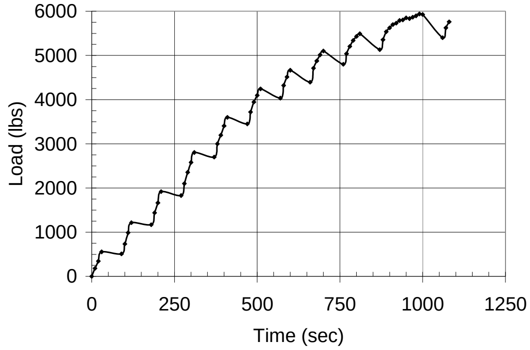

(a) Load vs. Time (US)

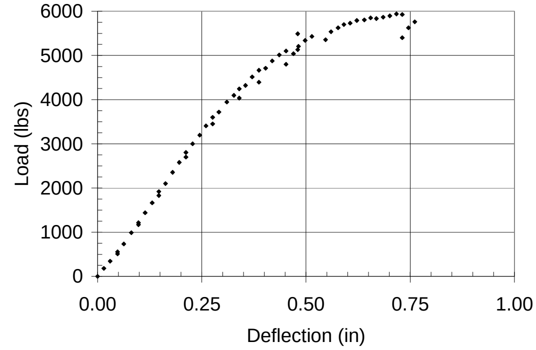

(b) Load vs. Deflection (US)

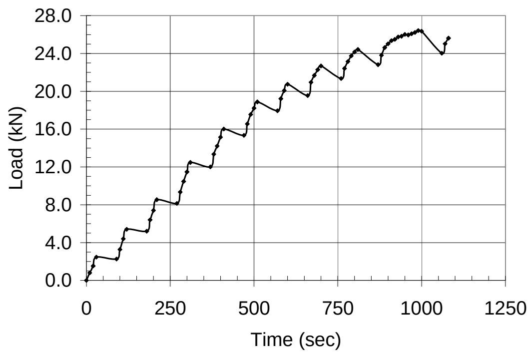

(c) Load vs. Time (SI)

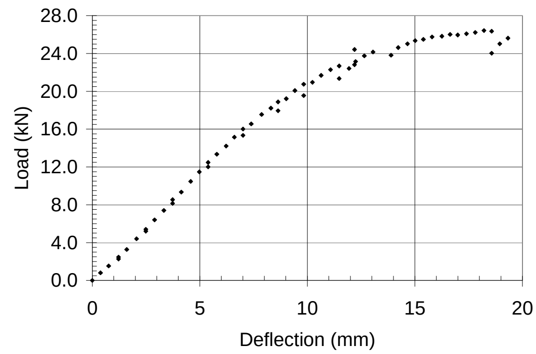

(d) Load vs. Deflection (SI)

Figure C45. Deflection Behaviors for Mat 45: Geometry 12

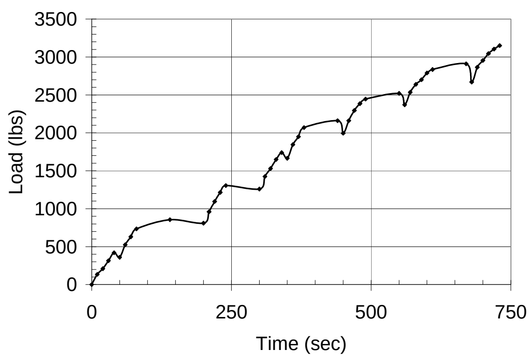

(a) Load vs. Time (US)

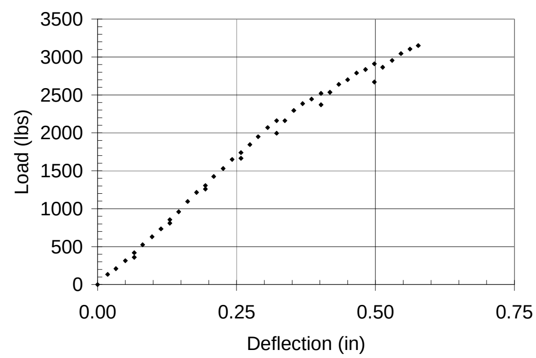

(b) Load vs. Deflection (US)

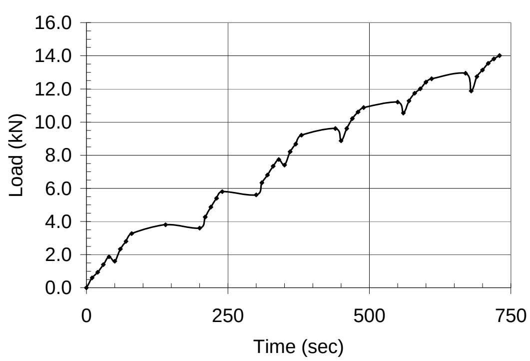

(c) Load vs. Time (SI)

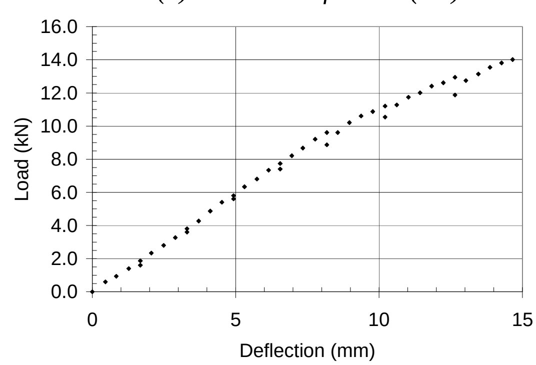

(d) Load vs. Deflection (SI)

Figure C46. Deflection Behaviors for Mat 46: Geometry 11

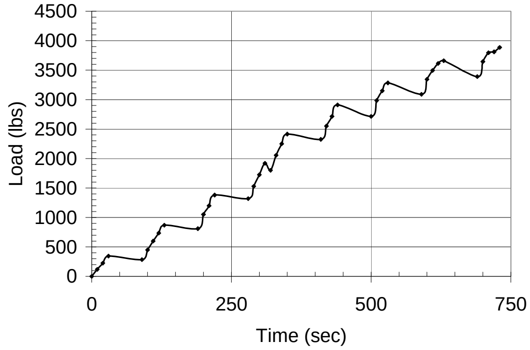

(a) Load vs. Time (US)

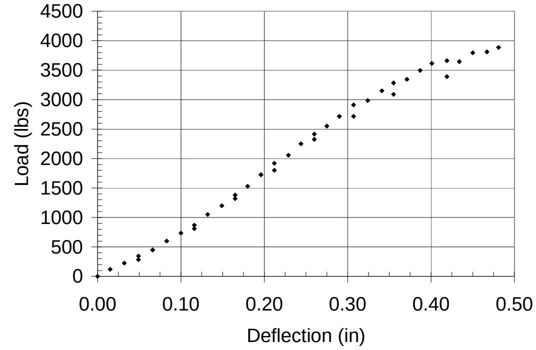

(b) Load vs. Deflection (US)

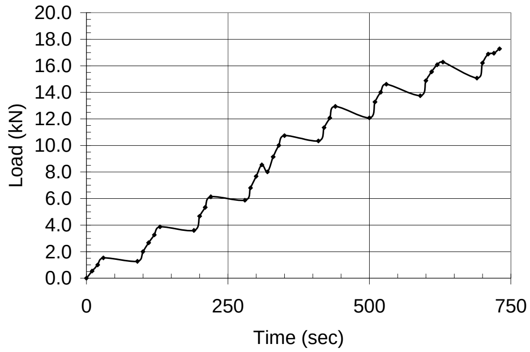

(c) Load vs. Time (SI)

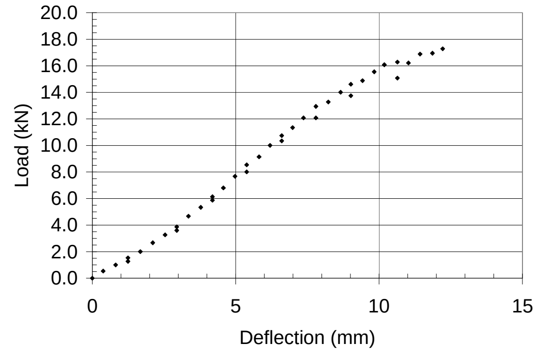

(d) Load vs. Deflection (SI)

Figure C47. Deflection Behaviors for Mat 47: Geometry 11

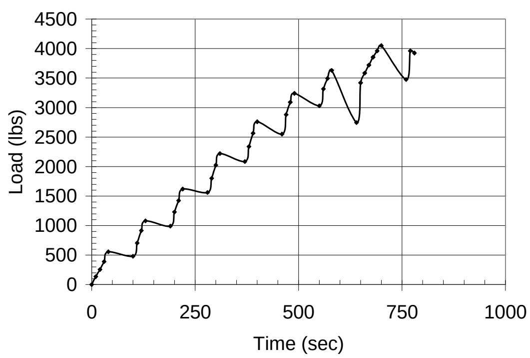

(a) Load vs. Time (US)

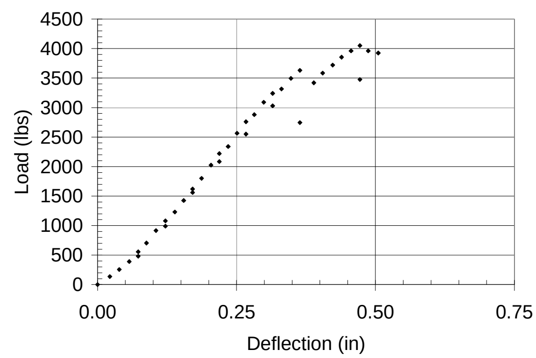

(b) Load vs. Deflection (US)

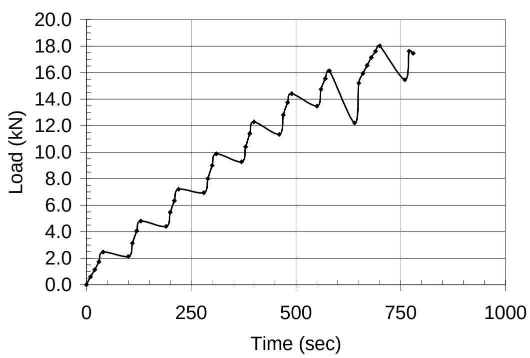

(c) Load vs. Time (SI)

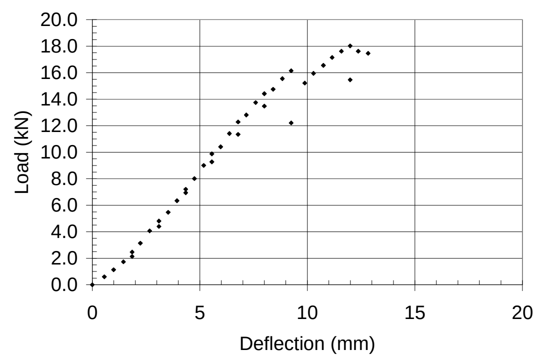

(d) Load vs. Deflection (SI)

Figure C48. Deflection Behaviors for Mat 48: Geometry 11

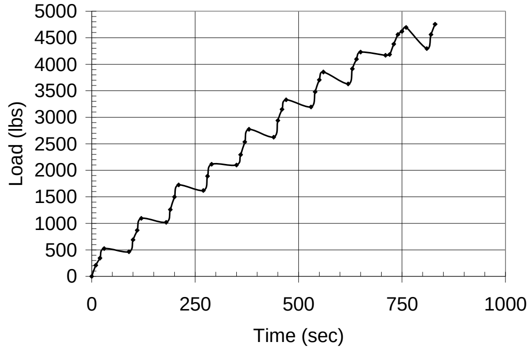

(a) Load vs. Time (US)

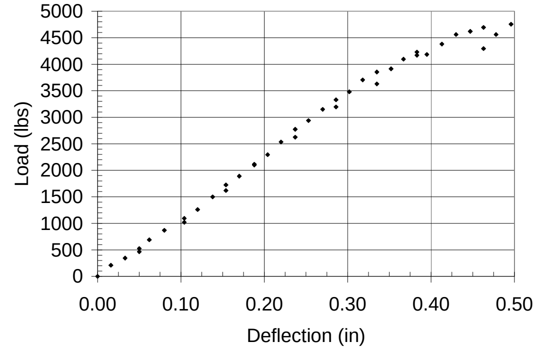

(b) Load vs. Deflection (US)

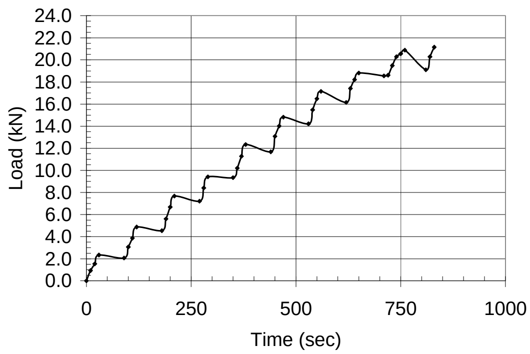

(c) Load vs. Time (SI)

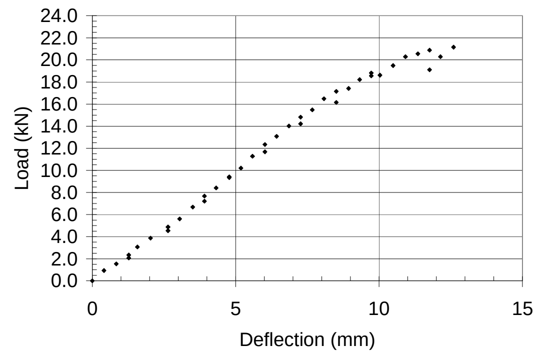

(d) Load vs. Deflection (SI)

Figure C49. Deflection Behaviors for Mat 49: Geometry 11

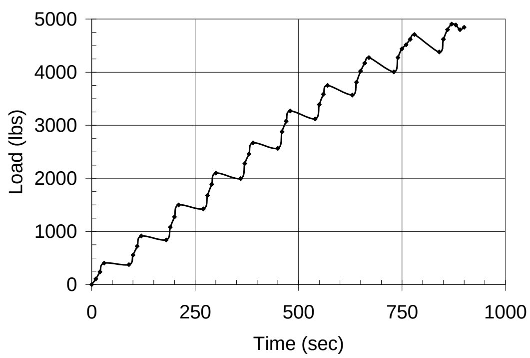

(a) Load vs. Time (US)

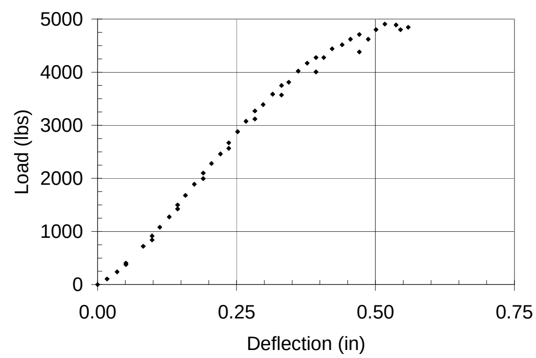

(b) Load vs. Deflection (US)

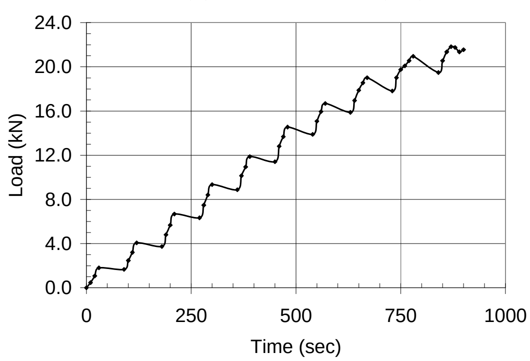

(c) Load vs. Time (SI)

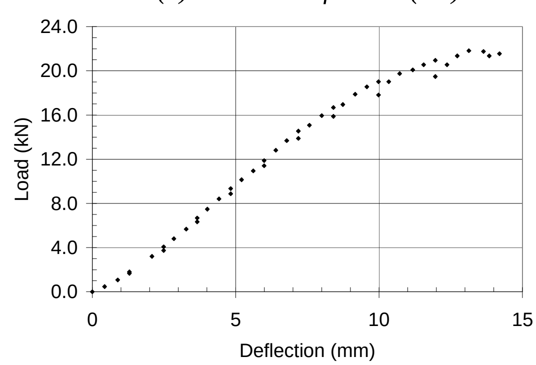

(d) Load vs. Deflection (SI)

Figure C50. Deflection Behaviors for Mat 50: Geometry 11

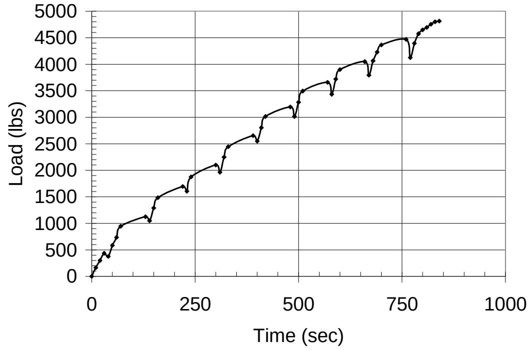

(a) Load vs. Time (US)

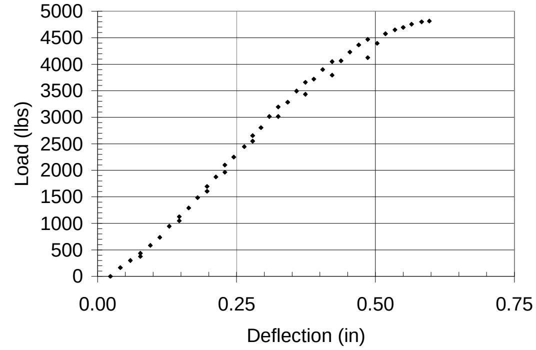

(b) Load vs. Deflection (US)

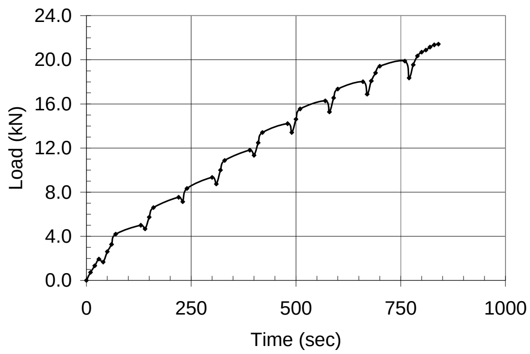

(c) Load vs. Time (SI)

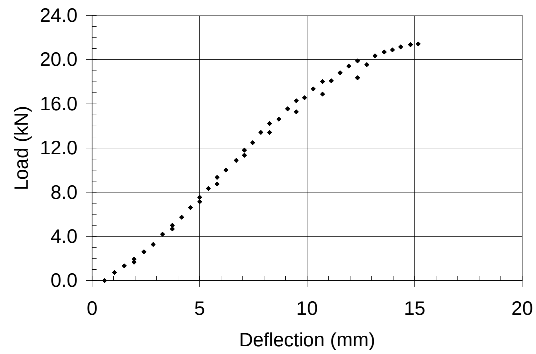

(d) Load vs. Deflection (SI)

Figure C51. Deflection Behaviors for Mat 51: Geometry11

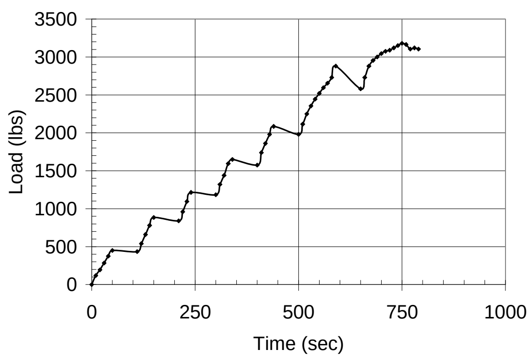

(a) Load vs. Time (US)

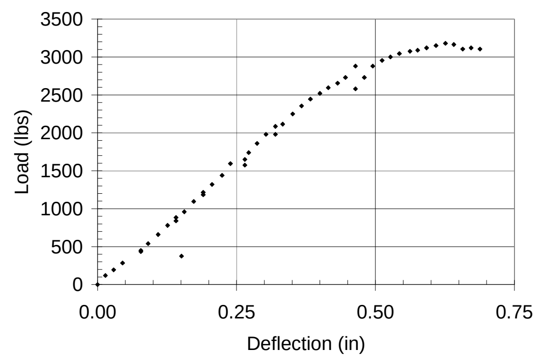

(b) Load vs. Deflection (US)

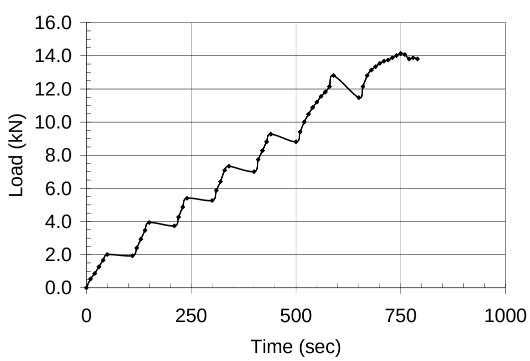

(c) Load vs. Time (SI)

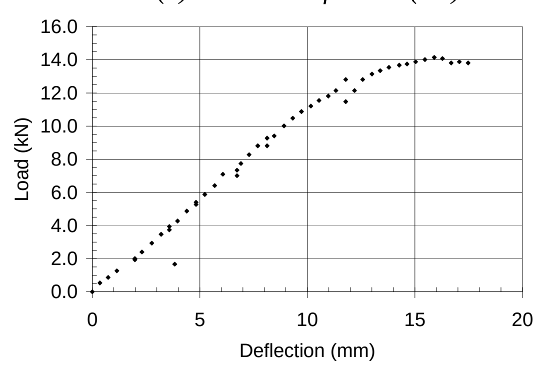

(d) Load vs. Deflection (SI)

Figure C52. Deflection Behaviors for Mat 52: Geometry10

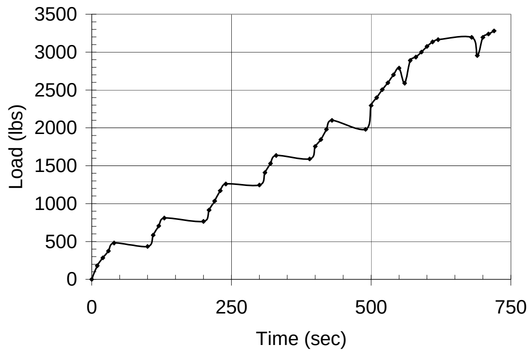

(a) Load vs. Time (US)

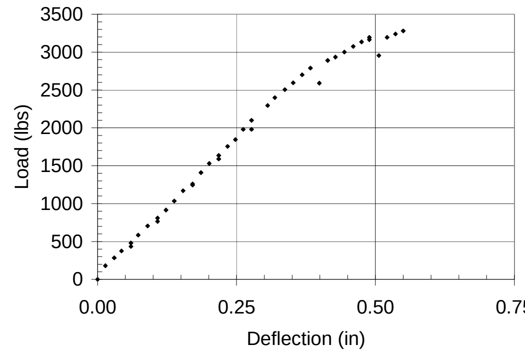

(b) Load vs. Deflection (US)

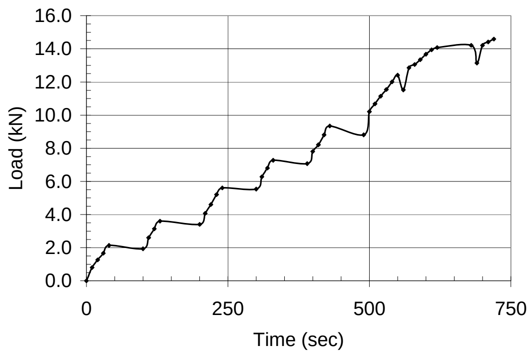

(c) Load vs. Time (SI)

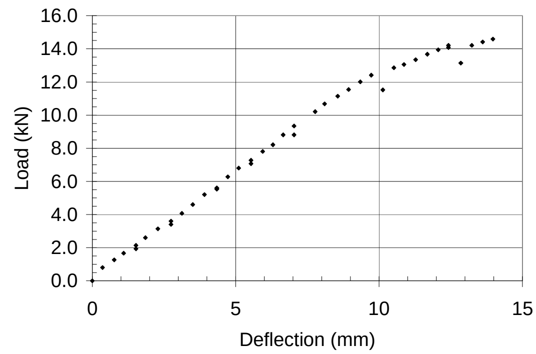

(d) Load vs. Deflection (SI)

Figure C53. Deflection Behaviors for Mat 53: Geometry 10

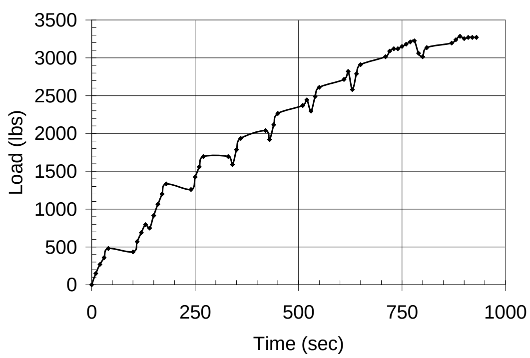

(a) Load vs. Time (US)

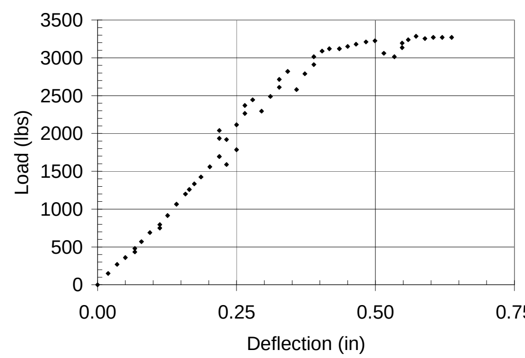

(b) Load vs. Deflection (US)

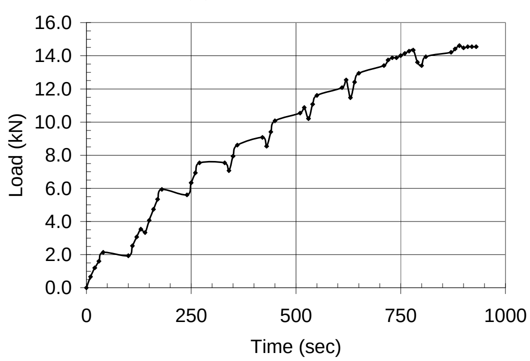

(c) Load vs. Time (SI)

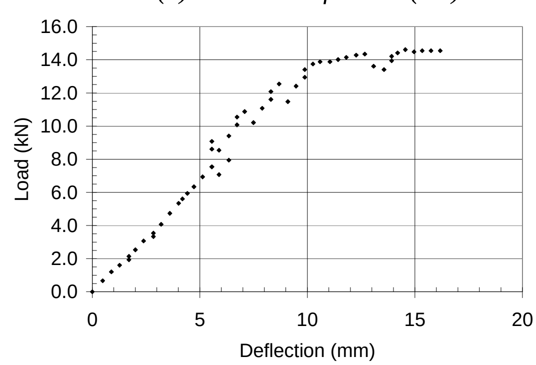

(d) Load vs. Deflection (SI)

Figure C54. Deflection Behaviors for Mat 54: Geometry 10

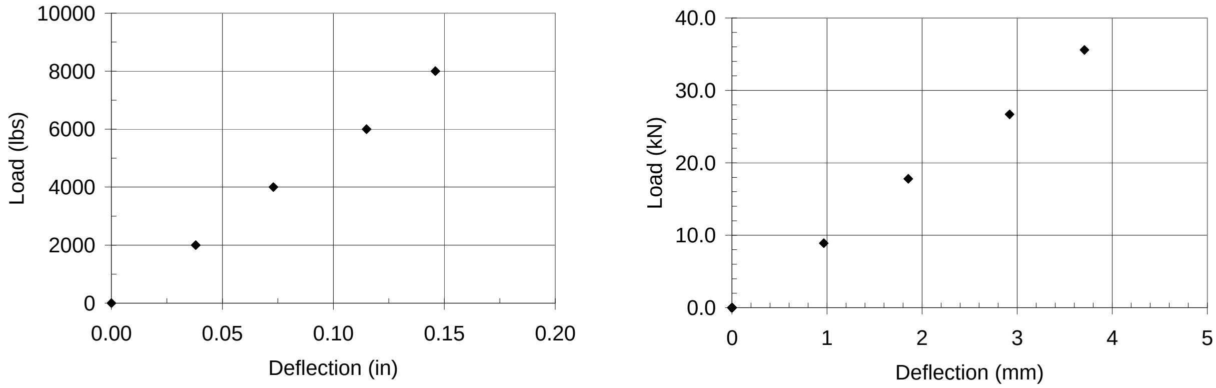

(a) Load vs. Deflection (US) *(b) Load vs. Deflection (SI)*

Figure C.55. Deflection Behaviors for Mat 55: Geometry 14

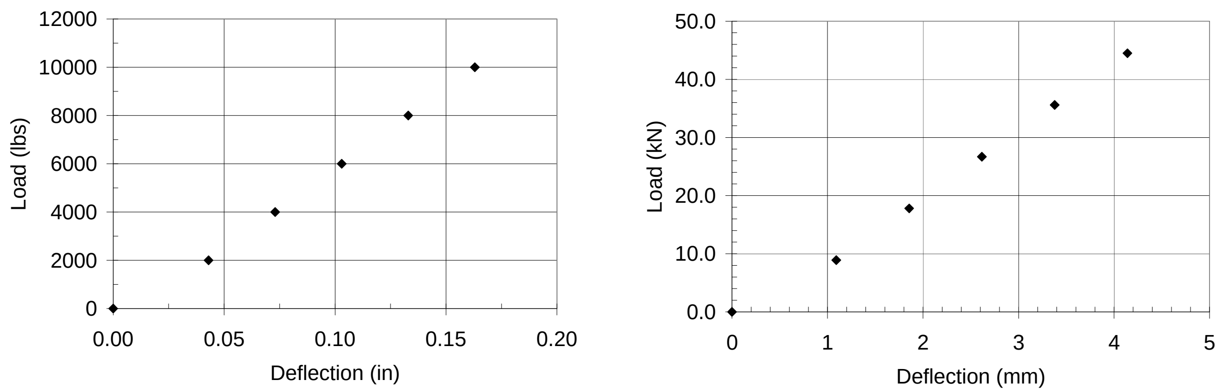

(a) Load vs. Deflection (US) *(b) Load vs. Deflection (SI)*

Figure C.56. Deflection Behaviors for Mat 56: Geometry 15

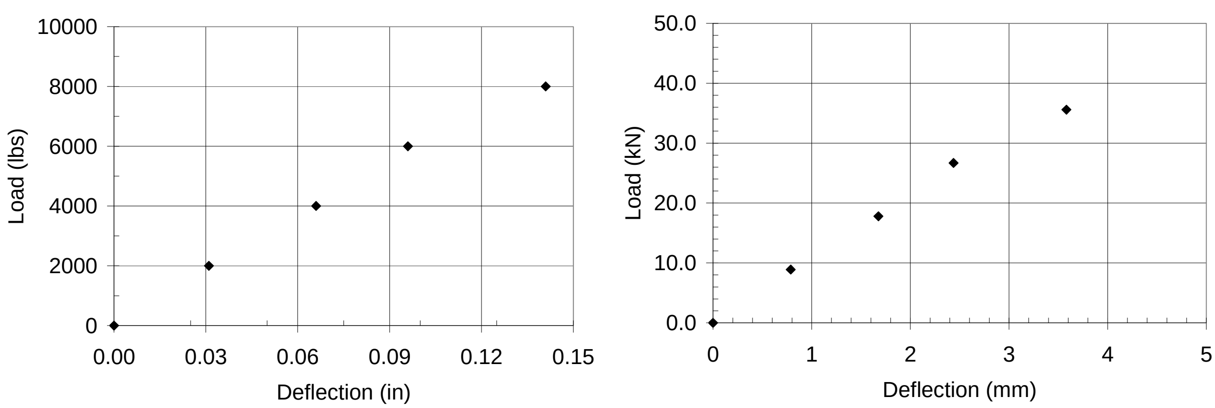

(a) Load vs. Deflection (US) *(b) Load vs. Deflection (SI)*

Figure C.57. Deflection Behaviors for Mat 57: Geometry 15

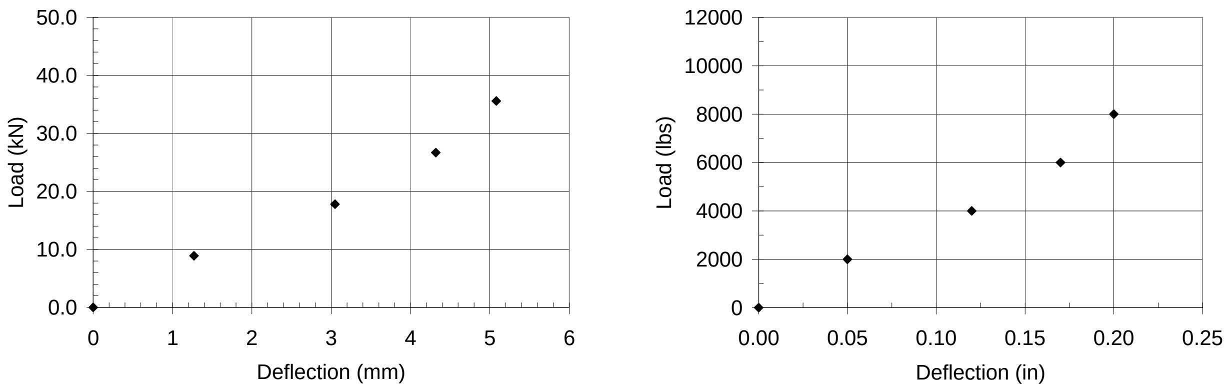

(a) Load vs. Deflection (US) *(b) Load vs. Deflection (SI)*

Figure C.58. Deflection Behaviors for Mat 58: Geometry 16

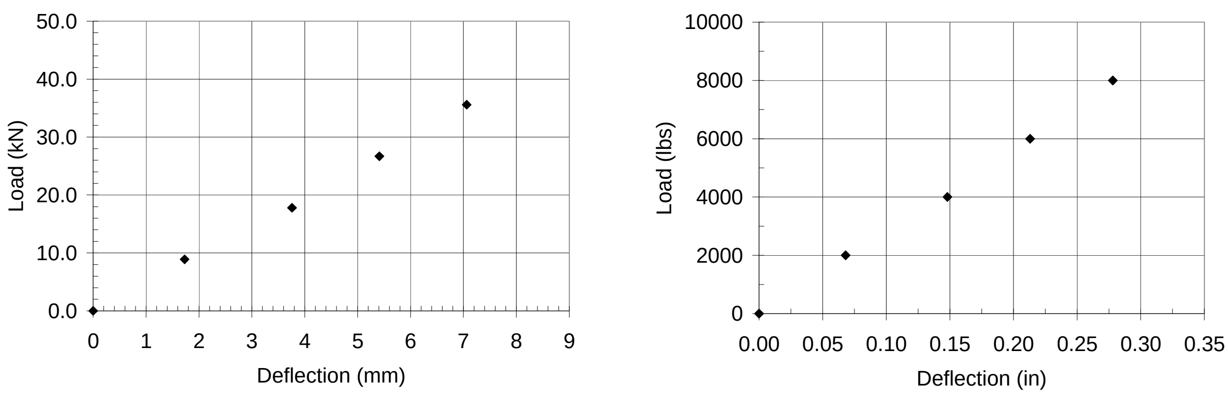

(a) Load vs. Deflection (US) *(b) Load vs. Deflection (SI)*

Figure C.59. Deflection Behaviors for Mat 59: Geometry 16

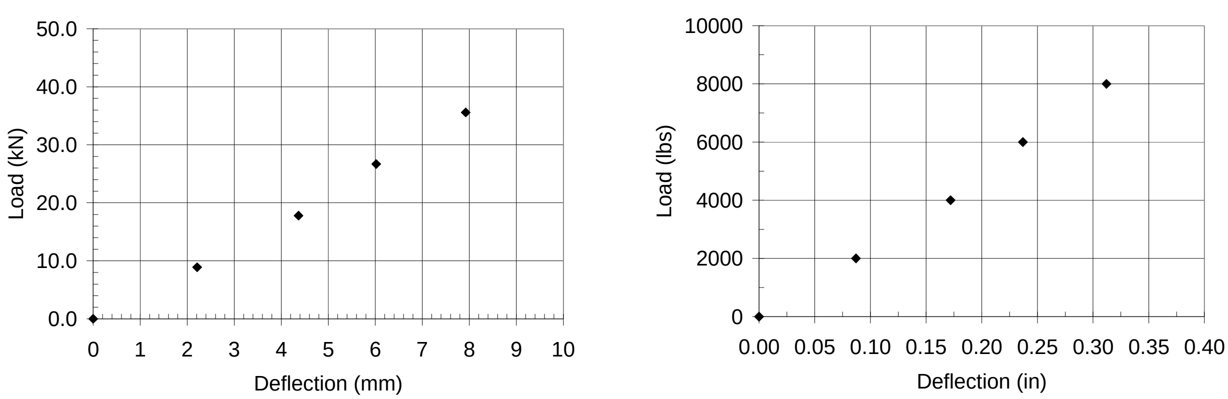

(a) Load vs. Deflection (US) *(b) Load vs. Deflection (SI)*

Figure C.60. Deflection Behaviors for Mat 60: Geometry 16

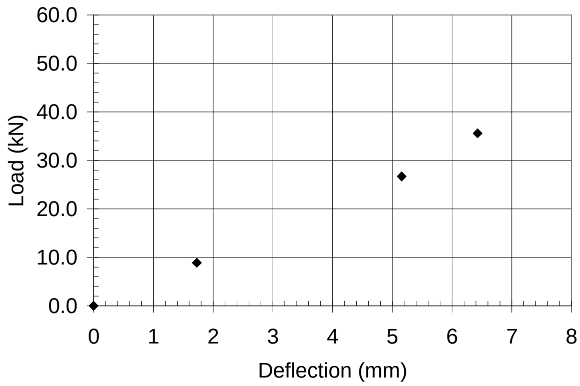

(a) Load vs. Deflection (US)

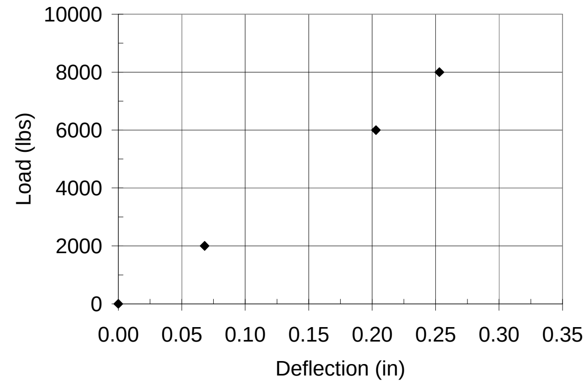

(b) Load vs. Deflection (SI)

Figure C.61. Deflection Behaviors for Mat 61: Geometry 16

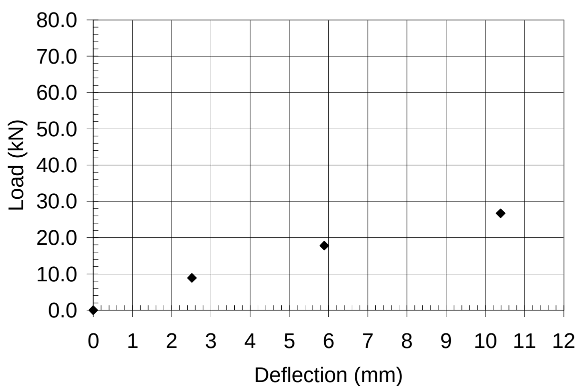

(a) Load vs. Deflection (US)

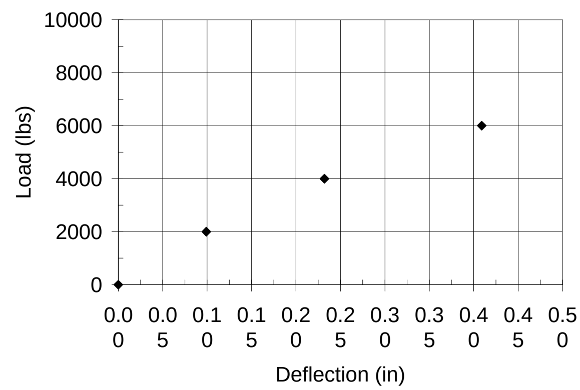

(b) Load vs. Deflection (SI)

Figure C.62. Deflection Behaviors for Mat 62: Geometry 17

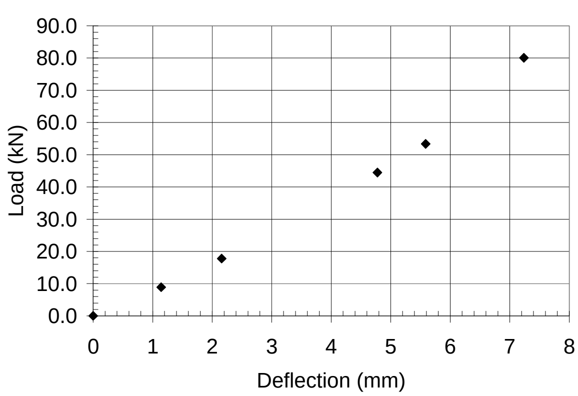

(a) Load vs. Deflection (US)

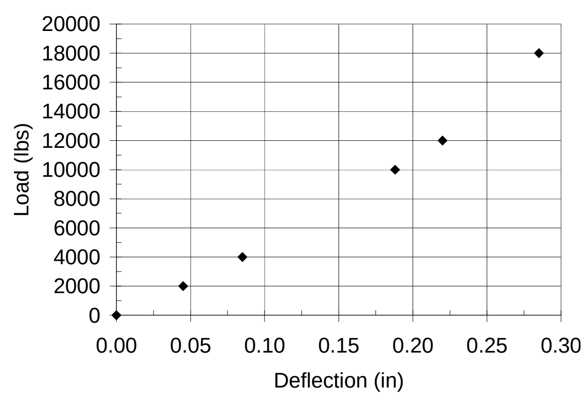

(b) Load vs. Deflection (SI)

Figure C.63. Deflection Behaviors for Mat 63: Geometry 18

APPENDIX D-STRAIN PLOTS

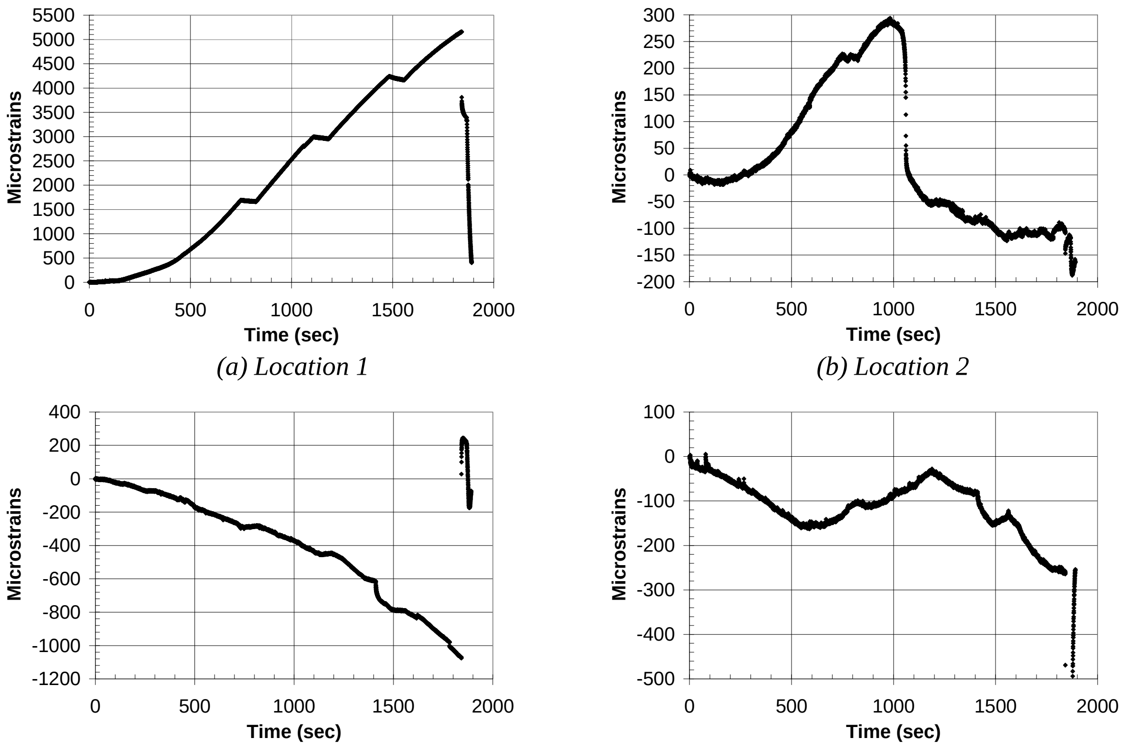

(a) Location 1 (b) Location 2

(c) Location 3 (d) Location 4

Figure D1. Strain v/s Time for Mat 1: Geometry 1

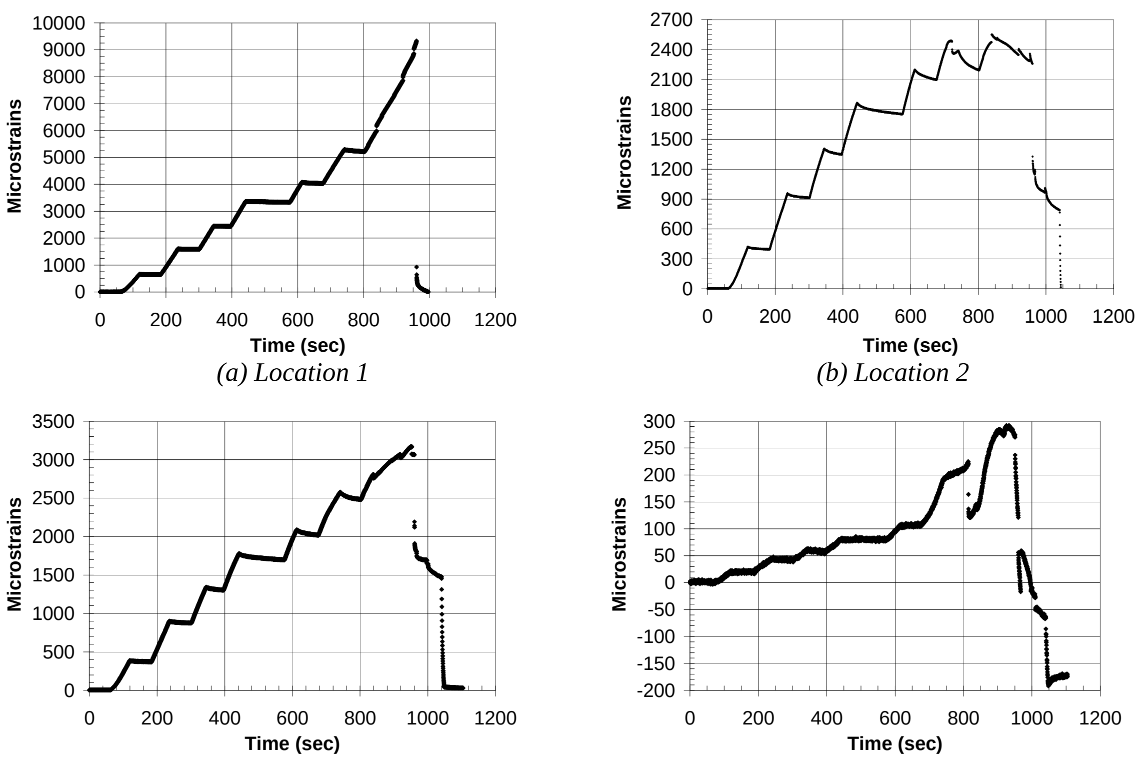

(a) Location 1 (b) Location 2

(c) Location 3 (d) Location 4

Figure D2. Strain v/s Time for Mat 2: Geometry 13

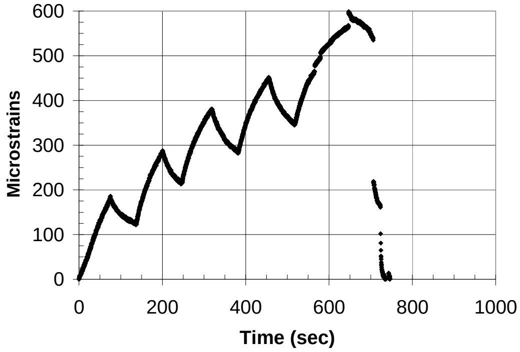

(a) Location 1

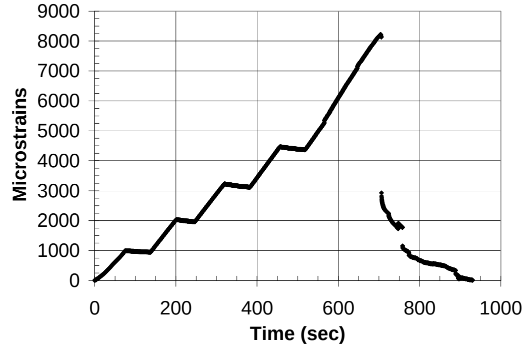

(b) Location 2

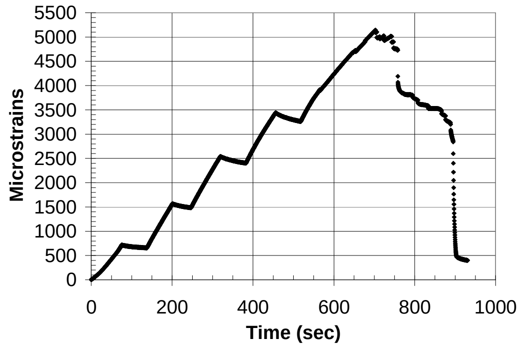

(c) Location 3

Figure D3. Strain v/s Time for Mat 3: Geometry 9

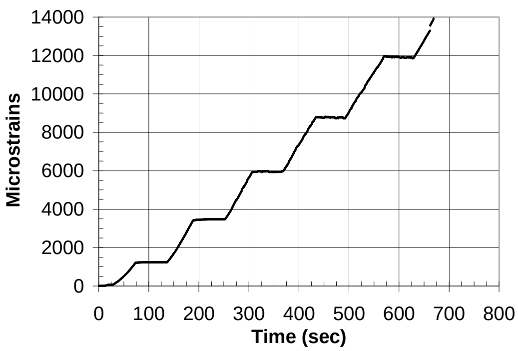

(a) Location 1

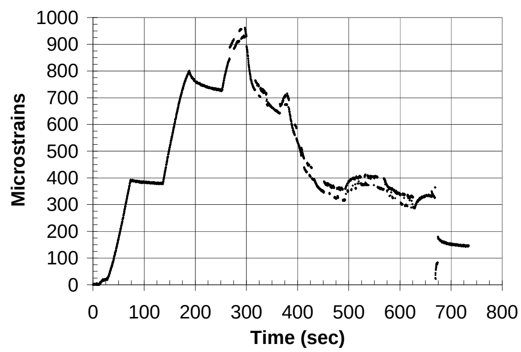

(b) Location 2

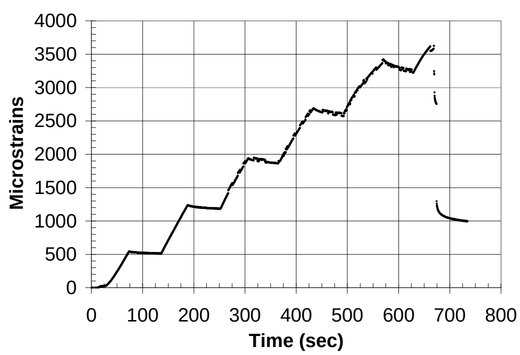

(c) Location 3

Figure D4. Strain v/s Time for Mat 4: Geometry 8

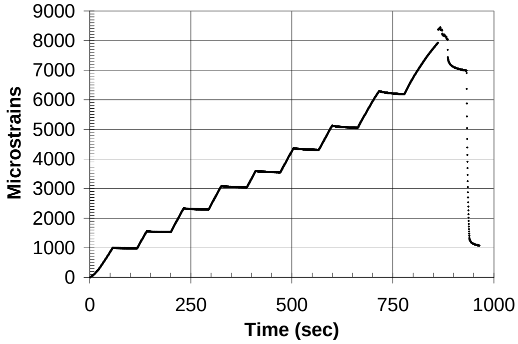

(a) Location 1

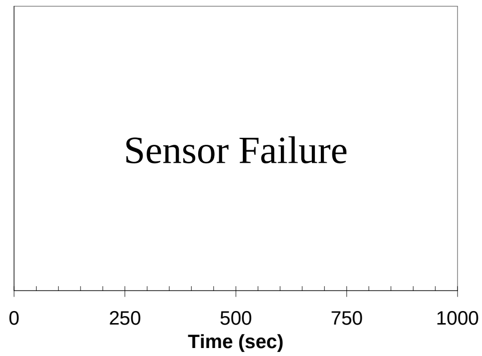

(b) Location 2

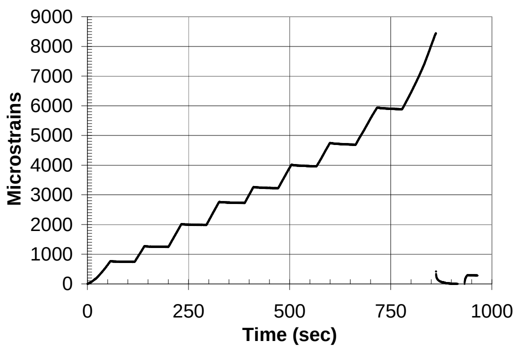

(c) Location 3

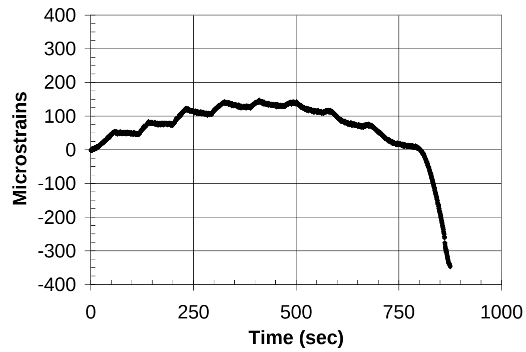

(d) Location 4

Figure D5. Strain v/s Time for Mat 5: Geometry 5

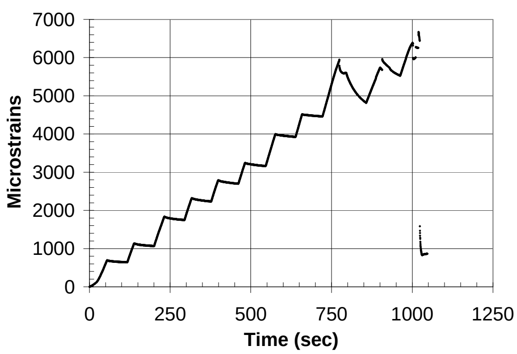

(a) Location 1

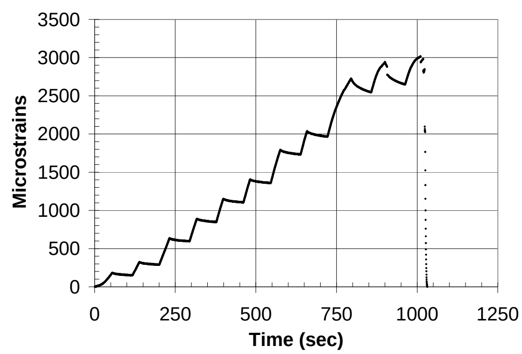

(b) Location 2

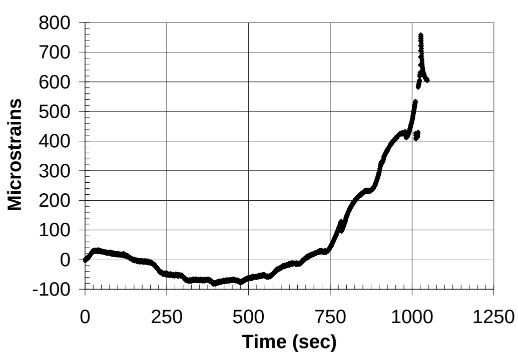

(c) Location 3

Figure D6. Strain v/s Time for Mat 6: Geometry 11

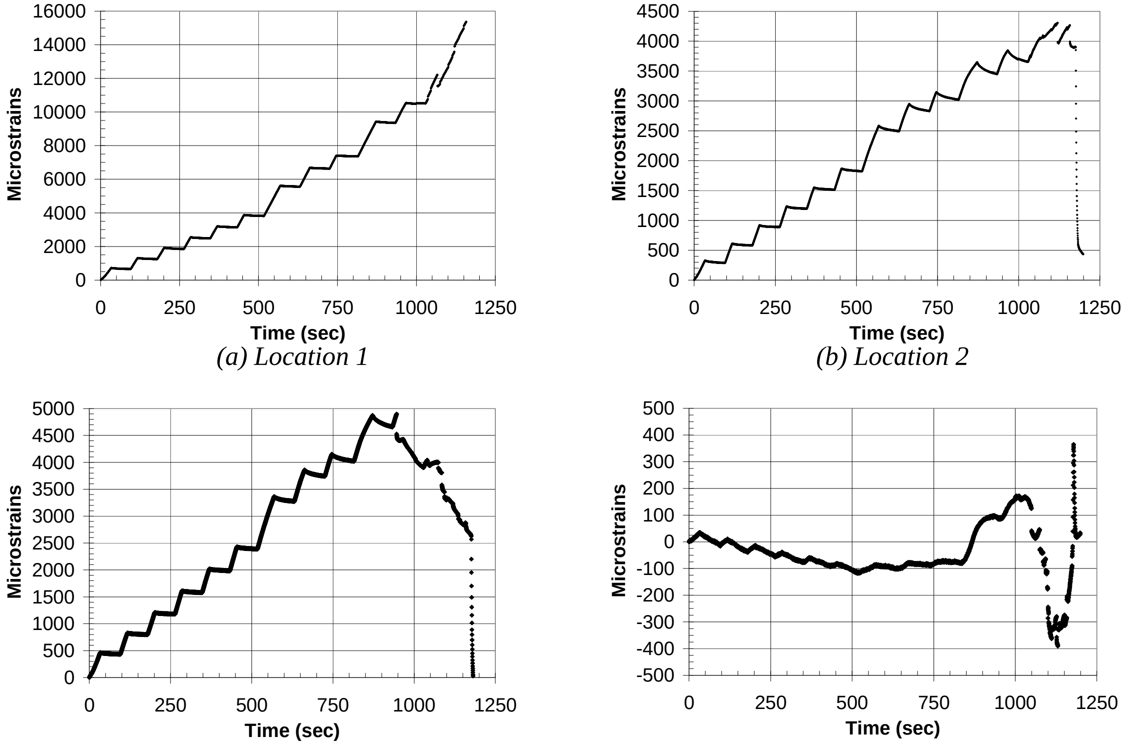

(a) Location 1 (b) Location 2

(c) Location 3 (d) Location 4

Figure D7. Strain v/s Time for Mat 7: Geometry 11

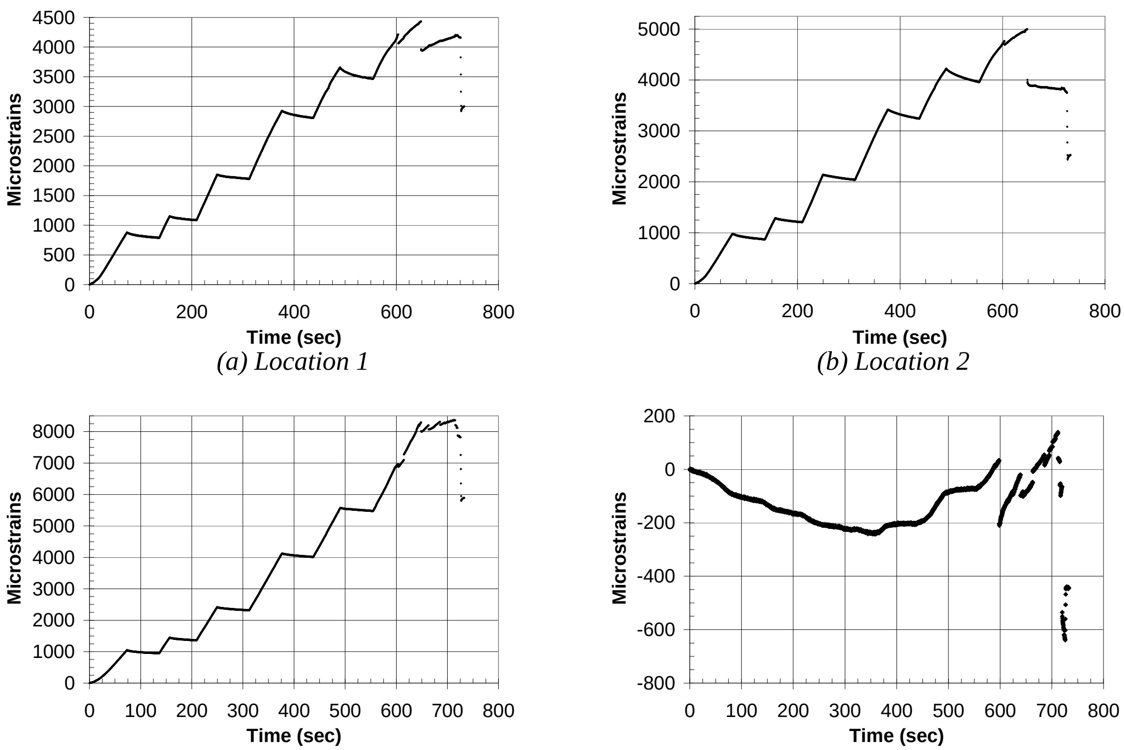

(a) Location 1 (b) Location 2

(c) Location 3 (d) Location 4

Figure D8. Strain v/s Time for Mat 8: Geometry 10

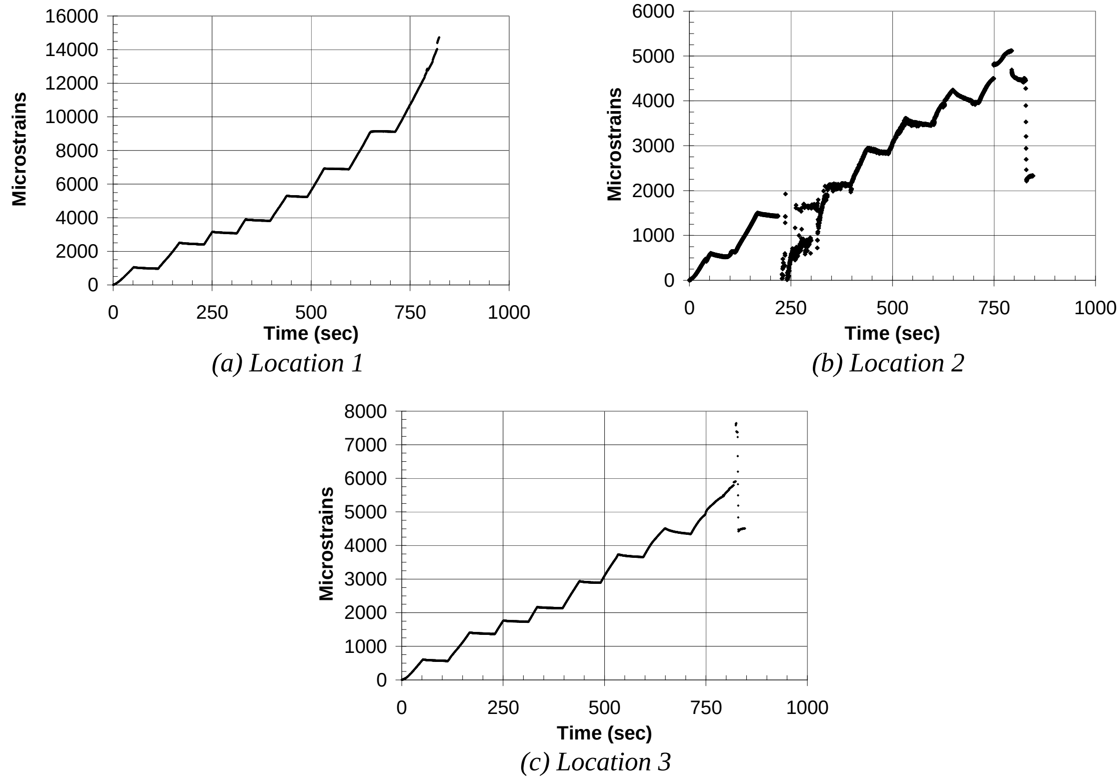

(a) Location 1 (b) Location 2 (c) Location 3

Figure D9. Strain v/s Time for Mat 9: Geometry 10

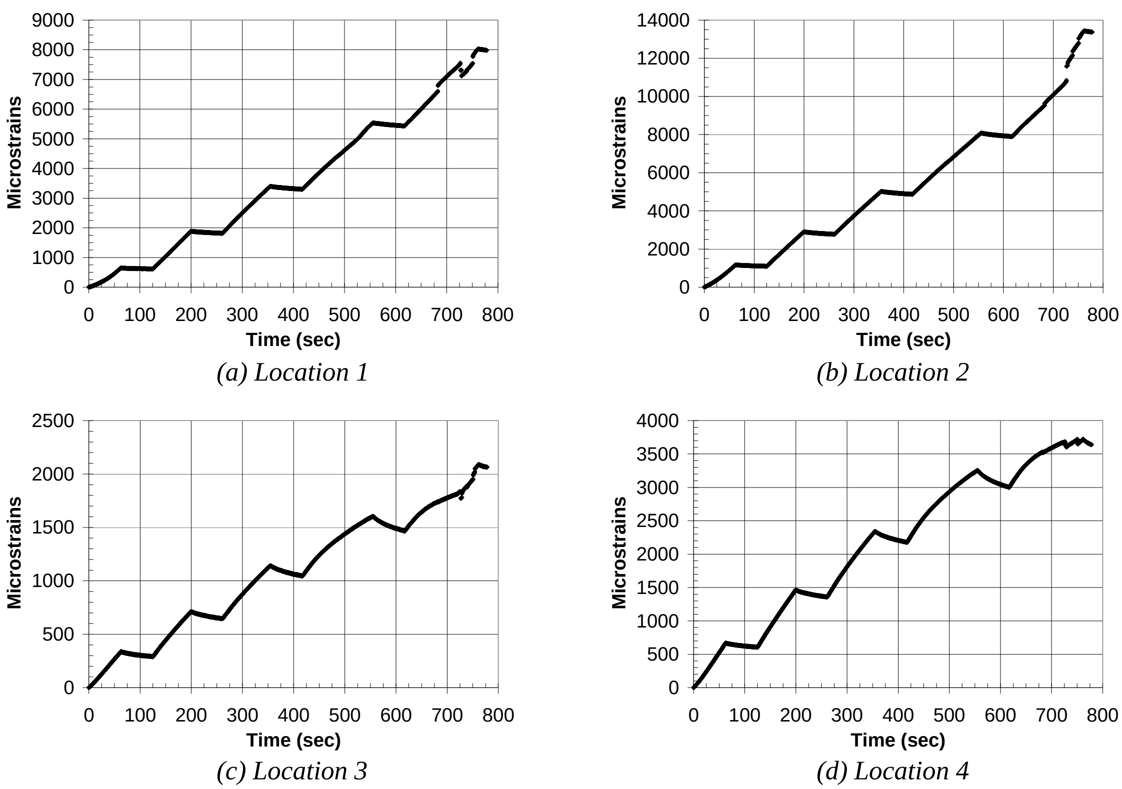

(a) Location 1 (b) Location 2 (c) Location 3 (d) Location 4

Figure D10. Strain v/s Time for Mat 10: Geometry 3

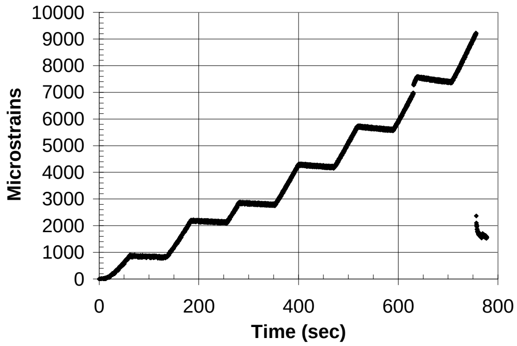

(a) Location 1

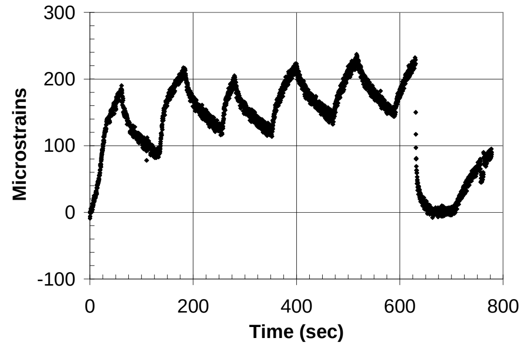

(b) Location 2

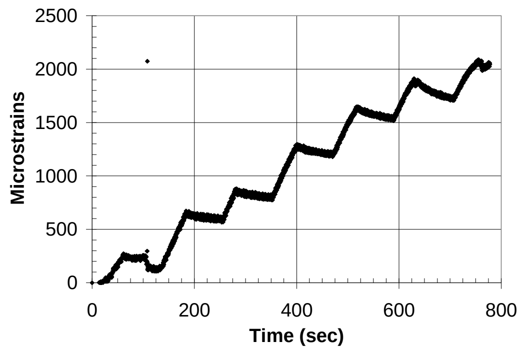

(c) Location 3

Figure D11. Strain v/s Time for Mat 11: Geometry 8

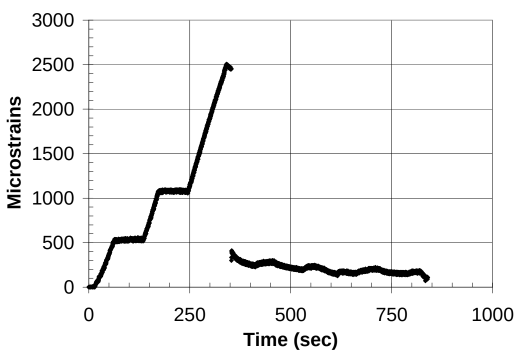

(a) Location 1

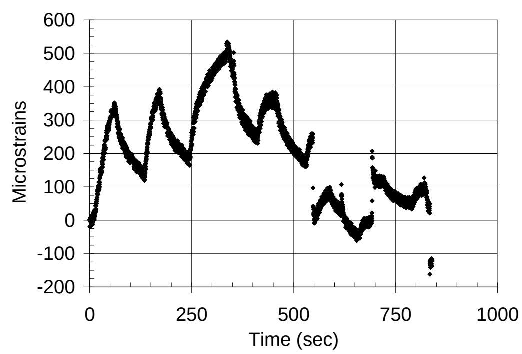

(b) Location 2

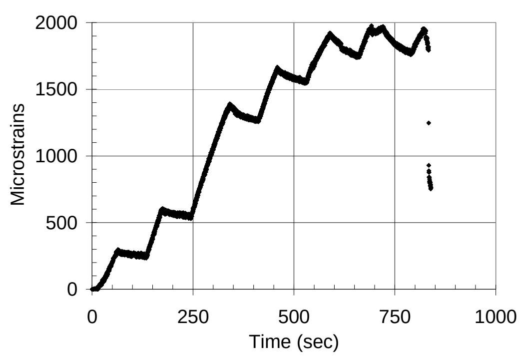

(c) Location 3

Figure D12. Strain v/s Time for Mat 12: Geometry 8

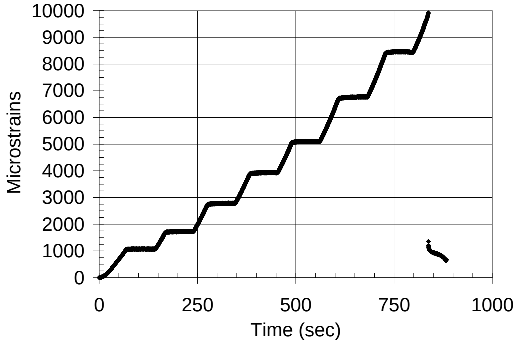

(a) Location 1

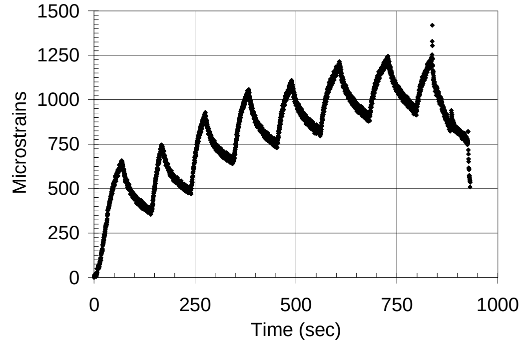

(b) Location 2

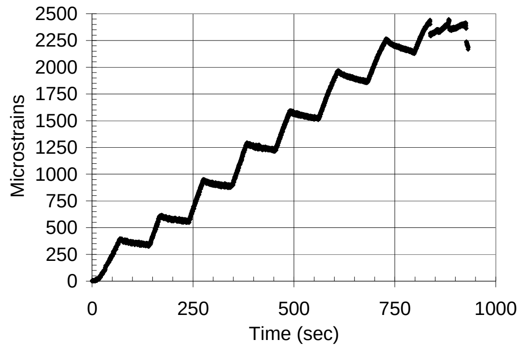

(c) Location 3

Figure D13. Strain v/s Time for Mat 13:Geometry 8

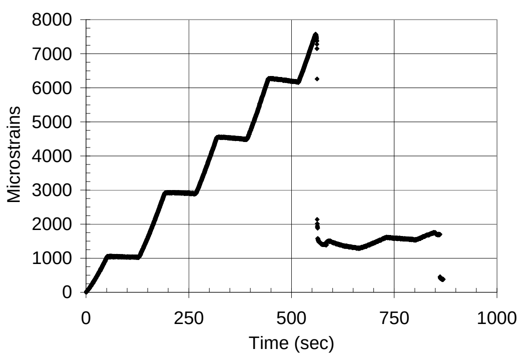

(a) Location 1

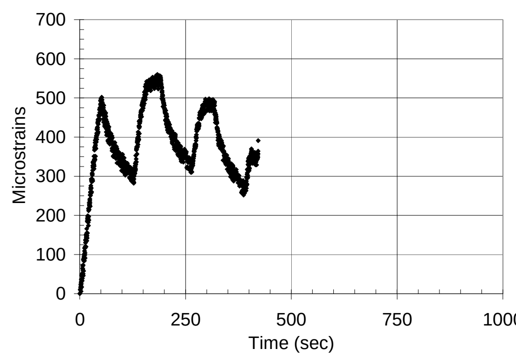

(b) Location 2

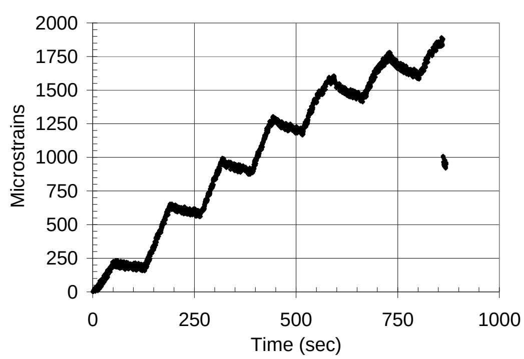

(c) Location 3

Figure D14. Strain v/s Time for Mat 14: Geometry 8

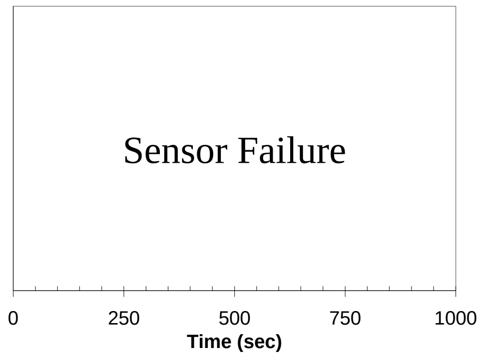

(a) Location 1

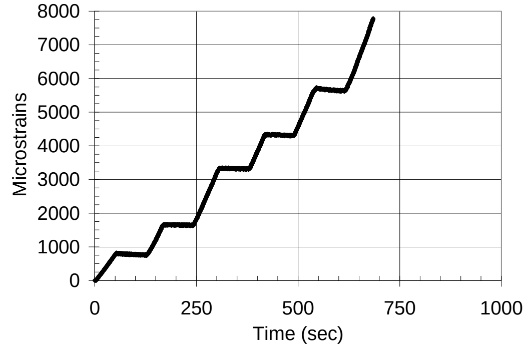

(b) Location 2

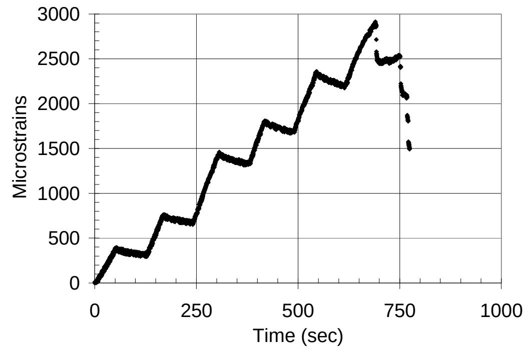

(c) Location 3

Figure D15. Strain v/s Time for Mat 15: Geometry 4

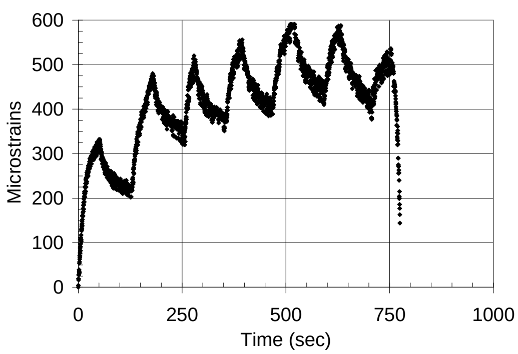

(a) Location 1

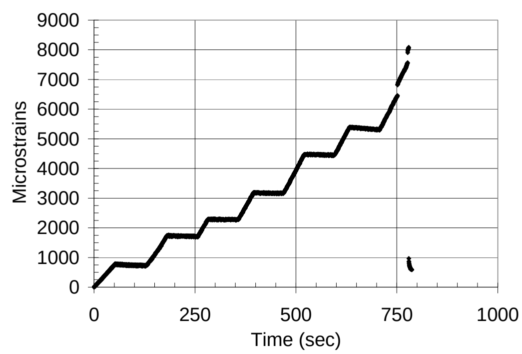

(b) Location 2

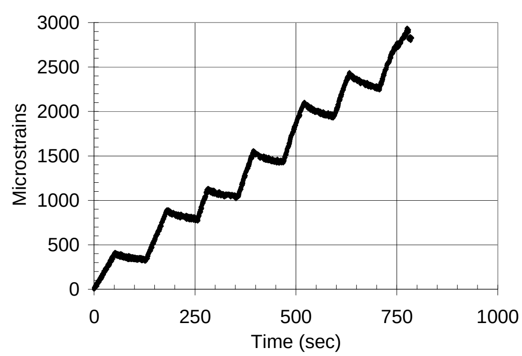

(c) Location 3

Figure D16. Strain v/s Time for Mat 16: Geometry 4

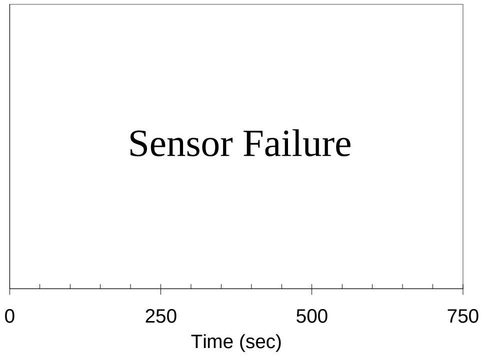

(a) Location 1

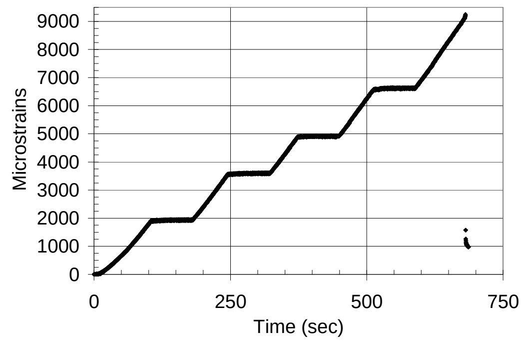

(b) Location 2

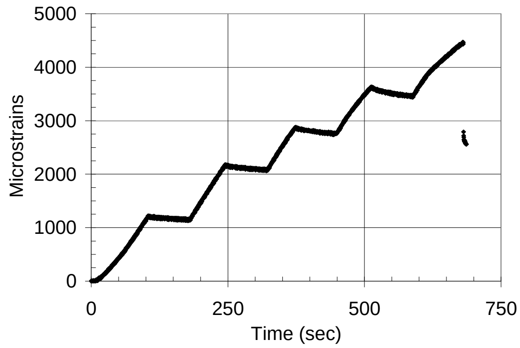

(c) Location 3

Figure D17. Strain v/s Time for Mat 17: Geometry 9

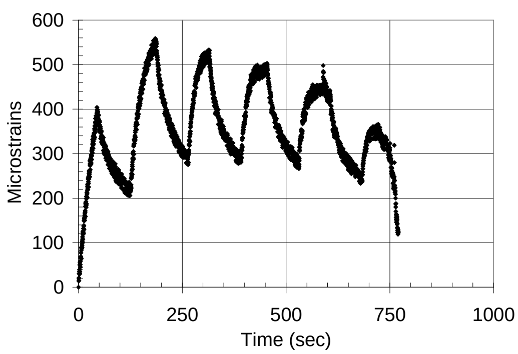

(a) Location 1

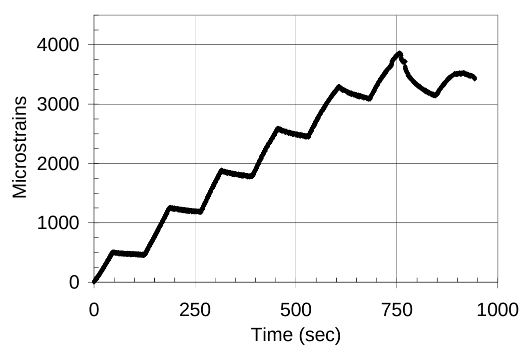

(b) Location 2

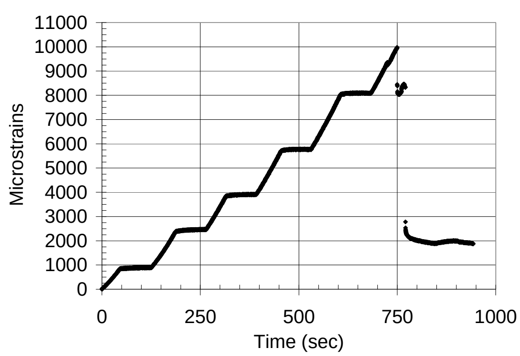

(c) Location 3

Figure D18. Strain v/s Time for Mat 18: Geometry 9

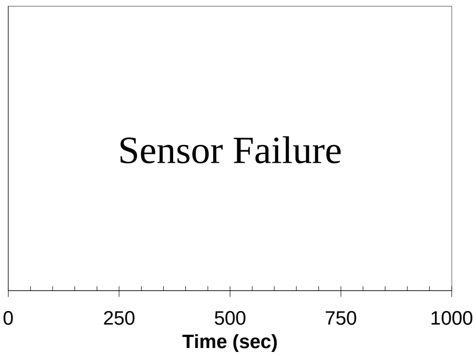

(a) Location 1

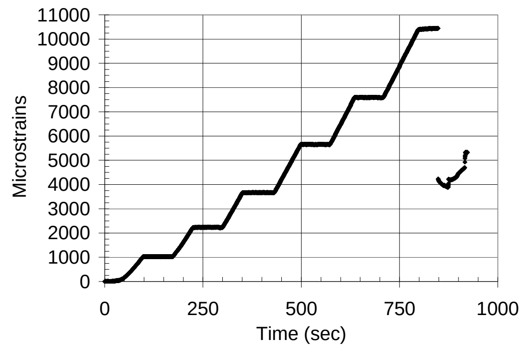

(b) Location 2

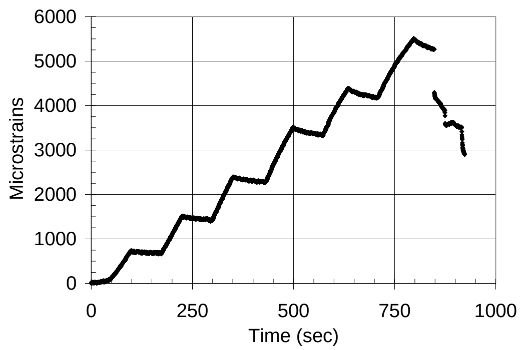

(c) Location 3

Figure D19. Strain v/s Time for Mat 19: Geometry 9

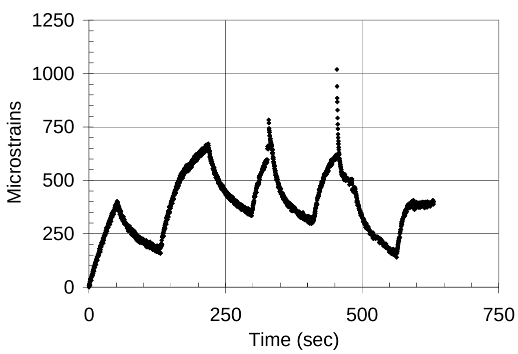

(a) Location 1

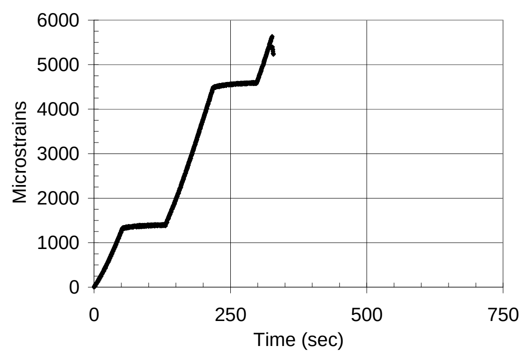

(b) Location 2

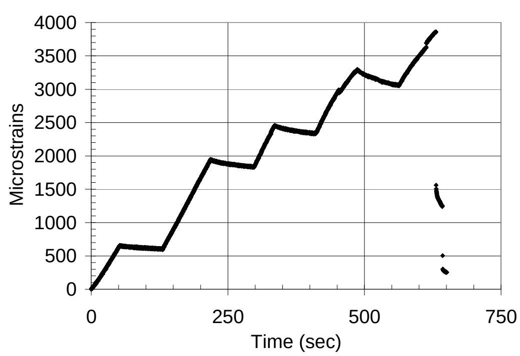

(c) Location 3

Figure D20. Strain v/s Time for Mat 20: Geometry 9

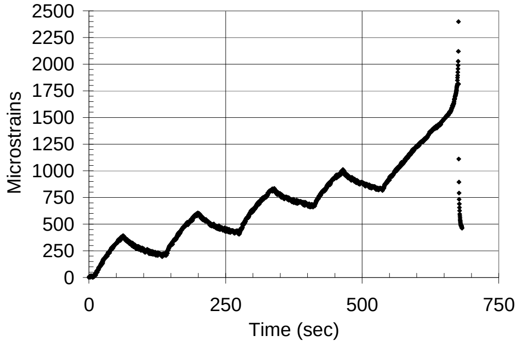

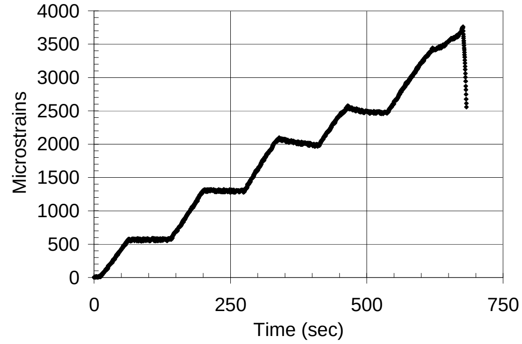

(a) Location 1 *(b) Location 2*

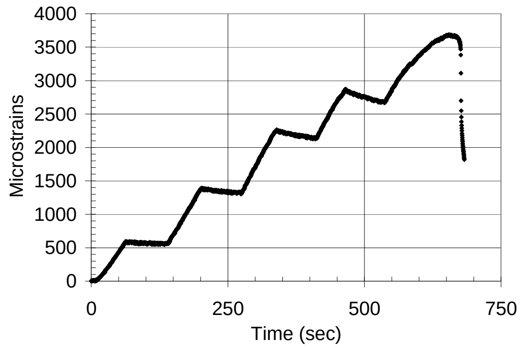

(c) Location 3

Figure D21. Strain v/s Time for Mat 21: Geometry 6

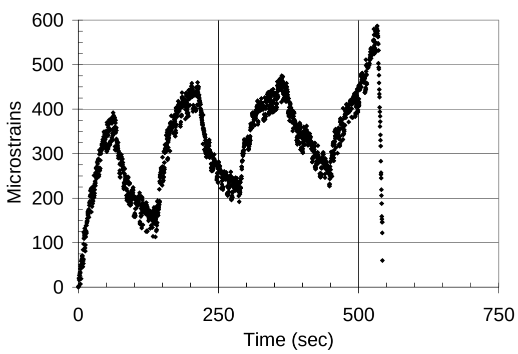

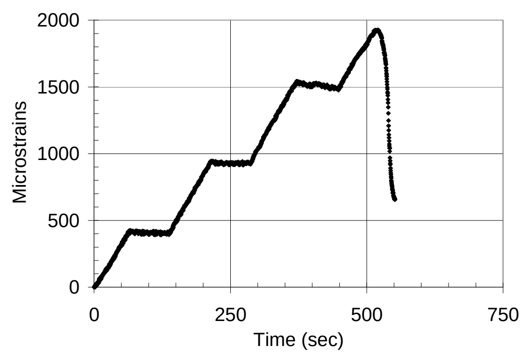

(a) Location 1 *(b) Location 2*

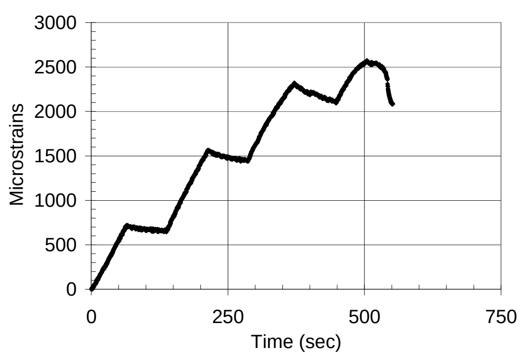

(c) Location 3

Figure D22. Strain v/s Time for Mat 22: Geometry 6

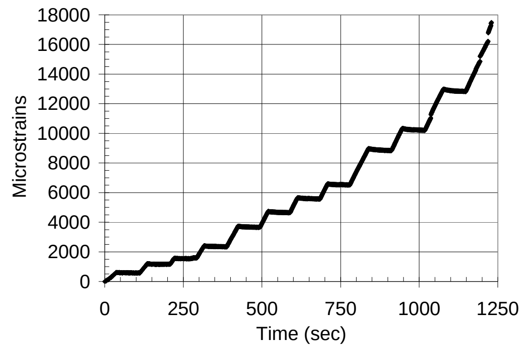

(a) Location 1

Figure D23. Strain v/s Time for Mat 23: Geometry 2

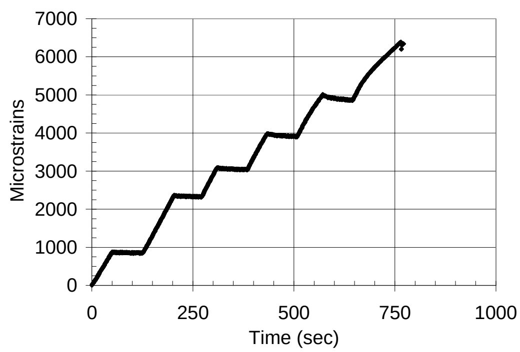

(a) Location 1

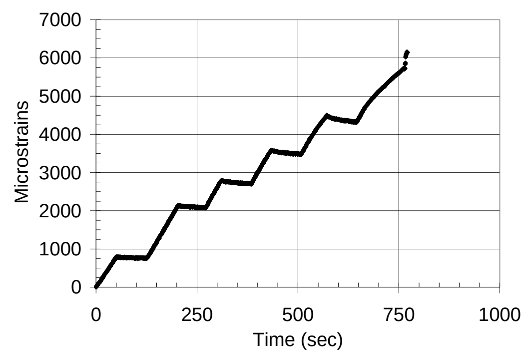

(b) Location 2

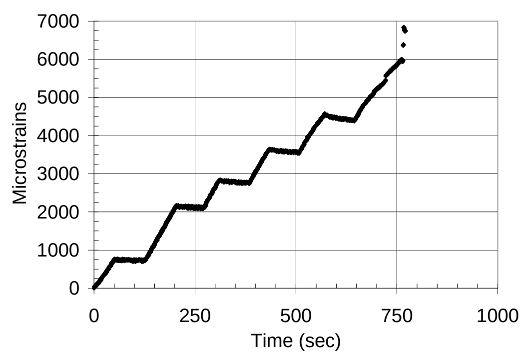

(c) Location 3

Figure D24. Strain v/s Time for Mat 24: Geometry 10

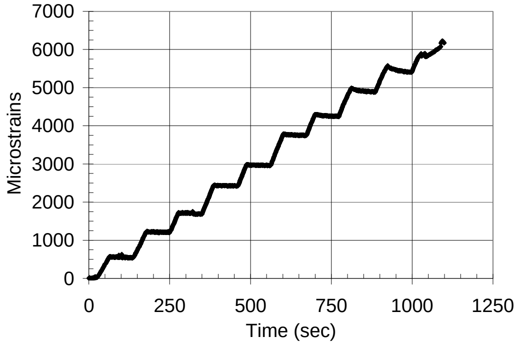

(a) Location 1

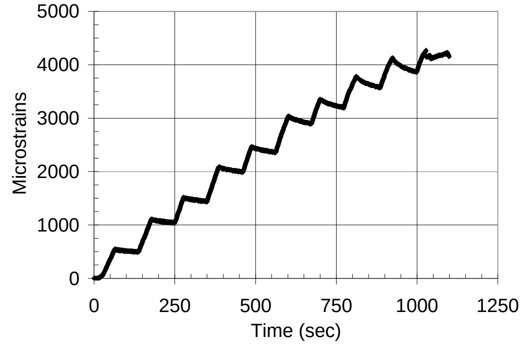

(b) Location 2

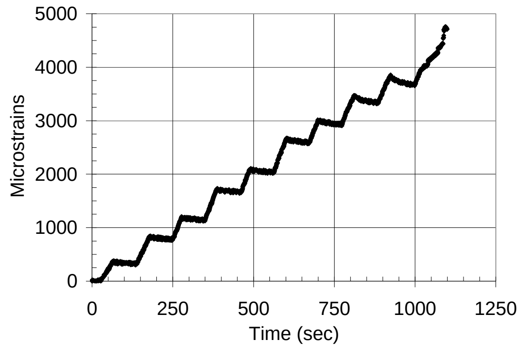

(c) Location 3

Figure D25. Strain v/s Time for Mat 25: Geometry 10

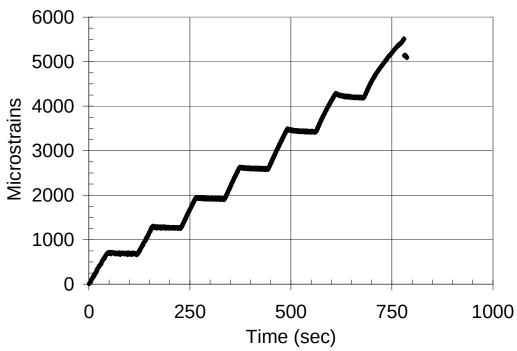

(a) Location 1

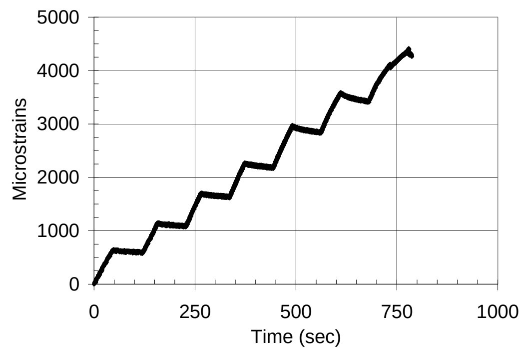

(b) Location 2

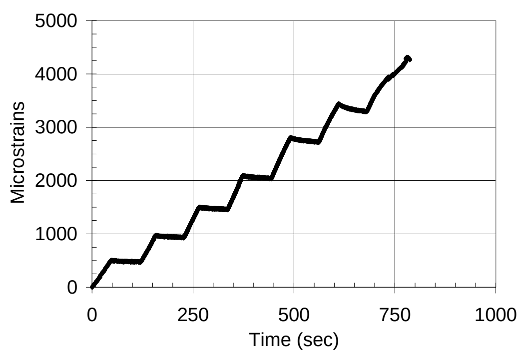

(c) Location 3

Figure D26. Strain v/s Time for Mat 26: Geometry 10

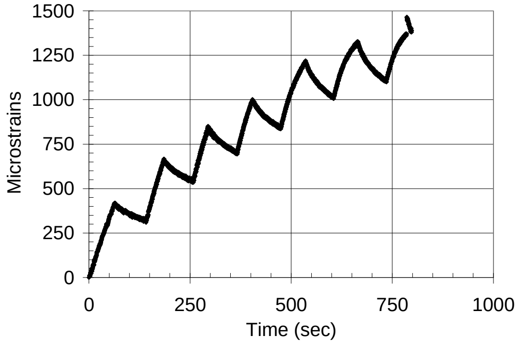

(a) Location 1

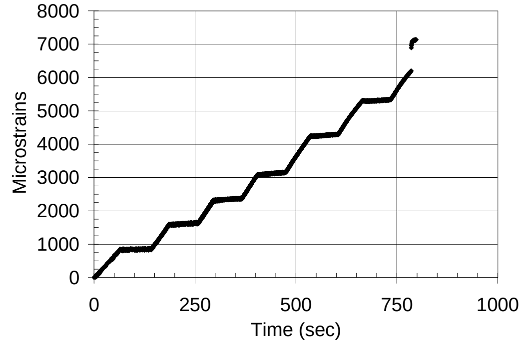

(b) Location 2

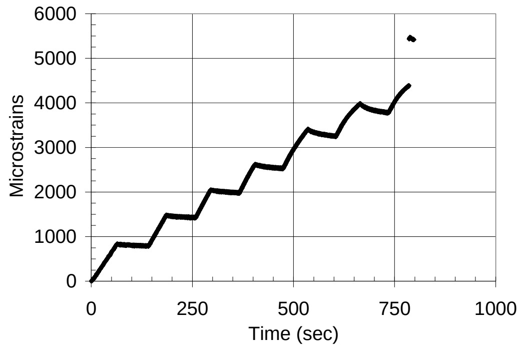

(c) Location 3

Figure D27. Strain v/s Time for Mat 27: Geometry 7

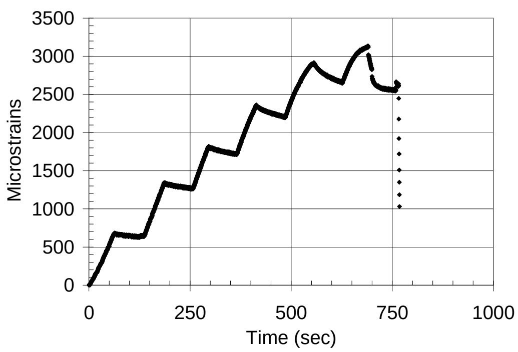

(a) Location 1

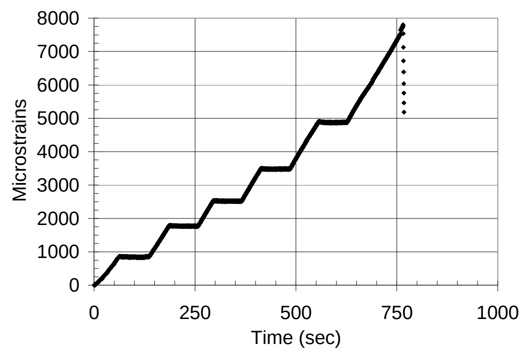

(b) Location 2

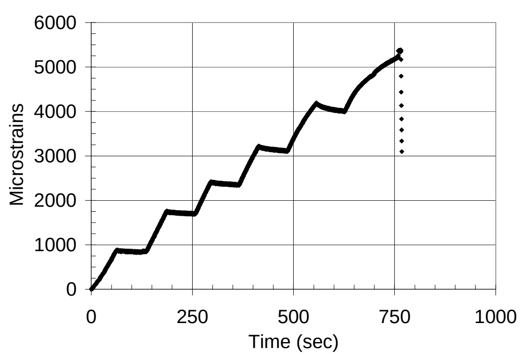

(c) Location 3

Figure D28. Strain v/s Time for Mat 28: Geometry 7

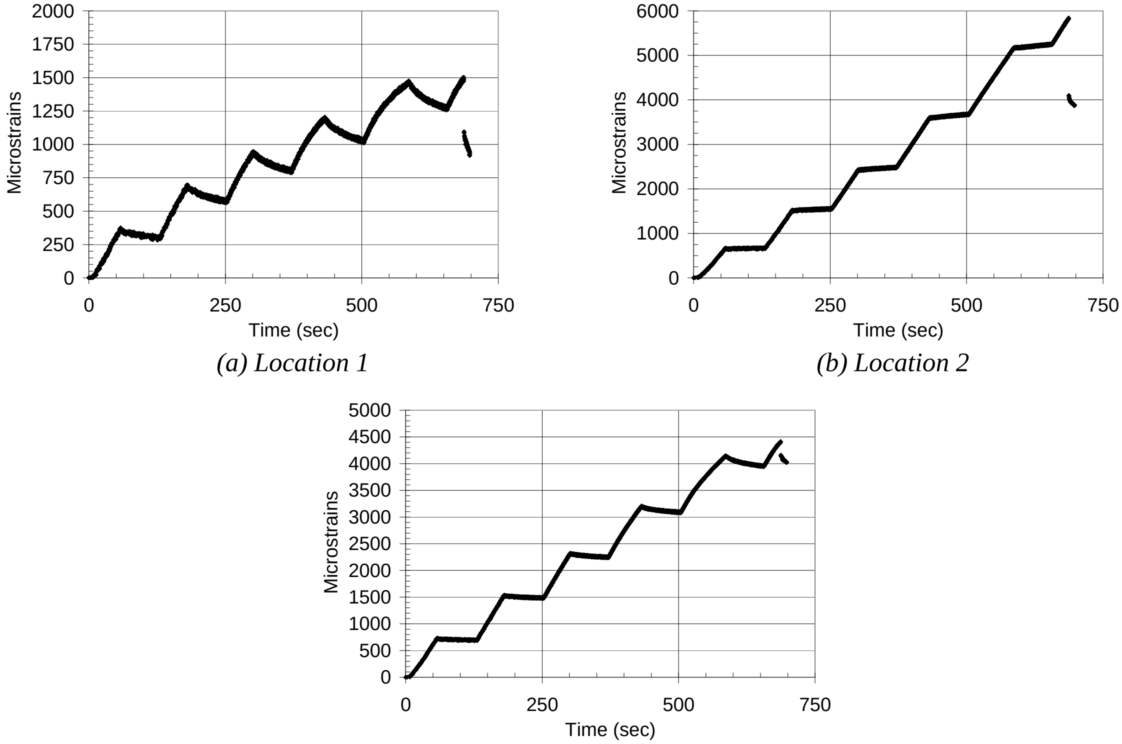

(a) Location 1

(b) Location 2

(c) Location 3

Figure D29. Strain v/s Time for Mat 29: Geometry 7

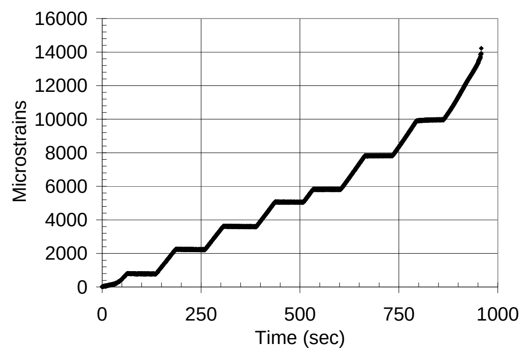

(a) Location 1

Figure D30. Strain v/s Time for Mat 30: Geometry 12

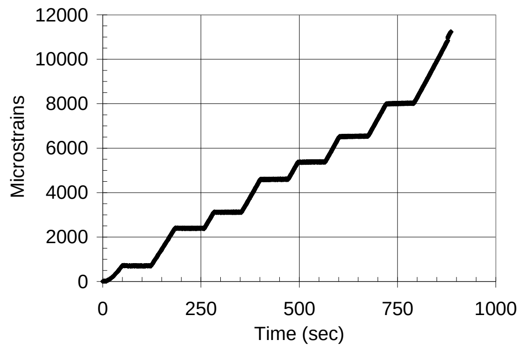

(a) Location 1

Figure D31. Strain v/s Time for Mat 31: Geometry 12

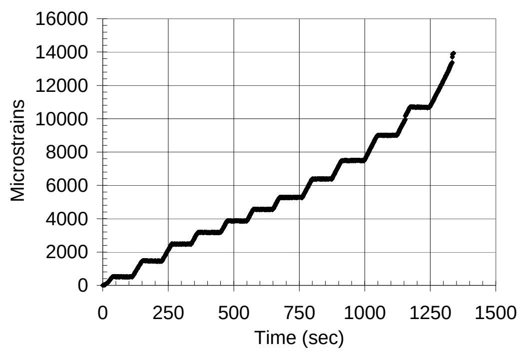

(a) Location 1

Figure D32. Strain v/s Time for Mat 32: Geometry 12

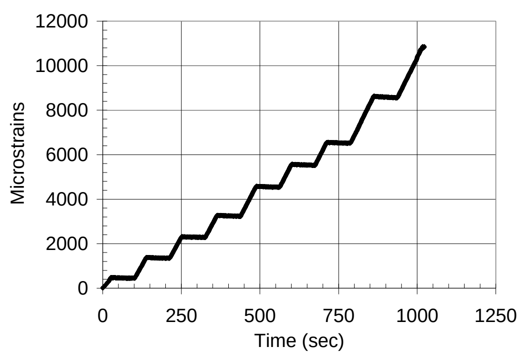

(a) Location 1

Figure D33. Strain v/s Time for Mat 33: Geometry 12

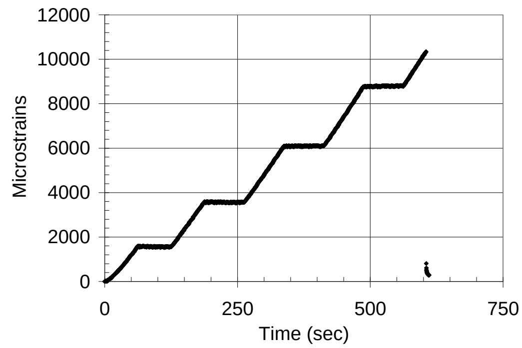

(a) Location 1

Figure D34. Strain v/s Time for Mat 34: Geometry 12

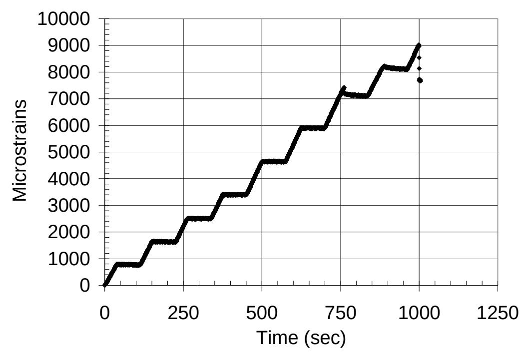

(a) Location 1

Figure D35. Strain v/s Time for Mat 35: Geometry 12

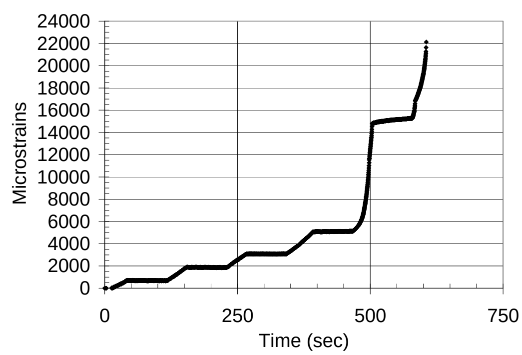

(a) Location 1

Figure D36. Strain v/s Time for Mat 36: Geometry 12

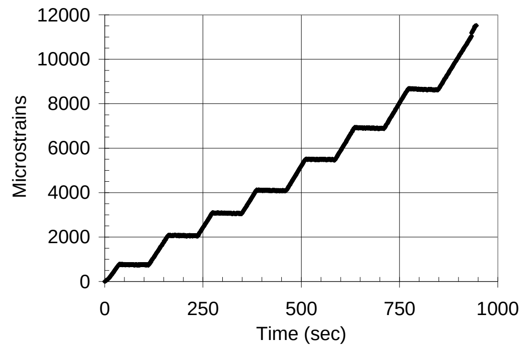

(a) Location 1

Figure D37. Strain v/s Time for Mat 37: Geometry 12

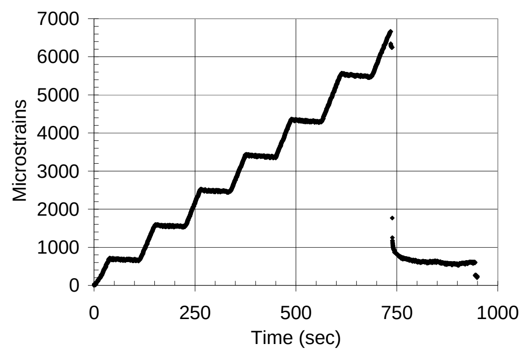

(a) Location 1

Figure D38. Strain v/s Time for Mat 38: Geometry 12

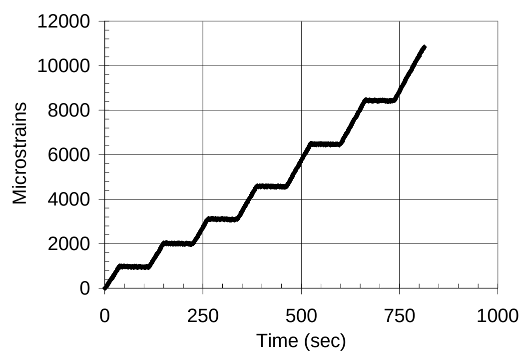

(a) Location 1

Figure D33. Strain v/s Time for Mat 39: Geometry 12

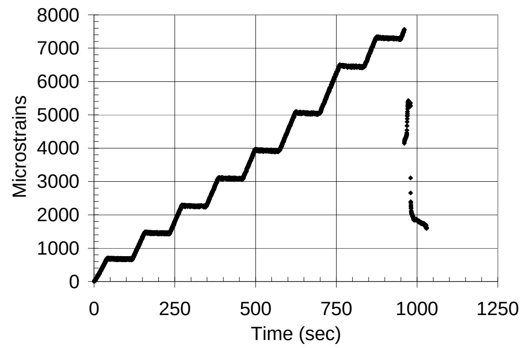

(a) Location 1

Figure D40. Strain v/s Time for Mat 40: Geometry 12

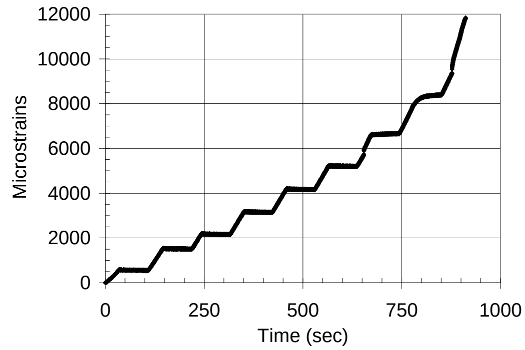

(a) Location 1

Figure D41. Strain v/s Time for Mat 41: Geometry 12

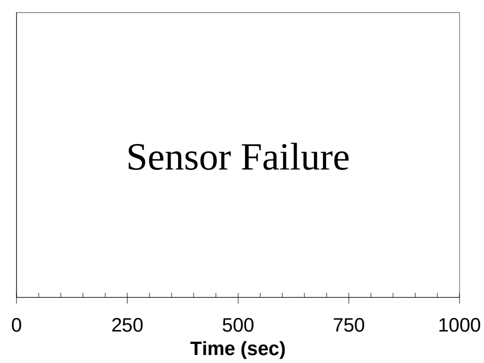

(a) Location 1

Figure D42. Strain v/s Time for Mat 42: Geometry 12

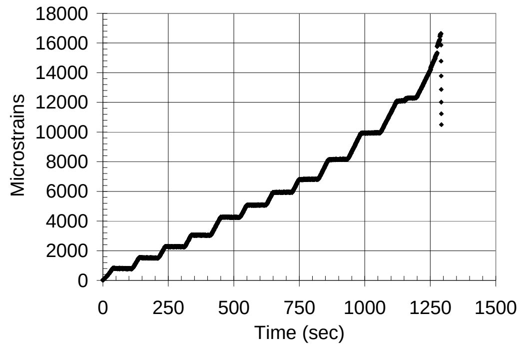

(a) Location 1

Figure D43. Strain v/s Time for Mat 43: Geometry 12

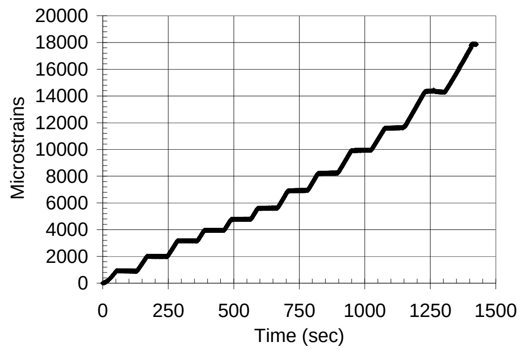

(a) Location 1

Figure D44. Strain v/s Time for Mat 44: Geometry 12

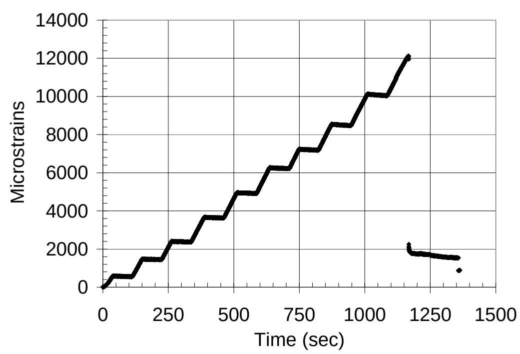

(a) Location 1

Figure D45. Strain v/s Time for Mat 45: Geometry 12

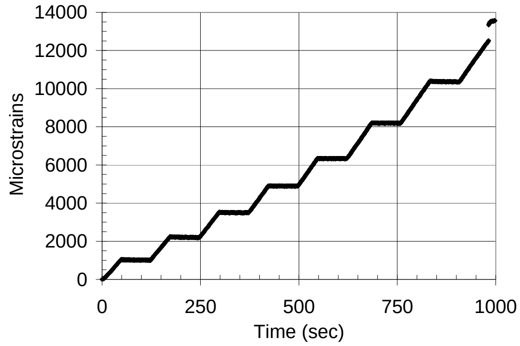

(a) Location 1

Figure D46. Strain v/s Time for Mat 46:Geometry 11

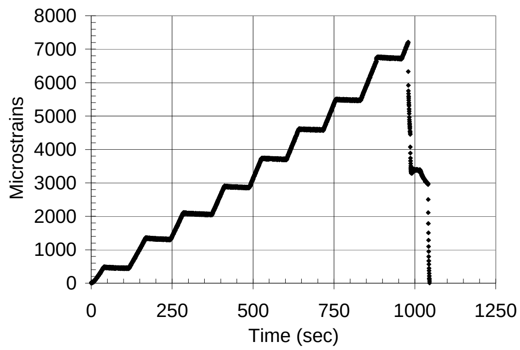

(a) Location 1

Figure D47. Strain v/s Time for Mat 47: Geometry 11

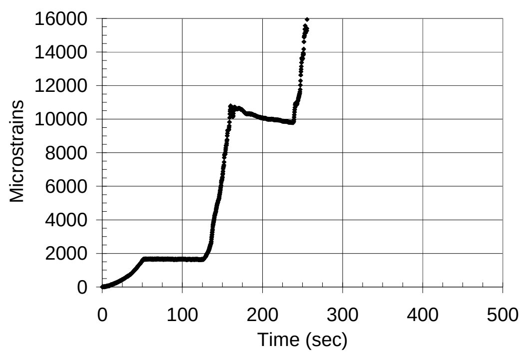

(a) Location 1

Figure D48. Strain v/s Time for Mat 48: Geometry 11

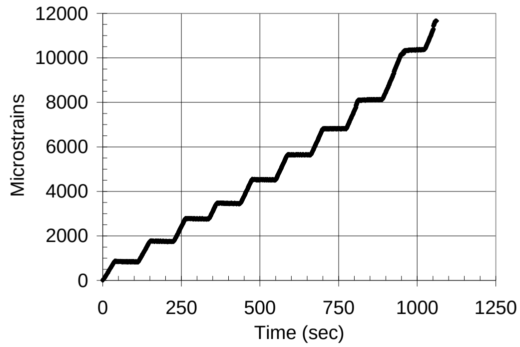

(a) Location 1

Figure D49. Strain v/s Time for Mat 49: Geometry 11

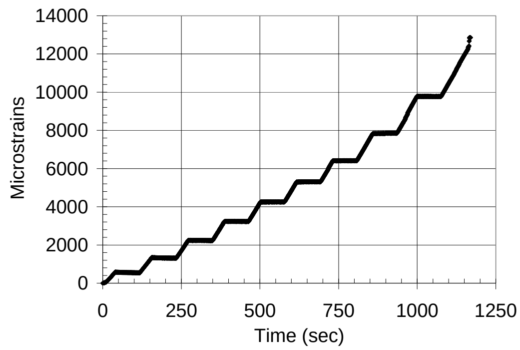

(a) Location 1

Figure D50. Strain v/s Time for Mat 50: Geometry 11

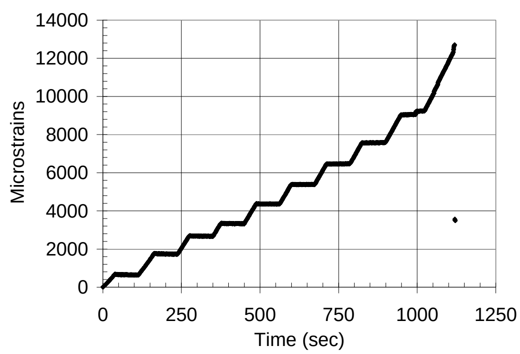

(a) Location 1

Figure D51. Strain v/s Time for Mat 51: Geometry 11

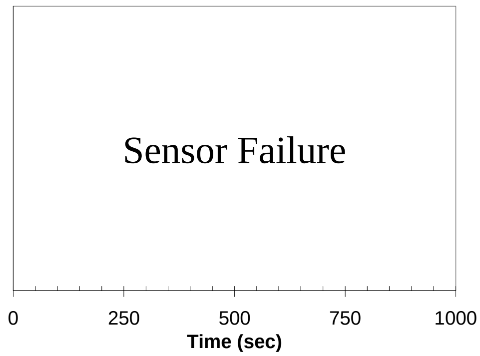

(a) Location 1

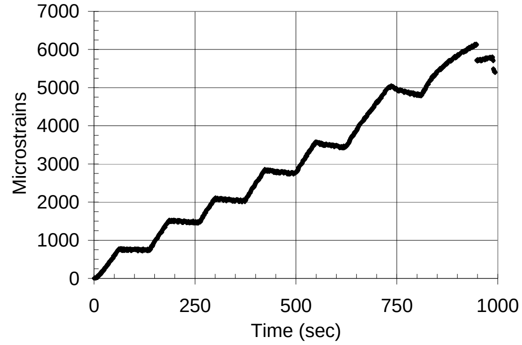

(b) Location 2

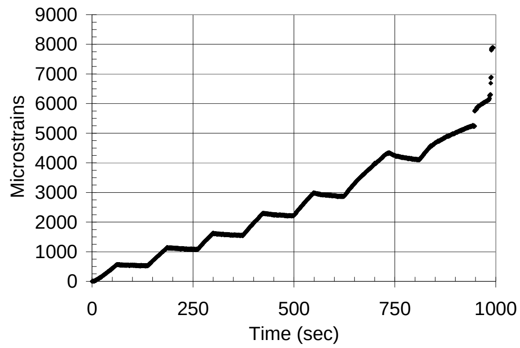

(c) Location 3

Figure D52. Strain v/s Time for Mat 52: Geometry 10

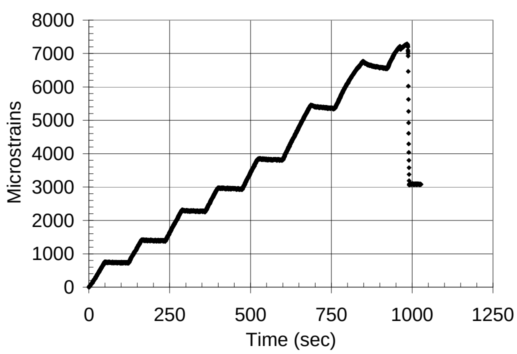

(a) Location 1

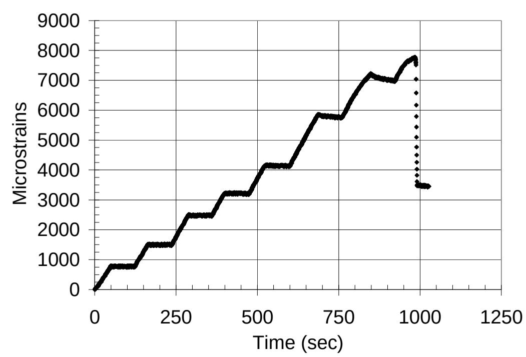

(b) Location 2

Figure D53. Strain v/s Time for Mat 53: Geometry 10

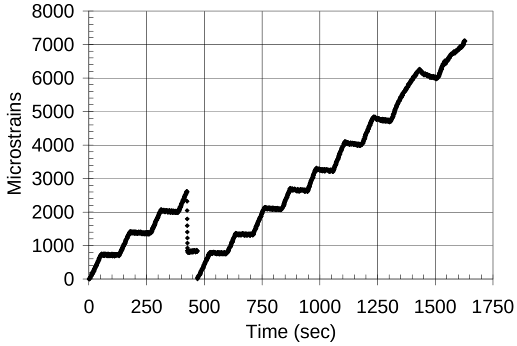

(a) Location 1

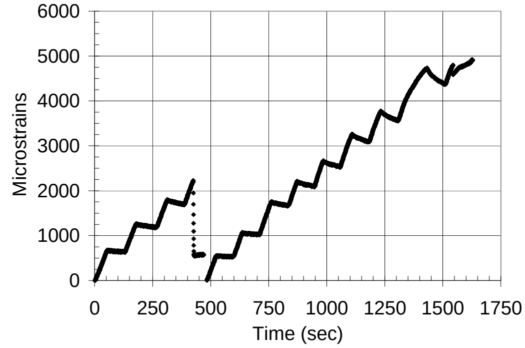

(b) Location 2

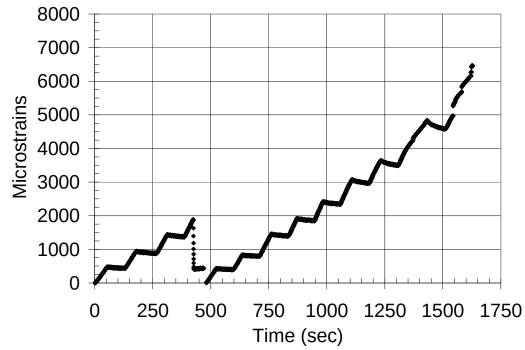

(c) Location 3

Figure D54. Strain v/s Time for Mat 54: Geometry 10

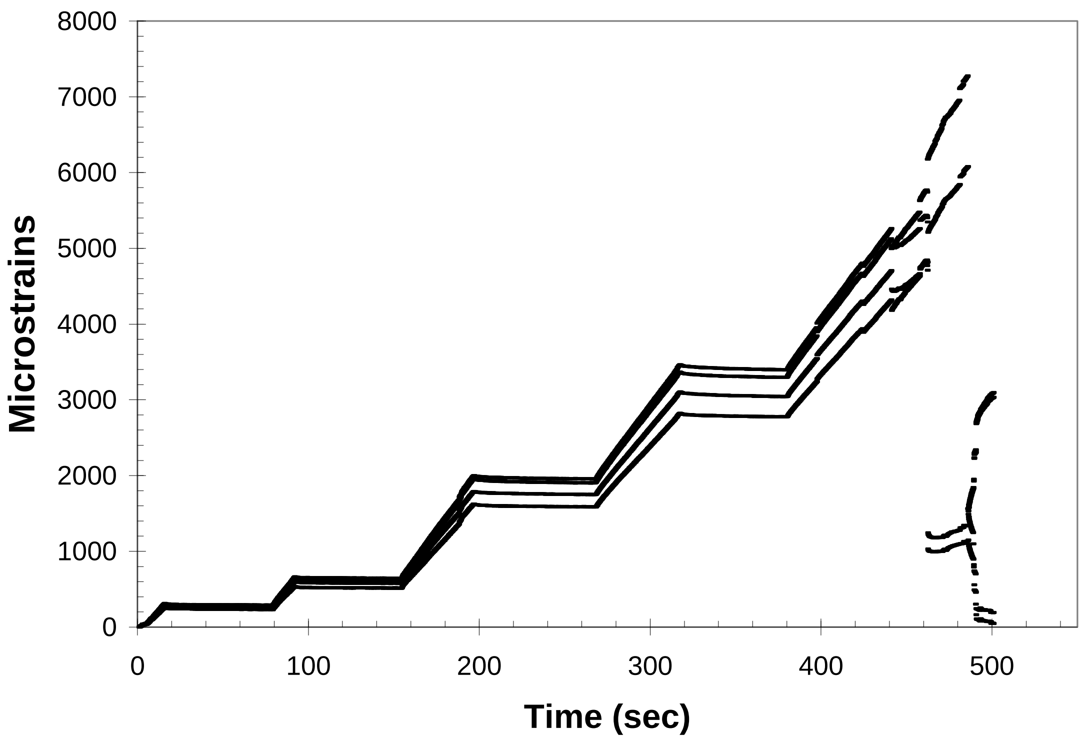

Figure D.55. Strain v/s Time for Mat 55: Geometry 14

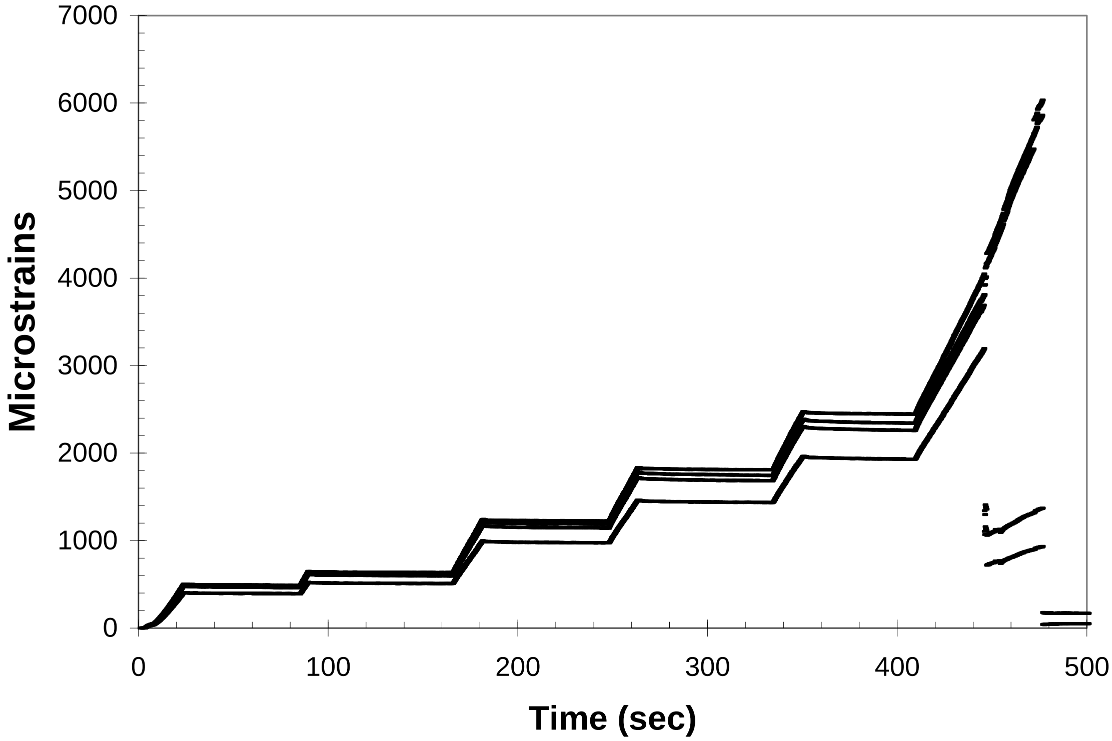

Figure D.56. Strain v/s Time for Mat 56: Geometry 15

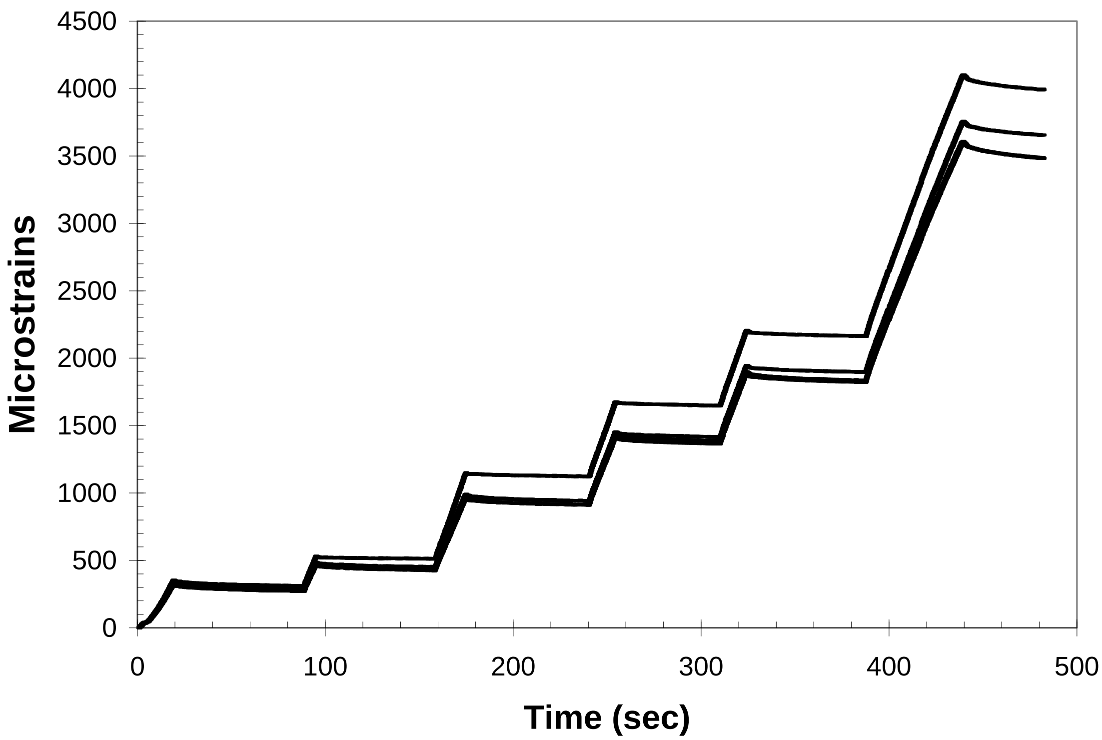

Figure D.57. Strain v/s Time for Mat 57: Geometry 15

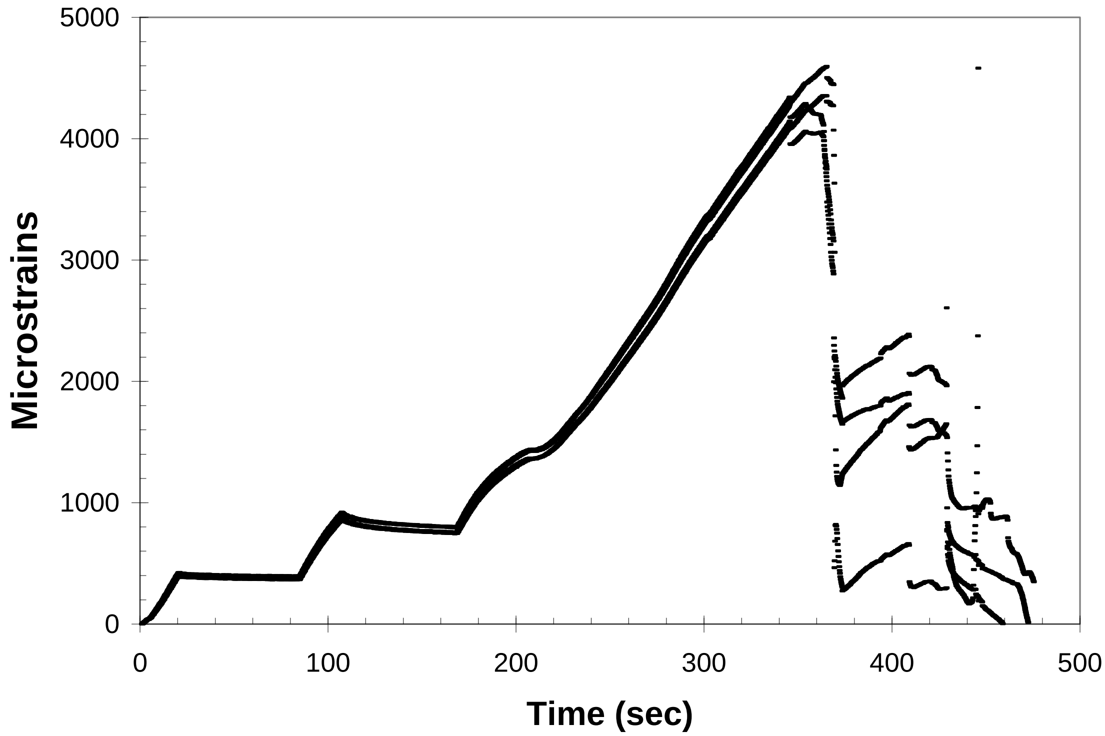

Figure D.58. Strain v/s Time for Mat 58: Geometry 16

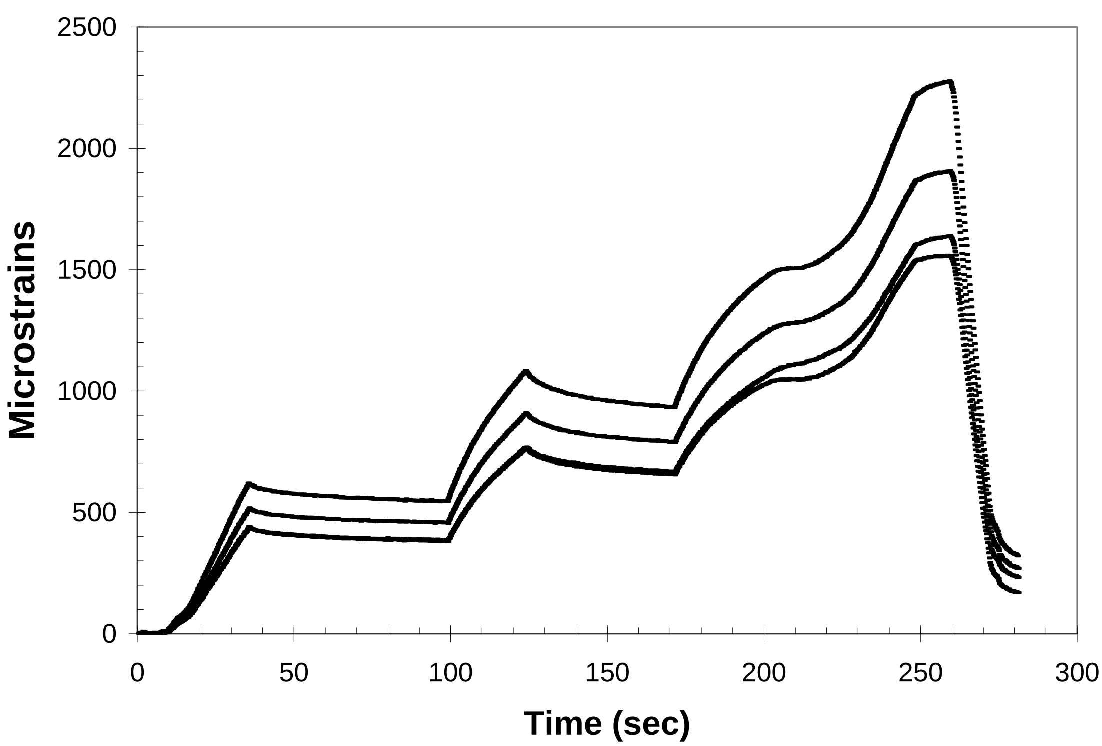

Figure D.59. Strain v/s Time for Mat 59: Geometry 16

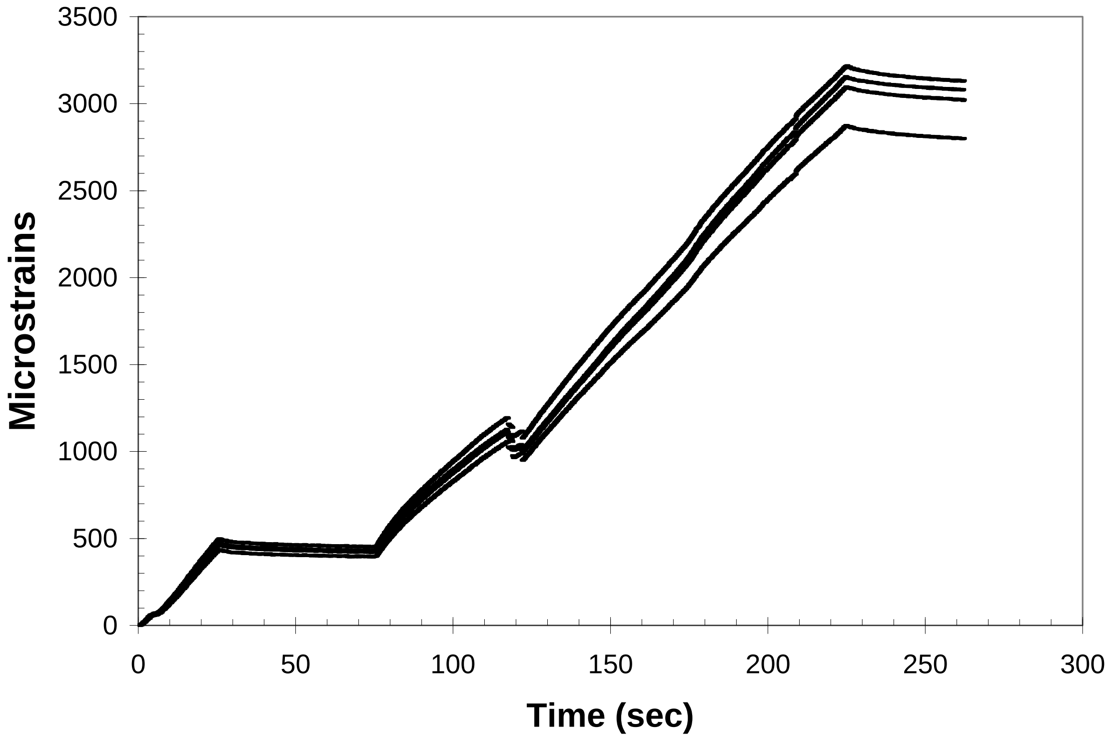

Figure D.60. Strain v/s Time for Mat 60: Geometry 16

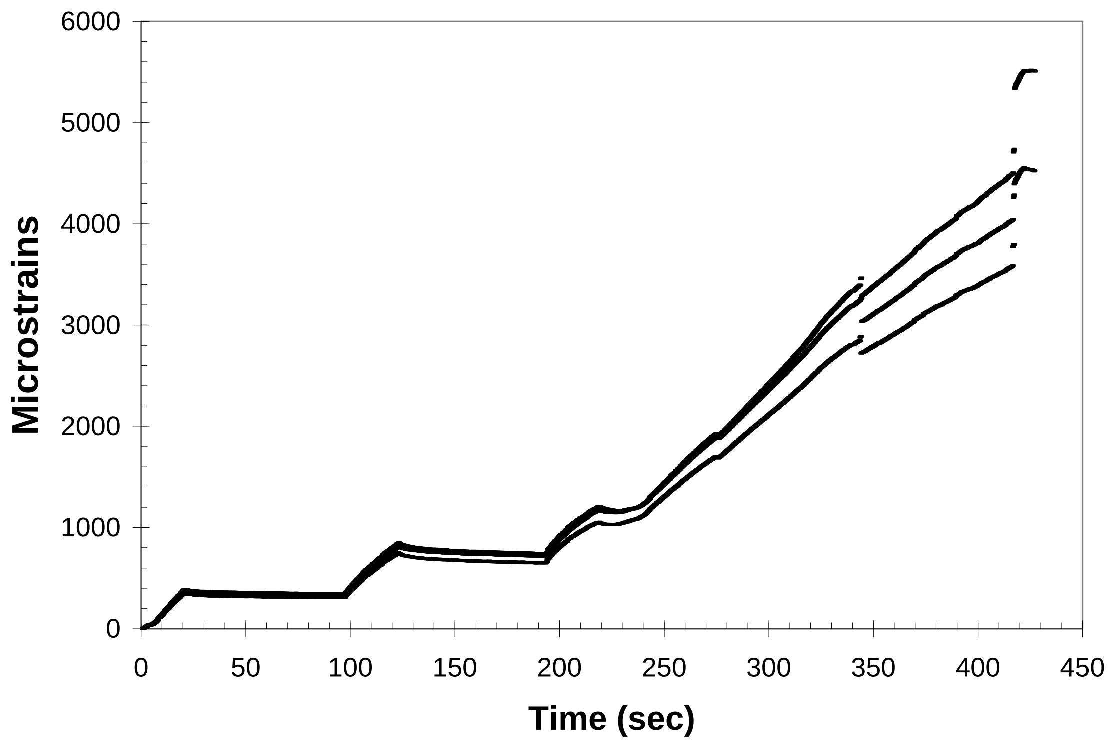

Figure D.61. Strain v/s Time for Mat 61: Geometry 16

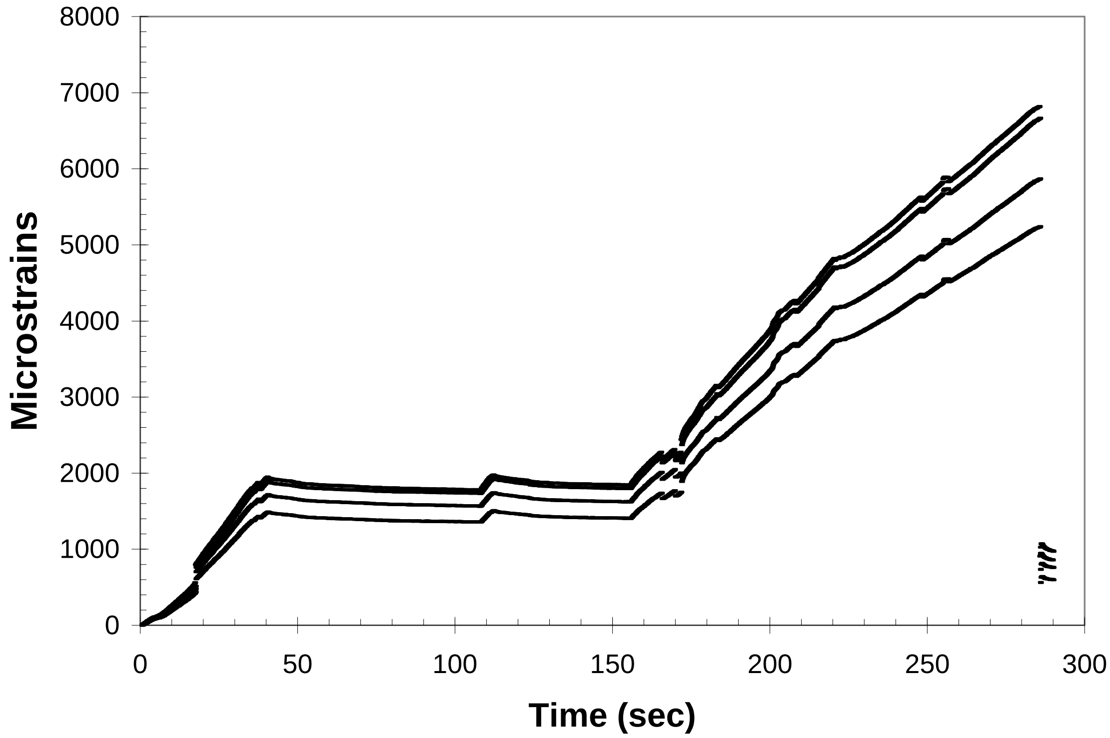

Figure D.62. Strain v/s Time for Mat 62: Geometry 17

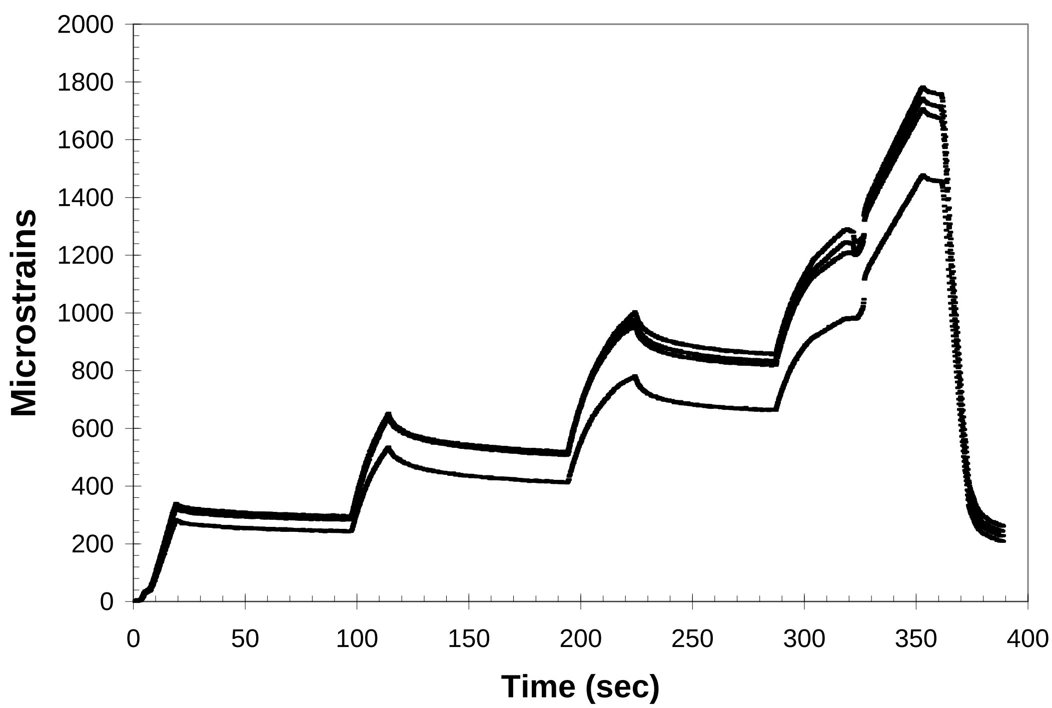

Figure D.63. Strain v/s Time for Mat 63: Geometry 18